UNIVERSIDADE DE SÃO PAULO
ESCOLA DE ENGENHARIA DE SÃO CARLOS

Gustavo Selem De Stéfano

About the State of the Art at Nanosatellite Docking Systems and Robotic Manipulation.

São Carlos

2022

Gustavo Selem De Stéfano

About the State of the Art at Nanosatellite Docking Systems and Robotic Manipulation.

Monografia apresentada ao Curso de Engenharia Mecatrônica, da Escola de Engenharia de São Carlos da Universidade de São Paulo, como parte dos requisitos para obtenção do título de Engenheiro Mecatrônico.

Advisor: Prof. Dr. Daniel Varela Magalhães

São Carlos

2022

Stéfano, Gustavo
About the State of the Art at Nanosatellite Docking Systems and Robotic Manipulation. / Gustavo Selem De Stéfano ; Prof. Dr. Daniel Varela Magalhães. – São Carlos, 2022.
124 p. : il. (preto.) ; 30 cm.

Monografia (Graduação em Engenharia Mecatrônica) – Escola de Engenharia de São Carlos, Universidade de São Paulo, 2022.

1. On-orbit docking. 2. On-orbit manipulation. 3. Attitude Sensing/actuation . 4. Design suggestions. 5. Course conclusion thesis. I. Prof. Dr. Daniel Varela Magalhães. II. Título.

Folha de aprovação em conformidade
com o padrão definido
pela Unidade.
No presente modelo consta como
folhadeaprovacao.pdf

Este trabalho é dedicado aos meus colegas do grupo Warthog Robotics. Não seria razoavel subestimar o imenso valor técnico e as belas amizades que me foram agraciadas após os anos de trabalho no grupo.

ACKNOWLEDGEMENTS

I would like to acknowledge the company and my peers at Endurosat AD. The former for embarking me on the internship that started this work and for having the forward-thinking mindset to invest in this research. The latter for serving as role models of capable engineers and most of all for openly sharing their knowledge.

ABSTRACT

Stéfano, G. **About the State of the Art at Nanosatellite Docking Systems and Robotic Manipulation.**. 2022. 124p. Monograph (Conclusion Course Paper) - Escola de Engenharia de São Carlos, Universidade de São Paulo, São Carlos, 2022.

This document aims to be a comprehensive report about on-orbit docking and manipulation systems for nanosatellites, more specifically with three or more units, as defined in NASA's State of the Art of Small Spacecraft Technology report (WESTON *et al.*, 2018). An overview of sensing and actuation for docking and manipulation missions is than presented and finally recommendations for such systems are proposed.

Keywords: On-orbit docking, Cubesat, Conclusion course thesis.

RESUMO

Stéfano, G. **About the State of the Art at Nanosatellite Docking Systems and Robotic Manipulation.**. 2022. 124p. Monografia (Trabalho de Conclusão de Curso) - Escola de Engenharia de São Carlos, Universidade de São Paulo, São Carlos, 2022.

Este documento explora o estado da arte em conectores para atracagem em orbita de nanosatelites, mais particularmente cubosats de três ou mais unidades, como definido em (WESTON *et al.*, 2018). Possíveis manipuladores robóticos, para serem utilizados em conjunto com os connectores ou nao, em mesma escala tambem são apresentados. Em seguida, temse uma revisão de atuadores, propulsores e sensores para *rendezvous*. Por fim, são oferecidas sugestões para missões de cubosat envolvendo atracagem e manipulação em orbita

Palavras-chave: LaTeX. Classe USPSC. Tese. Dissertação. Trabalho de conclusão de curso (TCC).

LIST OF FIGURES

LIST OF TABLES

LIST OF ABBREVIATIONS AND ACRONYMS

LEO	Low Earth Orbit
TRL	Technology Readiness Level
NASA	National Aeronautics and Space Administration
ESA	European Space Agency
JAXA	Japan Aerospace Exploration Agency
TRL	Technology Readiness Level
ADCS	Attitude Determination and Control System
I^2C	Digital Communication Protocol
GPIO	General Purpose Input Output
ISS	International Space Station
LIDAR	Light Detection and Ranging
DOF	Degree of Freedom
MEMS	Micro Electromechanical System
FEM	Finite Element Method
API	Application Programming Interface
IOT	Internet of Things

CONTENTS

1 INTRODUCTION

Docking and manipulation capabilities on large spacecrafts at LEO have been present for almost as long as space exploration itself (WILDE; CLARK; ROMANO, 2019). As smaller spacecrafts; in particular cubesats; are becoming more prominent, a significant push in the direction of miniaturization of these technologies have been noticed. Main governmental space agencies, such as NASA, ESA and JAXA, have declared the importance of such systems and their intent of pushing forward with their development as evidenced by Roger Walker overseeing ESA's CubeSat technology program in 2016:"The ability to autonomously rendezvous and dock CubeSats could enable in-orbit assembly of larger structures that simply would not be possible in any other way"[1]

The assembly of large structures on-orbit is indeed a very important application of such technologies, but equally important are on-orbit maintenance, assessment, refueling, cleaning and other activities that are included in the "on-orbit services" category(LI *et al.*, 2019). For a successful mission to be carried out under this scope it may be needed only docking, only manipulation or both. Commercial options for neither of those are available at the current time at the proposed scale, but significant efforts have been directed at it from multiple private companies and governmental agencies. Most of the projects presented here started no earlier than early 2000s and are only now starting to show higher TRLs.

The docking mechanism in the scope of this thesis have per objective to promote the transfer of electrical power, establish digital communication, and to provide mechanical stability across the connected satellites. This report includes research about the docking connector itself Sec.2; the actuation necessary for the docking procedure to succeed Sec.2.0.4, including the possibility of a robotic manipulator Sec.3 and the sensors and actuators necessary for proper attitude determination/estimation and control Sec.4. It then finishes with the author's suggestion to develop such a system Sec.5.

[1] https://www.esa.int/Enabling$_{S}upport/Space_{E}ngineering_{T}echnology/How_{t}o_{d}ock_{C}ubeSats$

2 CONNECTORS

In this document, "connector" means the physical component(s) attached to a satellite that makes contact with another one. They can be classified as a Probe/Drogue (also known as cup/cone) connector, where a male connector is distinguished from a female one and they can only be successfully connected with each other. This, more common, type usually results in a simple, although more restrictive design. Another possibility is an Androgynous connector, when they are virtually identical in both spacecrafts. This makes for a more versatile design, although usually more complex.

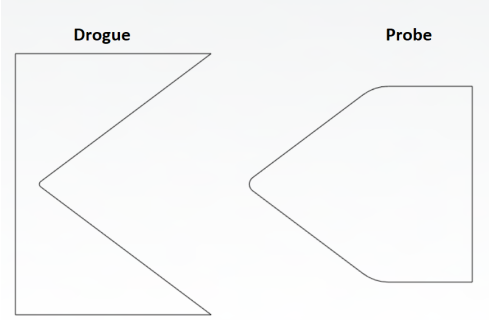

Figure 1 – Section view of a simplified Probe/Drogue connection.

The connector can be fixed directly into the spacecraft's structure or it can be mounted on an actuated system. The first option results in a simpler and lighter design, while the latter is capable of exposing and retracting the connector at will and help with it's alignment. It should also be considered that a satellite in space is a free floating base and movable parts demands a more capable Attitude Determination and Control System (ADCS).

There are other possible classifications for connector types. A soft connector is one that has dampening components in place to reduce the impact of the docking spacecrafts. These can be a simple spring, a single actuator designed to pre-capture the spacecraft and dock gently or even a robotic arm that pulls the two bodies together. This is useful for satellites with delicate instruments or sensible experiments on board, but adds complexity to the design.

The goal of this section is to examine different connector formats, and judge their design based on: capacity of fulfilling the set requirements (sec.), angular and lateral misalignment tolerance at docking and expected weight and complexity.

2.0.1 Requirements

There are three main goals set for the connector as for this research : establish digital communication, transfer electrical power and ensure a rigid mechanical link between the connected spacecrafts. Regarding communication, it is of the authors interest to adopt at least two of the following protocols: TIA-485 (TIA-485..., 2012) (also known as RS-485), TIA-422 (TIA-422..., 2014) (also known as RS-422) and I^2C. Based on the comparative table 1, this implies the necessity of 3 to 5 connections.

It is also of the author's interest to have available three to five General Purpose Input Output pins (GPIOs). The ground reference can be shared with the communication's ground to spare one extra conductor.

For the power transfer, two connections should be established for the positive voltage and ground. It must be able to support at least three amperes at 36V of potential difference. It is not recommended to share a power and a signal ground due to high risk of interference issues.

It is thus concluded that the docking system must be able to connect the two spacecrafts with 8 to 12 signal connections, two of them being power connections. It is also woth noting that other protocols are available for data transfer (WENZEL *et al.*, 2017), including the ones developed specifically for space applications such as SpaceWire(STANDARD,)

	RS-485	RS-422	I^2C
Max. No. of Connected Devices	Up to 32	Up to 10	Up to 1008
Flow of information	Multi-point	Multi-drop	Multi-point
Number of wires	2 (Half-Duplex) or 4 (Full-Duplex) +GND	4 (Full-Duplex) +GND	2 (Half-Duplex) +GND
Speed	Up to 10Mb/s	Up to 10Mb/s	Up to 3.2Mb/s
Noise immunity	High	High	Low
Observation	Moder industrial standard	-	Widely used on the "Maker Community"

Table 1 – Comparison between mainstream communication protocols in the nanosatellite community.

About the mechanical requirements, there are forces the connector is expected to withstand, they are represented in Fig.2. It should be able to resist tensile forces, pulling the spacecrafts apart perpendicularly to the mating surfaces; those forces are called here simply as "Tensile Forces". They can arise from thrusters being fired at the satellites; from

the centrifugal forces of a possible spin, intentional or not; from the differential drag of one of the spacecrafts in relation to the other on low earth orbit (LEO) and other factors.

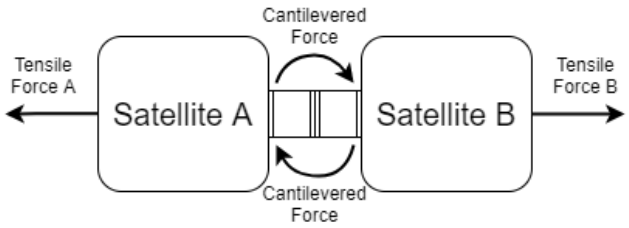

Figure 2 – Representation of the forces acting on the connector.

The rotation scenario can be used as reference for estimating the necessary connector strength. Suppose a 6U, 10kg (M) satellite, docked by it's top (smaller) surface and spinning at a rate of 0.5 Rad/s (W). Let's assume also an uniform mass distribution, resulting in the center of mass (COM) of the satellite being on its geometrical center and that the connector itself would add no more than 5cm (distance "R" from the top edge is 20cm). We can picture this scenario in figure 3. We can calculate the maximum tensile force on the connector using the simple formula:

$$F_t = M \cdot W^2 \cdot R$$

Substituting the values proposed, we can state that the minimum tensile force the connectors must resist is 0.5N. Adding a two fold safety factor the value goes to 1N.

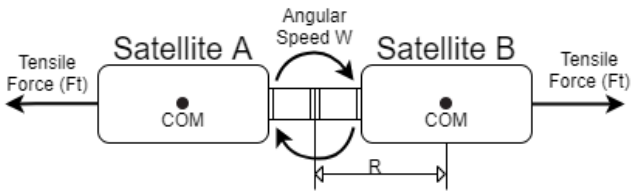

Figure 3 – Representation of the tensile force acting on a spinning pair of 6U satellites.

It should also be able to withstand torsion forces, here called "Cantilevered Forces", where a torque is generated between the connected spacecrafts. Those forces arise from the activation of an ADCS, firing of thrusters, differential drag on the atmosphere, etc.

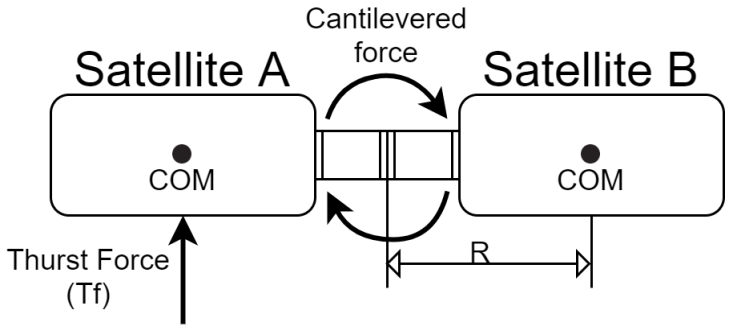

Figure 4 – Representation of cantilevered force acting at the connector at the firing of a thruster.

Consider a thruster firing at the center of one of the attached satellites and that the center of mass of the system resides at the connector's junction. A reasonable thrust force for such a system can be assumed to be up to 300nN (see section 4.1), which would result in a torque of 60mN.m. We can consider a conservative 1N.m as the minimum cantilevered forces that the connector would be required to withstand. This is a low value for any connector with a latching mechanism.

2.0.2 Connectors investigation

Here is exposed a comprehensive review of the work that has been done so far on this area. The first ten connectors are developed specifically for cubesats, the other ones are slightly too big for standard cubesats but can be miniaturized with relative ease. The addition of this latter group also provides useful insights into features and development patterns. Whiting each group, they are organised by relevance, i.e. the amount of data available, performance, technology readiness, etc.

2.0.2.1 MIT/NASA's SPHERES

The MIT's and NASA's SPHERES project aims to be a generic robotic platform in space, where different types of hardware and software can be tested. They were first sent to the International Space Station (ISS) in 2006 and to this day two of then remains on board, according to the official websites[1,2]. The relevance of the project in regards to this report, comes from the fact that the small robots are equipped with androgynous connectors, the Universal Docking Port (UDP) (RODGERS, 2006) (RODGERS *et al.*, 2005), that started its development on 2005 and is capable of docking two or more of then to each other.

[1] http://ssl.scripts.mit.edu/www/portfolio/spheres/
[2] https://www.nasa.gov/spheres/home

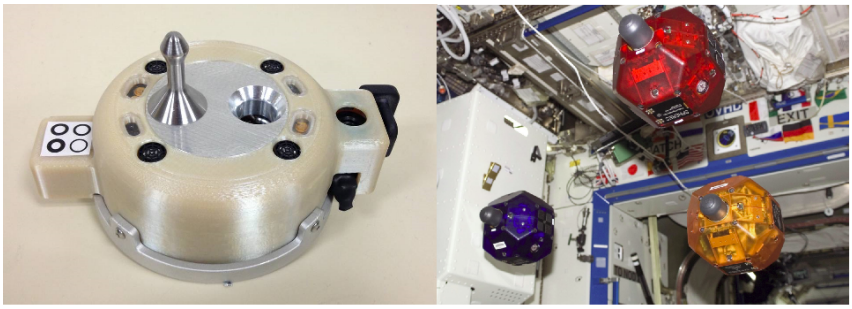

Figure 5 – MIT's SPHERES. The robots themselves floating on the ISS at b) and it's Universal Docking Port at a).

Other projects to utilise this connector are (DONG *et al.*, 2008) and (MILLER, 2015). The precision tolerances for this design is relatively high (MILLER, 2015). It is recommended $\leq 2°$ of angular accuracy and $\leq 10mm$ to ensure reliable docking. A level of precision that the SPHERES robots positioning sensors struggled to deliver.

The mass of the connector itself is 0.45Kg and the maximum tensile and Cantilevered forces are 27.5N.m and 110N, respectively. There are two brass tabs to transfer electric power. Given the position and size of those tabs, it should be possible to modify the connector and add more tabs with significant ease, although the reliability of such connections for digital communication should be investigated.

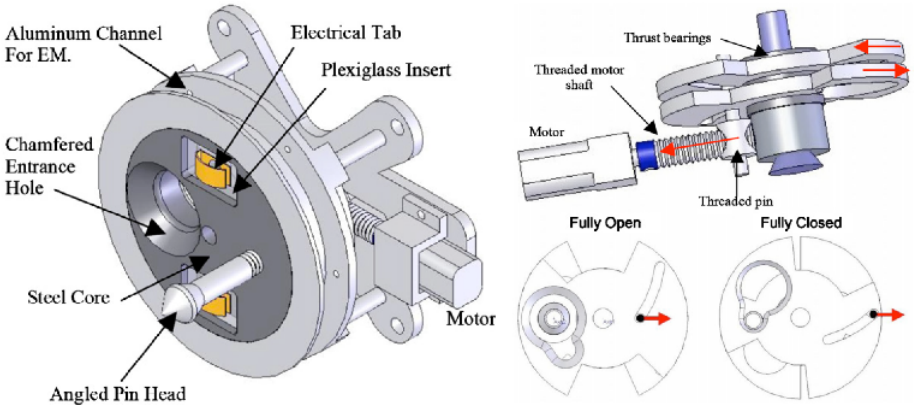

Figure 6 – CAD images of the UDP.

The mechanism is based on counter-rotating disks. When the pin head of the other satellite is inserted on the connector, an optical sensor detects its presence, which then activates the movement of the disk that ensures the head of the pin is firmly secured. To aid on the alignment, electromagnets are located at the mating surfaces. They are activated, both connectors with opposite polarity, at the moment the spacecrafts are proximity 10cm apart.

2.0.2.2 Padova Probe/drogue

This a research team from the Padova University that have developed a more traditional probe/drogue connector(BRANZ *et al.*, 2020). It is made so the probe protrudes from the spacecraft surface and still can fit inside a standard cubesat dispenser extra space region often called "tuna can". The drogue is completely passive and it is made to be attached to a satellite significantly heavier than than the probe's one. The system is designed to tolerate misalignments within the capabilities of the ADCS system, previously developed by the team(SANSONE; BRANZ; FRANCESCONI, 2018), where a mixture of visible camera and LED's fiducial markers are used. This requirement was fulfilled with great margins, so no electromagnetic alignment assistance was added. kinematic and dynamic simulations, as well as kinematic and dynamic tests confirmed the alignment margins on Fig.8, where lateral misalignment is related to the angular misalignment.

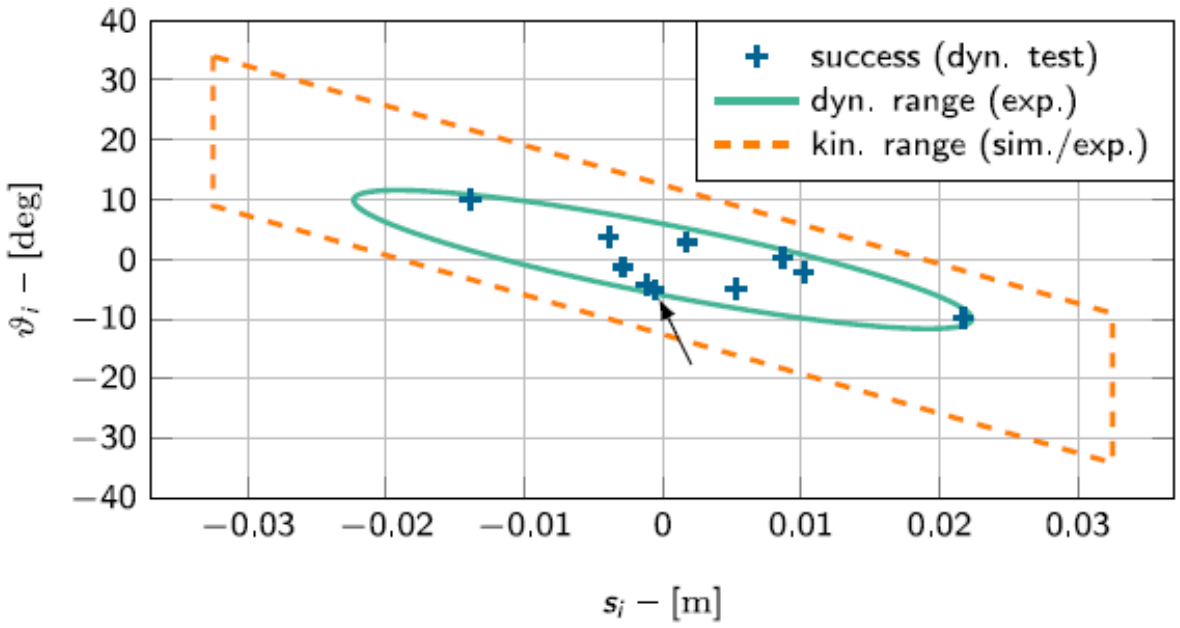

Figure 7 – Relation between lateral and angular misalignment for successful docking procedures. The orange line represents the range from the kinematic simulations and the green ellipse the range from dynamic simulations. Blue crosses represents the successful docking on breadboard testing.

The working principle is simple. After the insertion of the probe, the tip (marked in red at Fig.8) turns 90° and makes contact with the angled bottom of the alignment pins. This in turn generates an axial tension force between the surfaces of up to 25N. As stated by the team, the motor used is not capable of maintaining this force for long periods of time, a valid alternative would be to use a non backdrivable gear reduction to maintain the tension without power. An optic sensor is used to confirm a successful connection (marked in blue at Fig.8). The connector is already well sized for a cubesat application

considering the internal structure being approximately the size of a 0.5U. Regardless, the prototype presented was made out of plastic, using additive manufacture and made use of low cost components such as the hobby grade servo motor at the actuated tip.

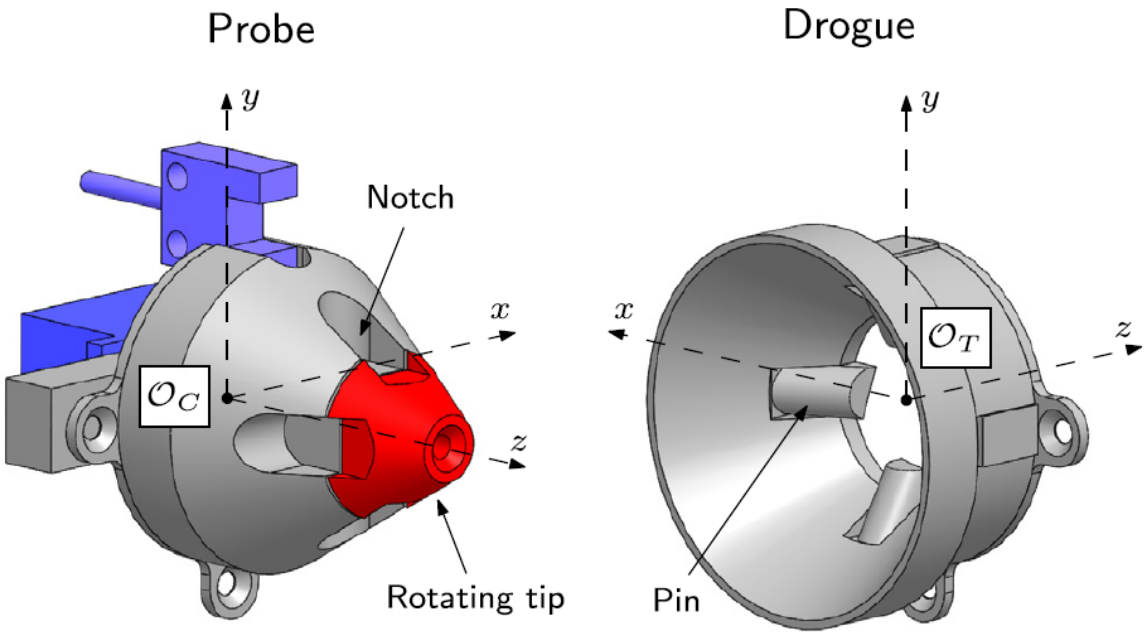

Figure 8 – Padova's probe/drogue connector with a rotating tip in red and a connection opto-sensor in blue.

2.0.2.3 AAReST

AAReST stands for Autonomous Assembly Reconfigurable Space Telescope. As the name implies, this mission has a very specific purpose, that is to use cubesats to demonstrate the possibility of on-orbit assembly of a telescope. This capability is very advantageous to telescopes, given that the aperture diameter of its lens is very important, but limited to the size of the rocket's fairing. The developers hope this technology will be the key to the construction of satellite telescopes with dozens of meters in diameter. The project started in 2009 as a partnership between the California Institute of Technology (Caltech) and the University of Surrey – Surrey Space Centre (SSC). The most recent launch time frame disclosed is 2019-2020[3], but it has not yet been launched.

Documentation on the project is abundant (ECKERSLEY *et al.*, 2017)(UNDERWOOD *et al.*, 2015)(MCKENNA, 2015)(AAREST. . . ,). The docking system was developed by Enda McKenna as a master thesis in 2015. The system is optimised for alignment precision, once it is to be used on a telescope array. As a result, it utilises the Kelvin Clamp principle, where the mating occurs only at three points of contact very well defined

[3] https://directory.eoportal.org/web/eoportal/satellite-missions/a/aarest

(Fig.10 b). In this case, a probe/drogue (Fig.10 a) arrangement is being used where the drogue has a bigger opening angle than the cone, allowing for a reliable alignment in every docking procedure. There is no electrical power being transferred for there are no electrical contacts. Information is transferred via a wireless link.

The idea is that, at least on the first mission, two 3U cubesat (called MirorSats) will detach from the initial formation. Then using traditional reaction wheels and cold gas thruster based actuation, will maneuver to be in line for reassembly. Those MirrorSats will be attached to a 15U CoreSat. The pointing requirements for the MirorSats are loose, while for the CoreSat is restricted and presents redundancy for the case of individual fails.

Figure 9 – Artistic representation of the AAReST project assembling on-orbit

The system relies on magnetic attraction for the approaching stage between the satellites. Electromagnets are controlled via Pulse Width Modulation (PWM) for adjusting the relative position and speed. The drogues and cones themselves, made out of Mild Steel (Fig.10 c), are used as a magnetic medium to focus the magnetic field lines, allowing for reliable control of the bodies. Once the connection is established, permanent magnets placed on the connectors are responsible for keeping them secure without power consumption. For undocking, the current on the electromagnets are directed in such a way to repel the spacecrafts apart and overpower the permanent magnet. This means that the unpowered holding Tensile Force of the docked system is limited by the maximum repelling force, in this case approximately 1N. If an extra holding force is needed for a predicted maneuver, the electromagnets are capable of providing about two extra newtons, at the expense of consuming 2.6A at 5 volts.

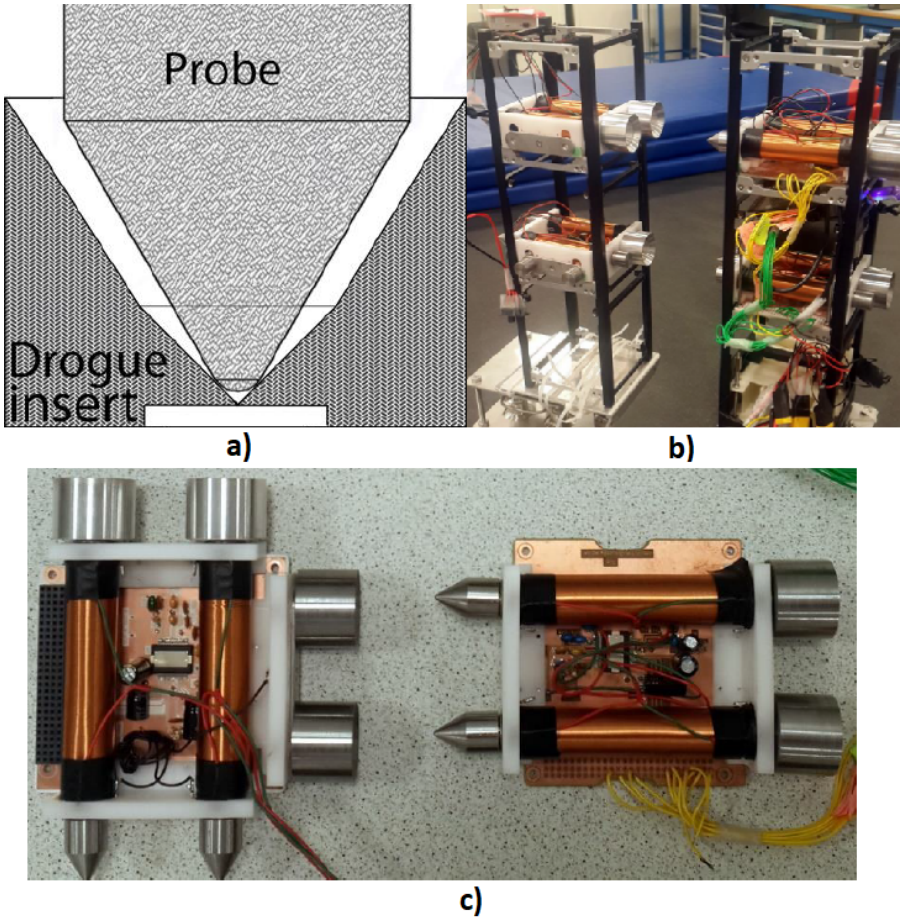

Figure 10 – a) The probe/drogue interface section view, highlighting the small point of contact. b) The docking experiment setup. c) The AAReST magnetic docking connectors.

The final docking stage is solely dependent on the magnetic attraction forces. One satellite should be positioned within a certain area (45° circle sector at Fig. 11) and at a certain angle, in relation to the other satellite, so the procedure can occur reliably. This angle (θ at Fig. 11) was observed to be dependent to the initial distance. At a distance of 30cm, the spacecrafts were able to dock reliably at angles between $+30°$ and $-30°$. The tests were performed on an air bearing table, so care must be taken when considering the results . This system should be considered for spacecrafts with high pointing accuracy performance, slow maneuverability and limited ADCS performance.

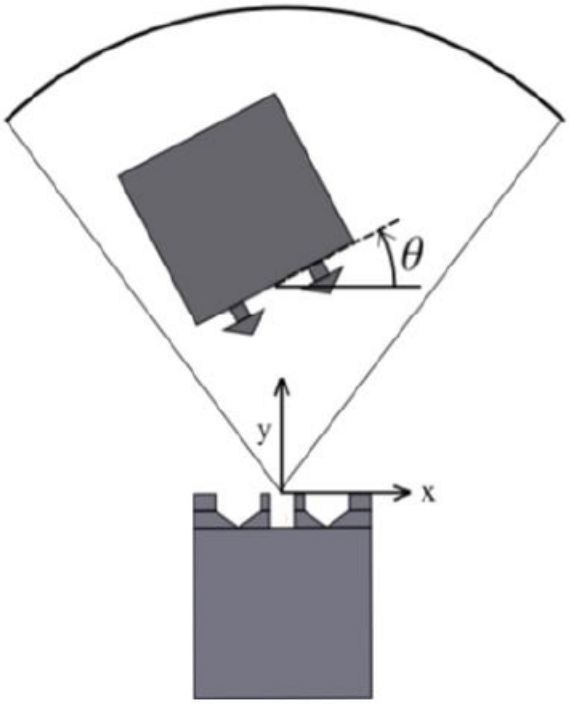

Figure 11 – Image representing the feasible docking area, the circle sector, and the alignment angle between the crafts θ.

Another mission called "Surrey Training Research and Nanosatellite Demonstrator 2" (STRaND-2)(BRIDGES *et al.*, 2013) aims to use this same connector, slightly modified for power consumption reasons. Unfortunately, this author could not find more information about the current state of the project.

2.0.2.4 OAAN

The On-orbit Autonomous Assembly of Nanosatellites (OAAN) is a NASA team, developing a permanent magnetic docking system for cubesats. There are two big distinctive factors of this project. First is the utilisation of Carrier-Phase Differential Global Position System (CDGPS) for estimating the relative position of the spacecrafts; instead of cameras; which is an enhanced form of GPS tracking. Second is that the docking system relies on permanent magnets, instead of electromagnets as the usual. Each connector has a magnetic dipole, so the forces generated by the earth magnetic field cancel out. The docking procedure relies on traditional attitude actuation until the crafts are in close proximity, afterward it deactivates its ADCS and lets the magnetic forces perform the final attraction and alignment. Other on board sensors attitude estimation are the usual star tracker, sun sensor, gyros and magnetometer. For attitude control, reaction wheels and magnetorquers are implemented and for translational control, cold gas thrusters.

Even though in theory the CDGPS is capable of centimeter-level accuracy, extensive filtering and air-bearing table testing was necessary to achieve this result (PEI, 2017).

Just like AAReST, the final approach of the cubesats are performed via magnetic forces, thus a capture volume must be reached in a certain range of distances and orientations for the procedure to be successful. This cone was extensively simulated via different approaches(PEI *et al.*, 2016). They concluded that the system is robust to 1σ at an initial axial distance of 4m and radial distance of 2m between the satellites.

Unfortunately, other mechanical details of the connector were not specified. The fact that an image system was able to be removed from the alignment sensors is a big advantage, but two big drawback of this system are: there is no way to separate the spacecrafts on-orbit once they are connected and any amount of non canceled magnetic dipole will greatly affect the spacecrafts attitude determination.

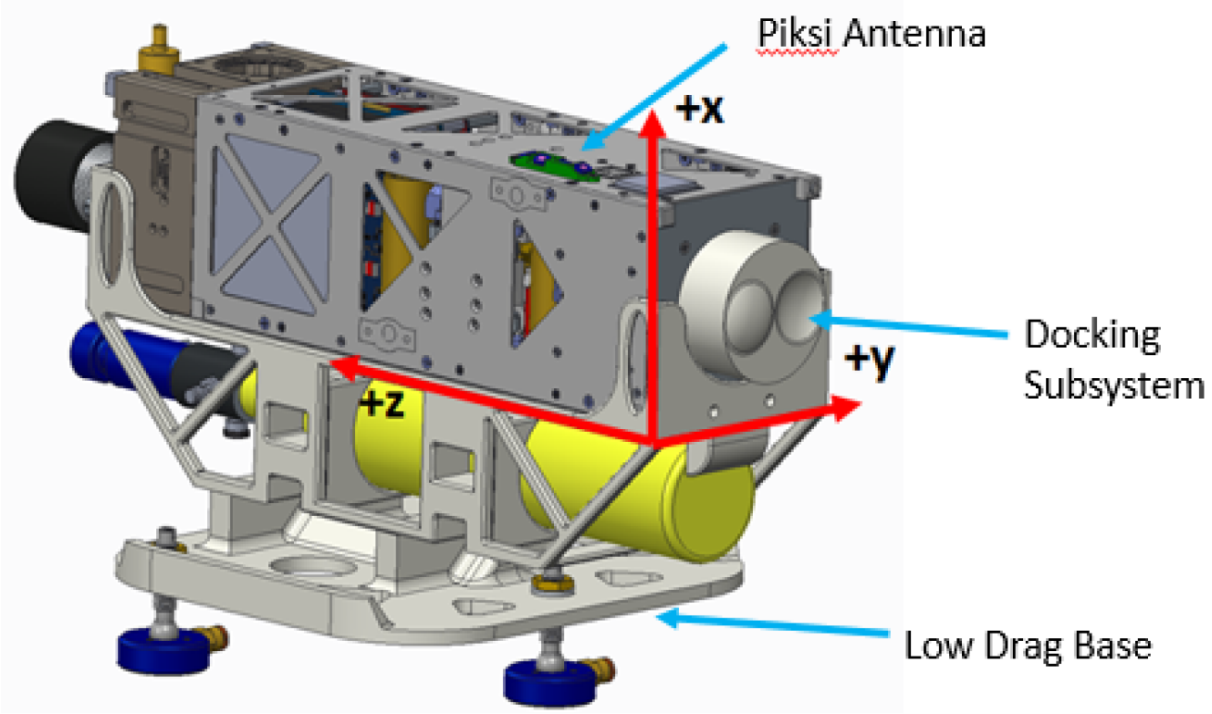

Figure 12 – CAD of OAAN satellite on its air bearing table rig. Highlighting of the CDGPS antenna (Piksi Antenna), docking connector and the matting surface between the rig and the table.

2.0.2.5 PACMAN

PACMAN(DUZZI *et al.*, 2018)) is yet another project from the university of Padova, the goal was to develop 1U magnetic docking demonstrators. They are solely maneuvered by the magnetic attraction between them. The chaser (called CUBE) is fitted with four induction coils on the mating surfaces corners. The target (called FFT) has one big central coil (Fig.13). Fig.14 shows the magnetic fields that arise from the system.

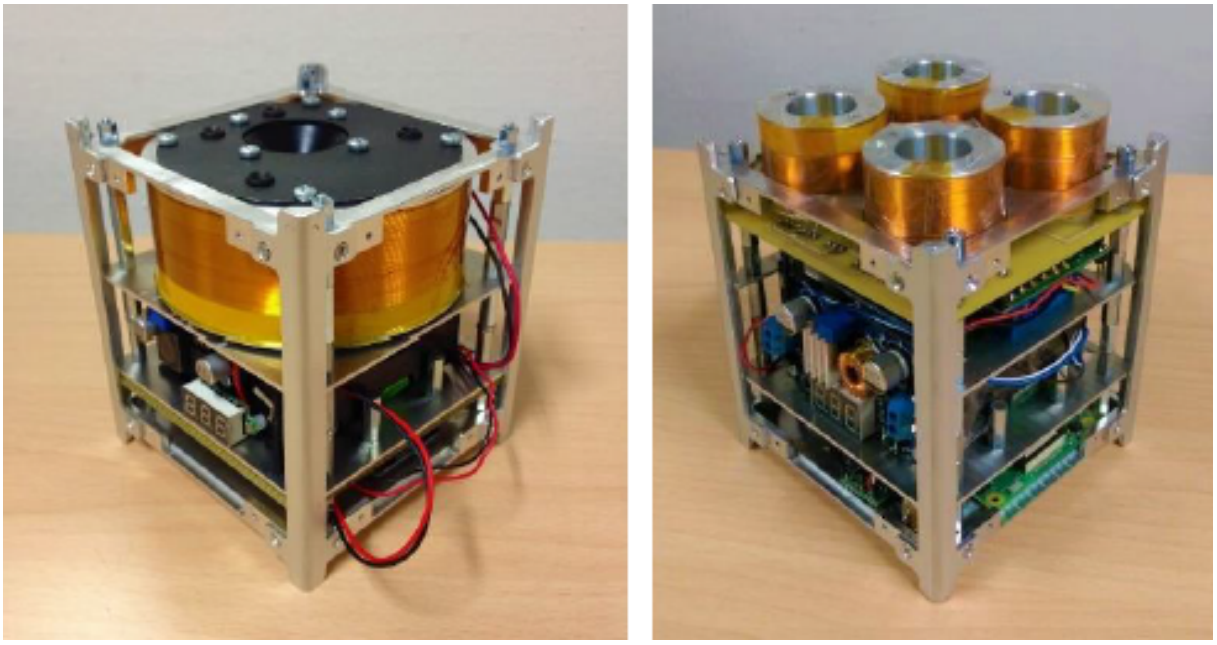

Figure 13 – PACMAN project cubesats. The target (at the left) with one big inductor and chaser on the right with four inductors for precise control.

The attitude sensing was done using a COTS raspberry pi camera and four fiducial LED's. The final system has an accuracy of less than 3° and ±5mm (DUZZI *et al.*, 2017). For attitude control, the four inductors at CUBE are independently modulated in order to achieve a smooth controlled docking. The team tested the system on zero g parabolic flights. The system was indeed capable of docking. However, residual magnetisation significantly affected the experiment.

Like the ARReST and the OAAN project, the system is fully reliable on magnetic forces for angular alignment and has no latching mechanisms. But a differential of this project is the utilisation of four electromagnets on the chaser, allowing for finer control. This concept could be implemented on other connectors.

2.0.2.6 CPOD

Tyvak Nano-Satellite Systems, a California company, is leading the development of the CubeSat Proximity Operations Demonstration (CPOD)((BOWEN *et al.*, 2015)) (BOWEN *et al.*, 2015)(BOWEN; VILLA; WILLIAMS, 2015). As the name suggests, the mission is a demonstrator, for the rendezvous and docking capabilities of the developed system. Two identical 3U satellites will be released as a 6U units and break apart. After that, they shall carefully maneuver and dock.

The cubesats are equipped with an ADCS capable of $< 0.15°$ in estimation accuracy; resulting from two star trackers fused with IMU data; and $< 0.25°$ in attitude control; from three reaction wheels and three magnetorquers.

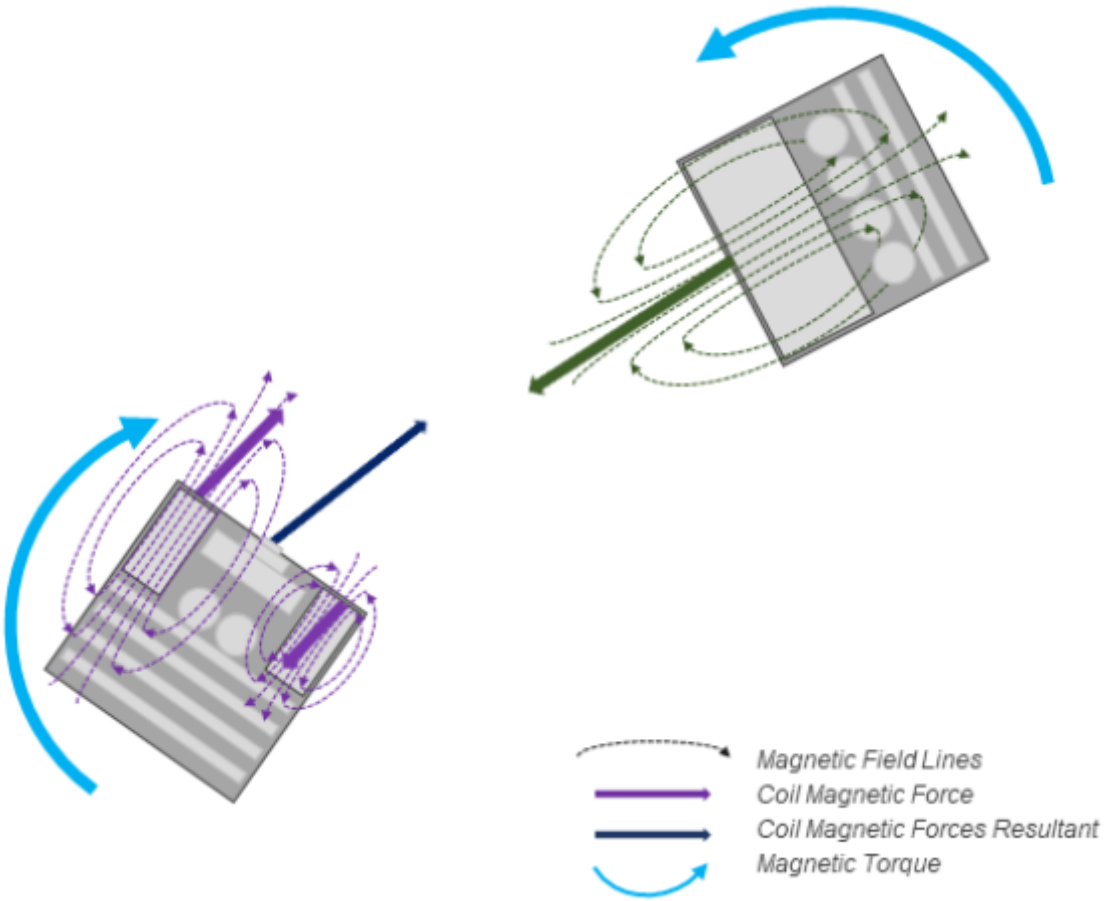

Figure 14 – PACMAN artistic representation of the chaser and the target cubesats maneuvering into each other and their magnetic lines created from the electromagnets.

There are four cameras for tracking (narrow field of view visible, wide field of view docking visible, wide field of view IR, and narrow field of view IR) (Fig. 15). A 3D model of the cubesats is stored on board, that is used for calculating each others pose using images on the visible range and thermal reflectivity. Using the OpenCV [4] platform the system is able to compensate for a number of aberrations on the imaging system like Sun glint, Earth albedo effects, etc. As the spacecrafts get closer, LEDs on the mating surfaces are used as fiducials.

[4] https://opencv.org/

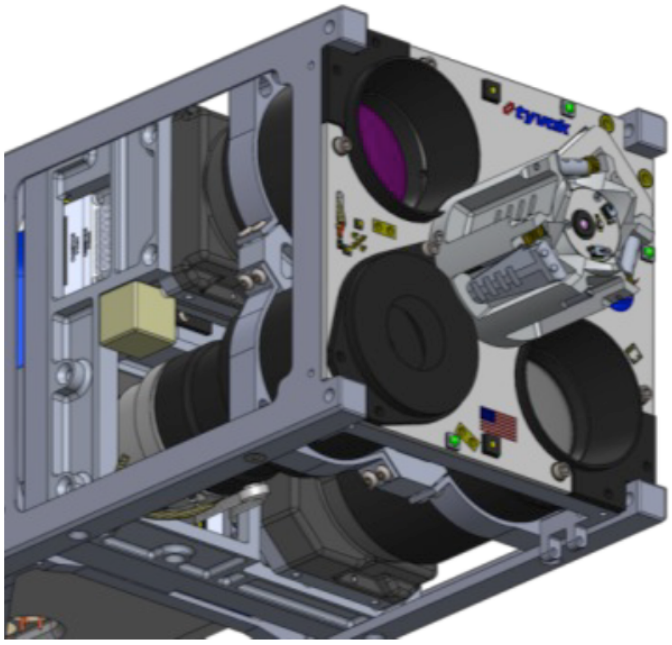

Figure 15 – CPOD matting surface with the docking port, fiducial LED's and alignment cameras.

The docking connector is androgynous. Three actuated fingers are deployed at the right moment to latch at the correspondent grooves at the other connector (Fig. 16). Electromagnets are used for the final 0.5m of approximation. Very little information is available other than that it was successfully tested at an air-bearing table(BOWEN; VILLA; WILLIAMS, 2015) and a quick description on page 102 at the final project presentation at ESA's NEBULA platform.[5]

The launch date was postpone multiple times, from 2015 to 2017 and now, according to NASA, the beginning of 2021[6]. In the meantime, the mission NANOACE, from the same company, was able to succeed in 2017, according to the company's website [7]. That mission tested the "Rendezvous and Proximity Operations (RPO) capability" of the satellite.

2.0.2.7 Electromagnetic Docking

((RAVINDRAN; VANCE; THANGAVELAUTHAM, 2020)) Is a quick paper that describes a purely electromagnetic docking system and focuses on the modeling, controlling and simulation of the system. The work is recent (2020) and very little information is available about the construction of the connector itself. Simulations and an air table experiment showed good initial results. The controller algorithms described can offer useful insights.

[5] https://nebula.esa.int/sites/default/files/neb_study/1261/C4000116866FP.pdf
[6] https://www.nasa.gov/directorates/spacetech/small_spacecraft/cpod_project.html
[7] https://www.tyvak.eu/missions/

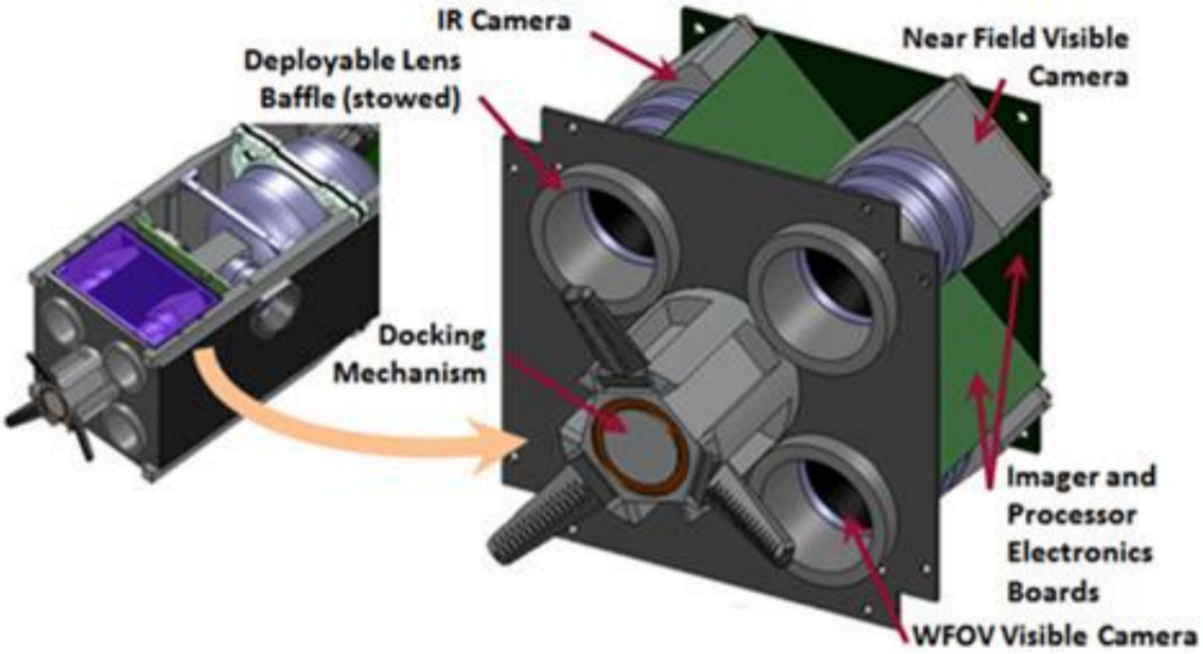

Figure 16 – CPOD connector with the latching mechanism ready for docking.

Figure 17 – NANOACE satelite.

2.0.2.8 ASDS

The Michigan Aerospace Corporation (MAC) developed a novel tether based connector mechanism called, Autonomous Satellite Docking System (ASDS)(RIVERA; MOTAGHEDI; HAYS, 2005) (HAYS *et al.*, 2004a), it allows for big alignment error margins between the satellites and provides a solid mechanical connection. Like on Fig.19, the mechanism is gendered, a cable comes out of the cone and is inserted into the drogue. After

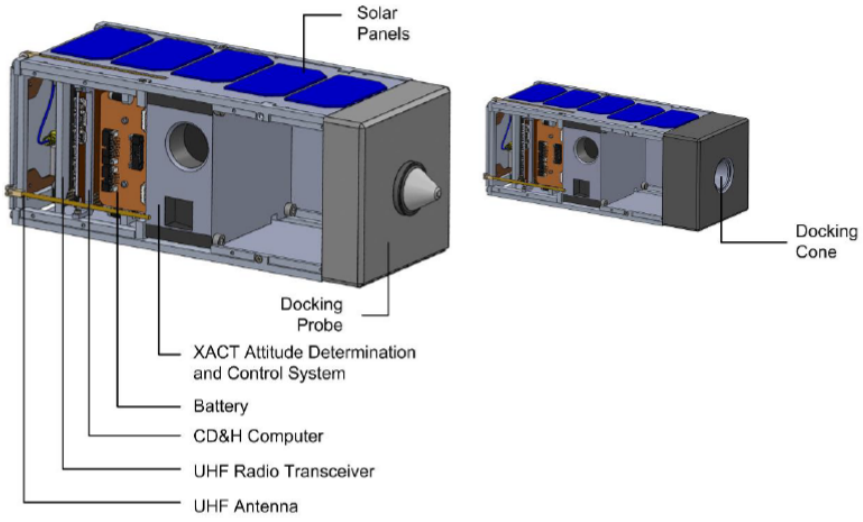

Figure 18 – Artistic representation of the simple proposed electromagnetic connector.

that soft connection, a latching mechanism then captures the cable and pulls it, allowing for the matting surfaces to make contact. The system was simulated on a Multibody Dynamics Simulation program (Adams [8]) and the results where calibrated on a air-bearing table(HAYS *et al.*, 2003) (HAYS *et al.*, 2004b). It was then successfully tested on a "zero g" parabolic flight with.

[8] https://www.mscsoftware.com/product/adams

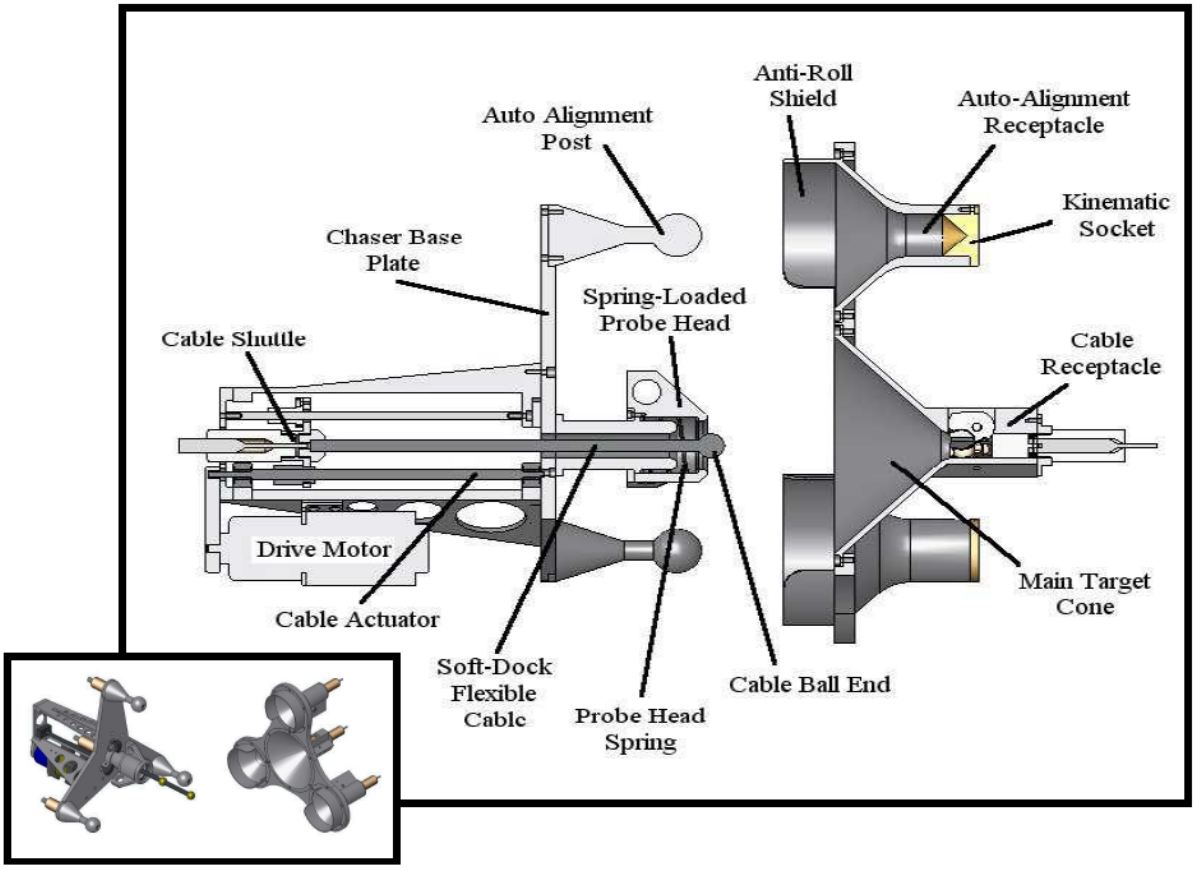

Figure 19 – Artistic representation of the docking connector from the Michigan Aerospace Corporation.

There are no electrical connections on this system. The three Kinematic Sockets; like on the ARReST project; allow for good and reliable alignment, and the latching mechanism gives good mechanical strength without permanent power consumption. It is the connector that allows for a large misalignment, due to the compliant nature of the system itself. It is also a complex connector and not very compact to be used in a cubesat. There is no information available in regards to the possibility of on-orbit testing. It is also worth mentioning that the mechanism is patented under the code US6742745B2 and US7104505B2. There are other tethered satellite missions, like STARS(NOHMI, 2009) for instance, but their goals and mechanisms fall out of the scope of this report.

2.0.2.9 RACE

RACE[9] stands for Rendezvous Autonomous CubeSats Experiment and it was commissioned by the European Space Agency (ESA). The goal is to have two 6U cubesats; currently being developed by GOMspace, with the assistance of GMV (for guidance), Micos (for the navigation camera) and Almatech (for the docking mechanism); docking

[9] https://gomspace.com/race.aspx

on-orbit. The development stated in 2019 and unfortunately, there is very little information available. Little can be done other than speculating over an artistic rendering at Fig.20.

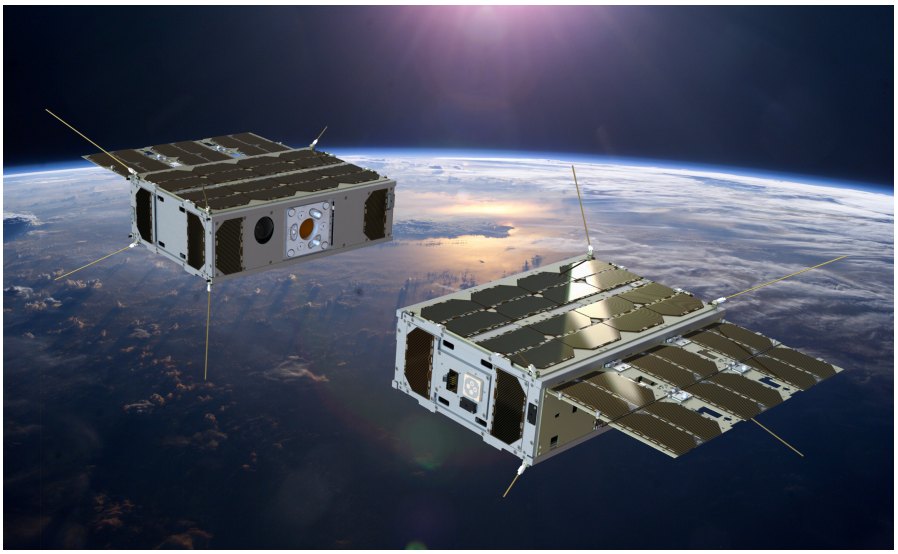

Figure 20 – Artistic representation of the RACE project.

2.0.2.10 TED-sat

Tethered Electromagnetic Docking is an unusual type of docking connector, researched by yet another team from the Padova University(OLIVIERI *et al.*, 2017). This system employs a tethered projectile that is launched by the chaser cubesat. The target cubesat is equipped with an electromagnet that steers and captures the object. The chaser then retracts the tether and soft docking is performed. The system is in its preliminary stages, the main concepts and mathematical model of the electromagnetic forces was tested successfully at the ZARM Drop Tower in Bremen. The main advantages of this docking system is the loose requirements for alignment between the two spacecrafts. Due to the novelty and the relative bulkiness of the system as a whole, there were no further investigations about the concept in this report.

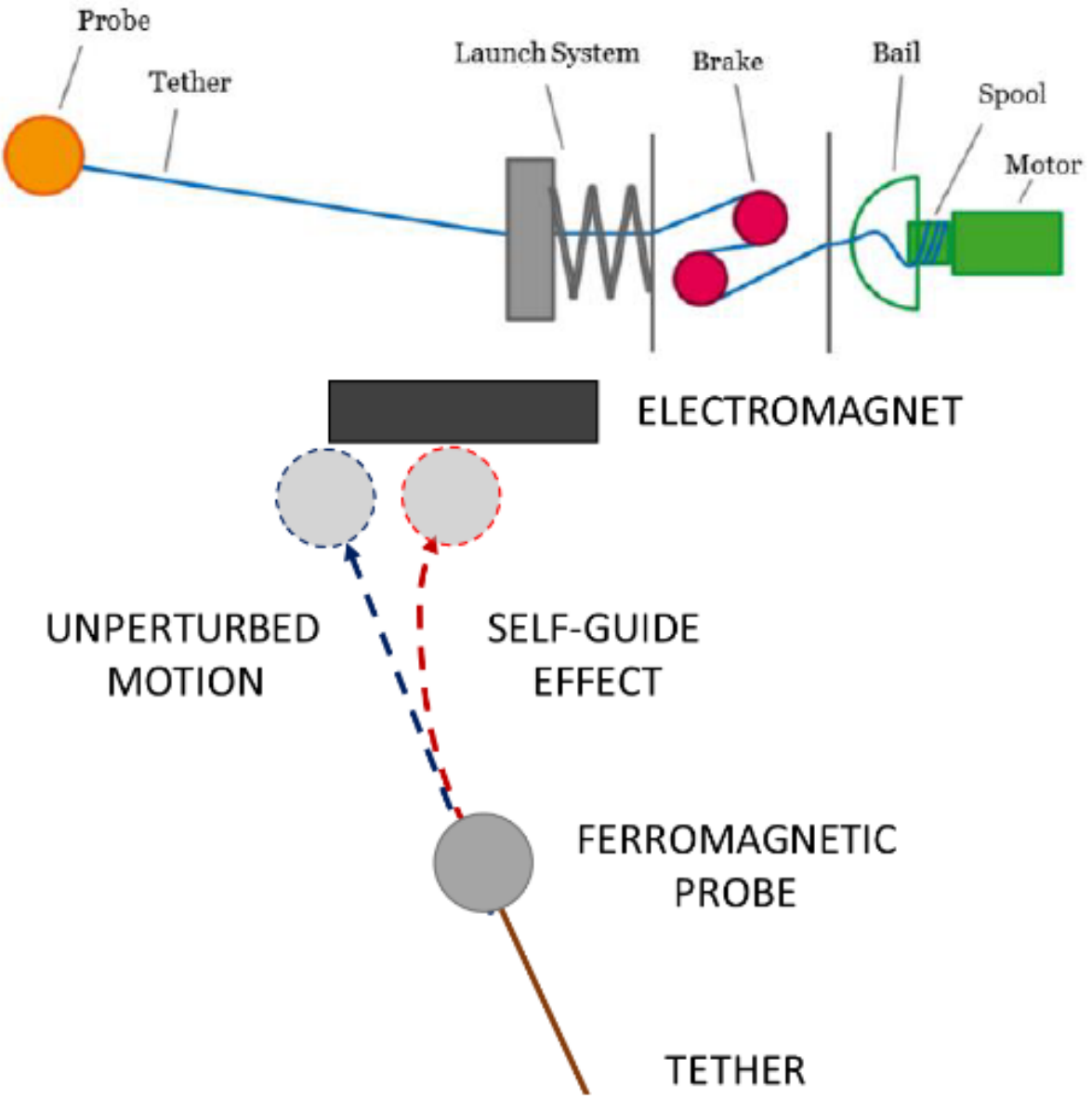

Figure 21 – TED-sat firing, brake and retrieve mechanism on the top. Magnetic directioning of the fired projectile into the target.

2.0.2.11 SIROM

This project started in 2016 with the EU H2020 Strategic Research Cluster (SRC) in Space Robotics Technologies. It was an ESA public funded program that aimed to develop 6 key technologies that allow and standardize robotic space exploration[10], it's developments was made open source. The Standard Interface for Robotic Manipulation of Payloads in Future Space Missions[11](SIROM) was the fifth operational grant (OG) and, as the name suggests, was responsible for developing a standard connector to be used between two payloads or between manipulators and payload. The connector is androgynous and

[10] https://www.h2020-infuse.eu/src/
[11] http://www.h2020-sirom.eu/

capable of transmitting mechanical, electrical and thermal loads; it is not optimized for nanosatellites, but it could be miniaturized. Fig.22 shows the connector itself, notice that the purple hooks are made to latch with the purple pockets.(BRINKMANNA,) describes the design requirements.

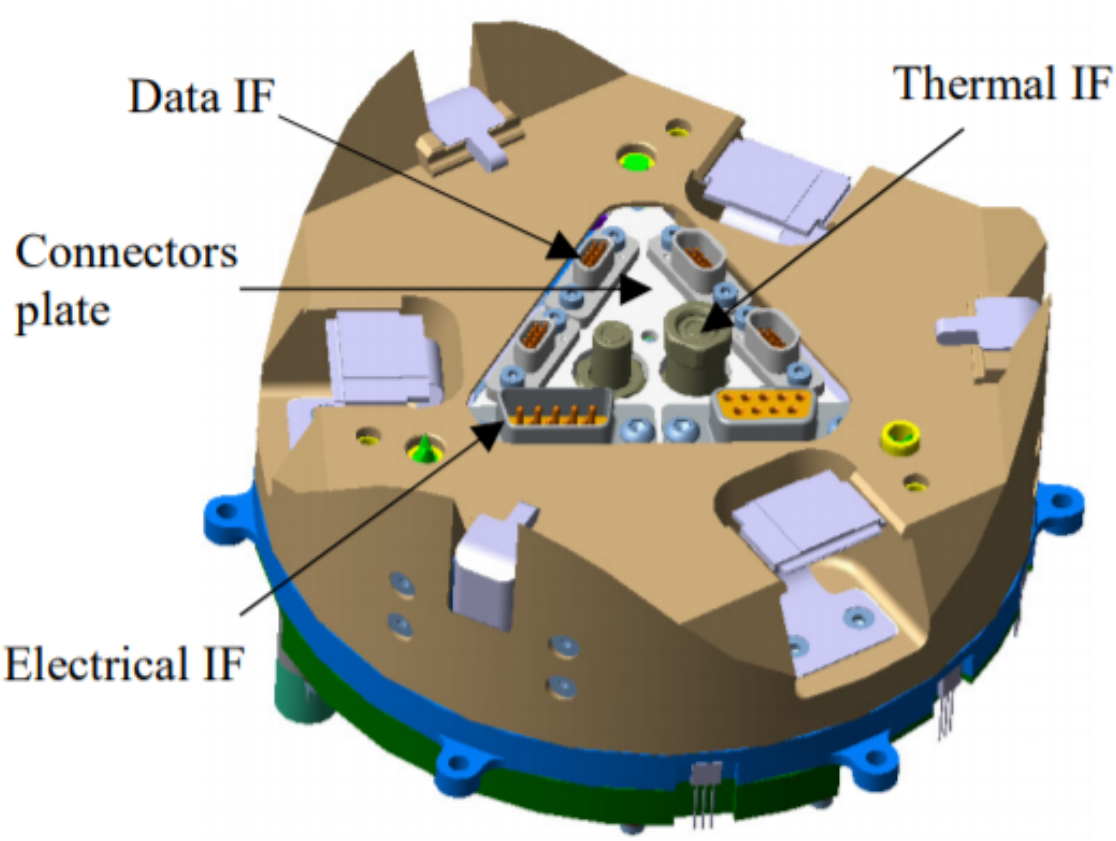

Figure 22 – SIROM connector artistic representation. Purple parts at the edge composing the latching mechanism. Multiple different connectors at the center. Waved edge for roll alignment.

The idea is that the connectors are going to be guided by manipulators. A crucial aspect underlined is the waveform at the edge of the connector. The team estimates that the last 5cm before making contact will be guided only by position and force feedback from the manipulator, given the field of view and focal length of the camera. This edge format ensures the correct docking even with minor misalignments. The angular tolerance for connection is tight; only 1.5°; but the lateral tolerance is more reasonable at 10mm.

The connector is to be used mainly on-orbit and on rovers. Neither of those applications were implemented at the moment, but tests with robotic manipulators showed positive test results. For relative position measurement at laboratory test, ArUco markers were utilized as fiducials in conjunction with RGB cameras, it served to prove the concept but it would probably not serve as a final solution. The program was deemed successful

(STANDARD. . . ,) and the resulting design is publicly available[12].

2.0.2.12 HotDock

Space Application Services[13] is currently selling an interface based on the SIROM connector and trying to improve on its weakness highlighted in Fig.23. The figure is taken from the research at project PULSAR(ROGNANT *et al.*, 2019), which is within the scope of the e Space Robotics Technologies Strategic Research Cluster (SRC) in Horizon 2020. The connector is called HotDock, and it was chosen to be part of three of ESA's H2020 developments (OG8 PULSAR, OG9 MOSAR and OG11 PRO-ACT) and to NASA's "T-REX" mission(HOTDOCK. . . , a). Like SIROM, the connector is not optimised for cubesats and would need to be miniaturized.

Characteristic	HOTDOCK	SIROM	IBOSS
Envelope Dimension (not including electronics)	156mm / 130mm ⌀ 65mm height	120mm ⌀ 75mm	120mm (220mm with thermal) ⌀ 50mm
Mass	1.2kg	1 kg (without electronic)	0.8kg (2.5kg with thermal)
Androgynous Design	X	X	X
90deg Symmetry	X		X
Allowing Diagonal Engagement	X		X
Position Finding by Form-Fit	X		
Locking Support by Form-Fit	X	X	
Sealing	X		
Can force passive side to dock/undock	X (Full)	X (elec)	X (mech)
Docking sequence duration	< 30 sec	[8 min, 2.6 min] c.f. motor control	< 30 sec
Load Transfer Axial (no SM)	20.000N (Theoretical)	1600 N (simulation)	6.000N
Load Transfer Radial (no SM)	TBC	TBC	[90-300]N
Load Transfer Moment (no SM)	1.500Nm (Theoretical)	50Nm (simulation)	360Nm
Power Transfer	[1kW] @ 100V	120W @ 100V	2.5kW
Data Transfer	Ethernet/TTE/SpaceWire, CAN	SpW/CAN	Ethernet/CAN
Thermal Transfer	Thermal tube (design)	Thermal tube	Thermal plate

Figure 23 – Table comparing features from three types of connectors studied: HOTDOCK, SIROM and IBOSS.

The company offers three types of connectors:active, passive and mechanical; including or not the latching mechanism, thermal transfer or electrical connections. This extra flexibility allows for the client to choose the best options for its requirements considering weight and complexity. HotDock has a high misalignment tolerance of 15mm and 10°, possible thanks to the edge format of the connector, a modified version of the SIROM wave. The latching mechanism is a patented rotating one, that uses one BLDC motor with gear reduction and complex mechanisms to actuate the whole system. The

[12] https://cordis.europa.eu/project/id/730035/results
[13] https://www.spaceapplications.com/products/hotdock

connectors include a novelty that is the use of hall effect sensors, in conjunction with permanent magnets, to allow the close alignment of the connectors. Is a simple and cheap way of doing so, and works from a very close distance until contact, which is usually dead band for camera based sensors. For the electrical connection, 48 POGO pins are used for their misalignment and dust tolerance. They are positioned in a 90° symmetry, like the connector itself (Fig.24).

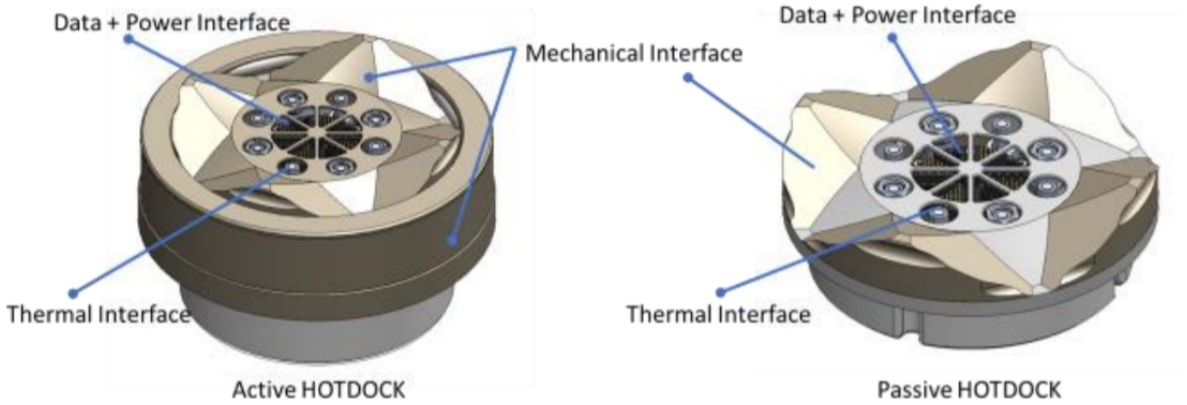

Figure 24 – HOTDOCK connector. Different type of latching mechanism and one extra crest at the edge (allowing for 90deg symmetry) in relation with the SIROM connector it was based on.

The connector was tested with a robotic arm[14] and were planned to be implemented in a number of different missions in 2021. It is almost an ideal connector as it fulfills all the requirements highlighted in section 3.1. but the need of miniaturization, for cubesat applications, still remains. It is idealized to be used with manipulators for alignment and insertion, as can be seen at the service manual (HOTDOCK. . . , b).

2.0.2.13 ASSIST

The ASSIST program is an ESA initiative (MEDINA *et al.*, 2017). It is formed by a conglomerate of companies; GMV,MOOG, NTUA, DLR, OHB, TAS; and the main goal is to offer on-orbit servicing. The program's goals are not precisely in line with this report scope, but it's mentioning is relevant nevertheless given the possibility of miniaturisation and adaption of the connector. The refuelling capability of this connector was stressed, but is also capable of providing data and electrical power connection. The drogue will be positioned on a larger satellite, and the docking procedure will be soft (also called zero force capture), once one of the requirements is not to alter the orientation of the client satellite. It is also intended for the servicing satellite to have a robotic manipulator to aid on the docking procedure.

[14] https://spacewatch.global/2019/10/spaceapps-hotdock-takes-centre-stage-at-iac-2019/

As seen on Fig.25, the connector consists of alignment pins, fluid coupling, electrical connector and a pantograph. The latter is able to expand once penetrated the drogue and generate tension forces. The electrical connector is a typical DB9. The tolerances for misalignments is clearly not high, but that is accounted for by the presence of the robotic arm and the higher capabilities of bigger satellites.

For the close proximity attitude estimation (< 5km), the system uses LIDAR and retro reflectors, due to their relative immunity to light variation. Cameras are added to the probe and 2D markers are used on the drogue for better alignment. Kinematics and dynamics simulations were performed using the GNCDE[15] (Guidance Navigation and Control Development Environment) simulator. They were then confirmed by air-bearing table tests. The system was also supposedly tested on vacuum, but there are no more details about it.

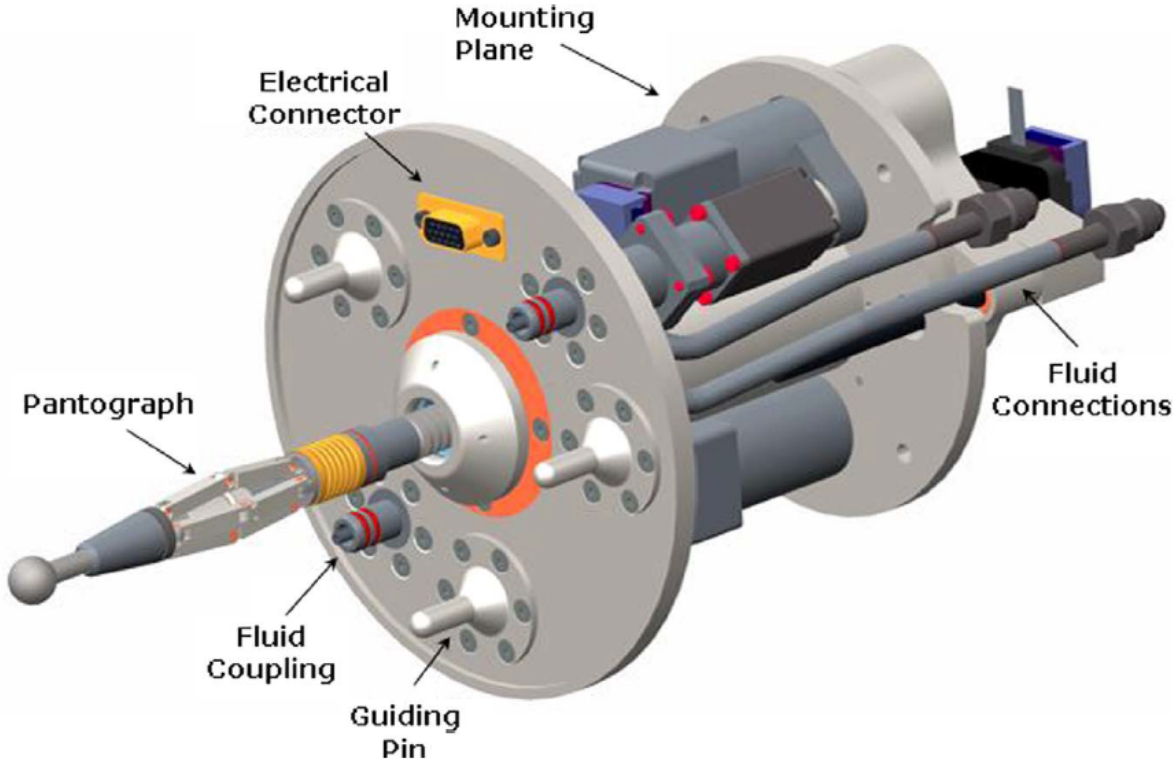

Figure 25 – ASSIST connector artistic representation. Retracted pantograph on the middle, alignment pins and connector at the edge.

2.0.2.14 ARCADE

The goal of the Autonomous Rendezvous Control and Docking Experiment (ARCADE)(BARBETTA *et al.*, 2015)(BOESSO; FRANCESCONI, 2013) was to be a demonstrator for attitude determination, control and docking technologies. The experiment was

[15] https://www.gmv.com/en/Products/gncde/

not analogous to an on-orbit environment, for it was performed on a stratospheric balloon (BEXUS 17) on a testing rig, with one transnational and one rotational DOF(Fig.26). Nevertheless, the technology developed by the Italian team is well designed and documented, and it should be easily adaptable to micro-gravity conditions.

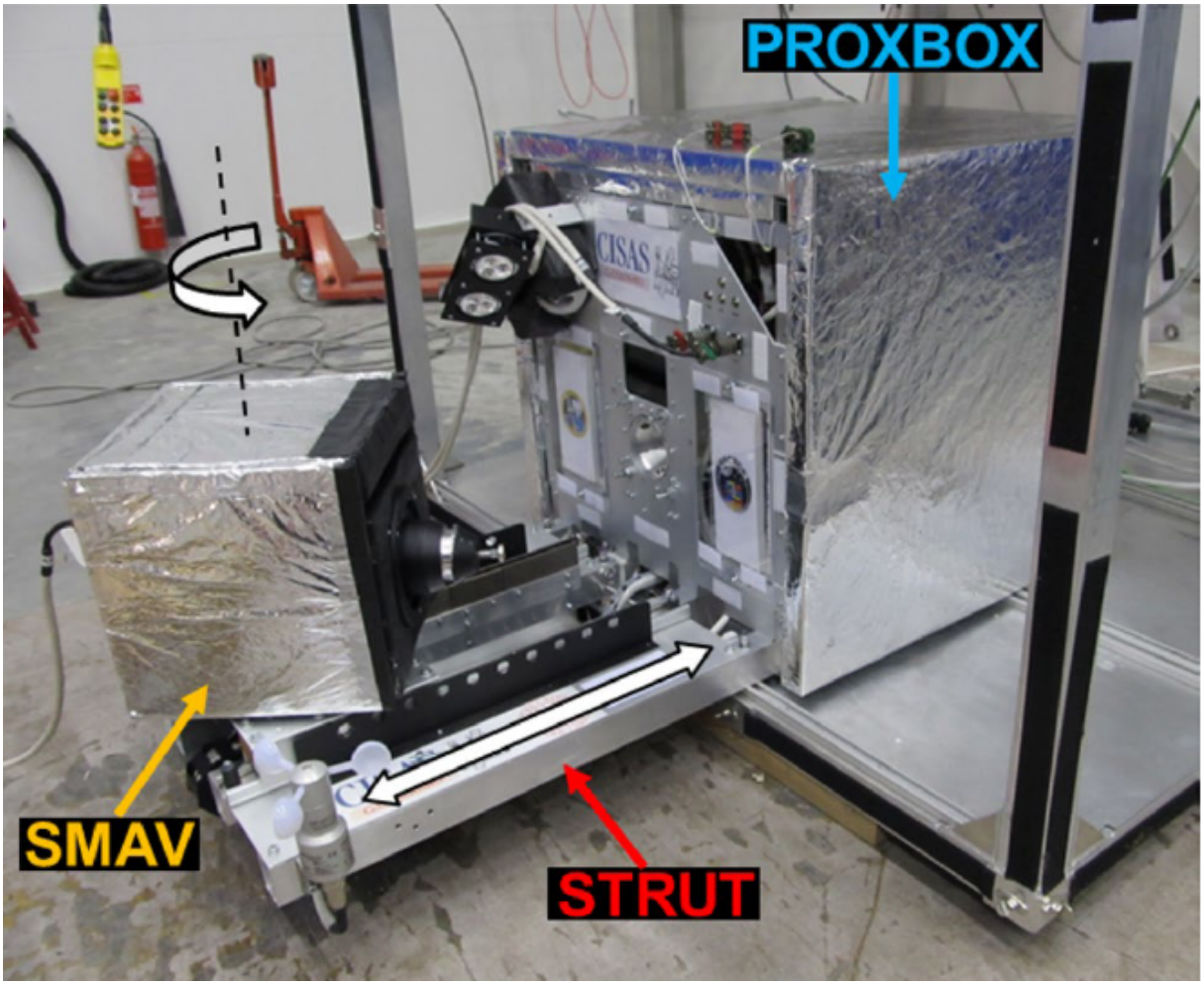

Figure 26 – ARCADE test rig, the white arrows represents the DOFs of the system.

The connector developed is an aluminium probe/drogue type (Fig.27). It is a center symmetrical design, containing three locking, normally closed, solenoids mounted on the drogue and one big matching groove on the probe. Micro switches and optocouplers are used to judge a successful docking. It is also a soft docking system, once the spring mounted magnetic tip of the probe is captures by the drogue and pulled inwards by a small linear actuator. The mechanical matting forces are dealt with by the solenoids and a spring loaded disc on the base of the connector.

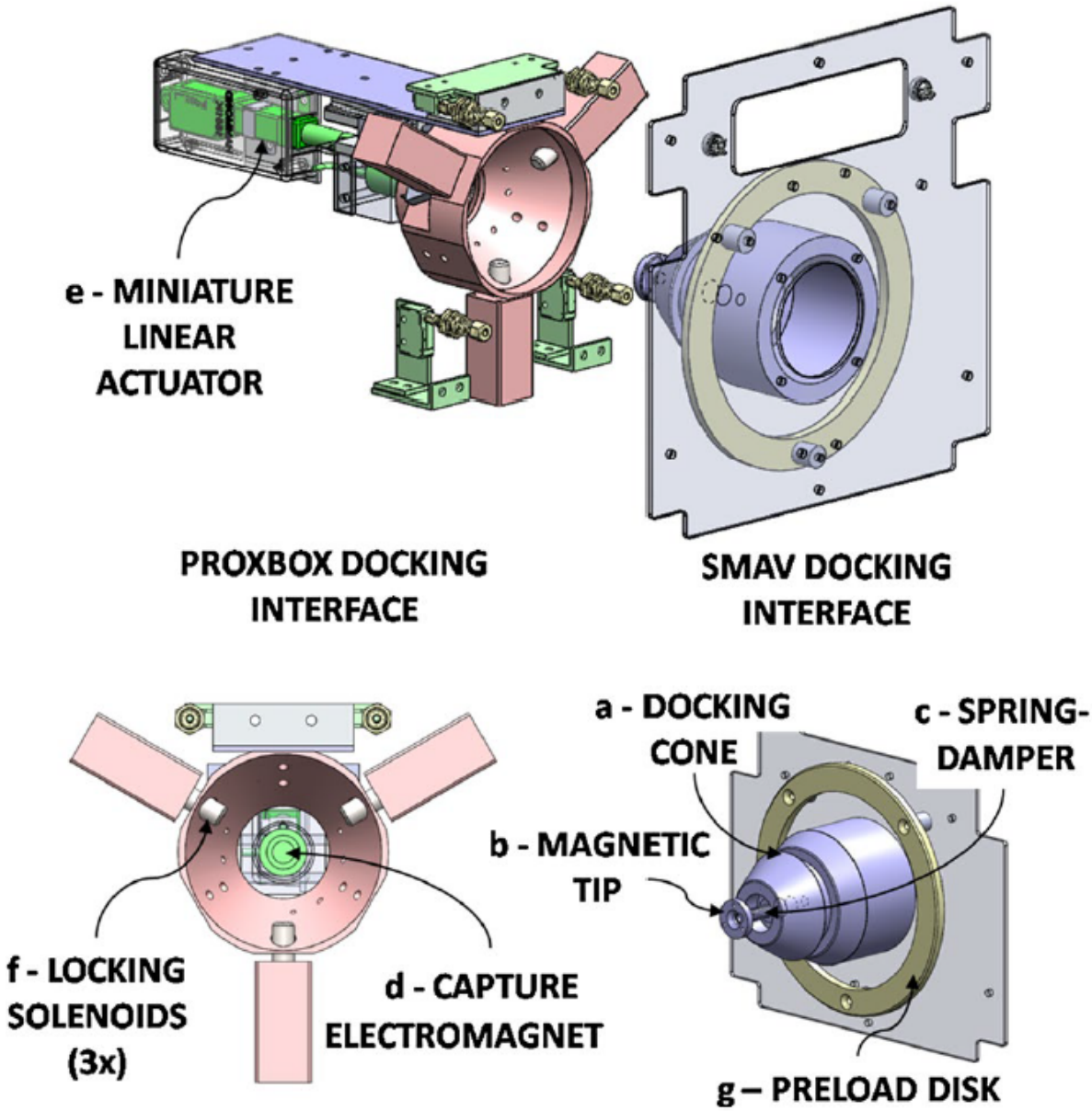

Figure 27 – ARCADE probe/drogue connector highlighting each major component of the system.

Given that the connector was developed having cubesats and also small aerial vehicles in mind, it was given great attention to the minimum and maximum relative velocities between the two spacecrafts in order to have a successful connection. Multi-body dynamic analysis and later on experimental testing, showed that these values ranged from 50 to 100mm/s. in regards to misalignment, it was confirmed to be tolerable up to 5°. One significant difference in this project is the sensing, which is composed of traditional magnetic sensors and gyroscope MEMS but also an Infrared (IR) system. This attitude estimation was determined to have an accuracy of 5mm and 1.5° of average error, It should be however be considered the limited conditions of the experiment as an on-orbit analogy.

Some elements of the connector presented might not be the best fit for a cubesat. One of the requirements of the design was to offer a pushing force when undocking, this is desirable for an aircraft system, but in a on-orbit environment it would result in difficulties controlling the spacecraft. The latching mechanism itself does not consider the rotational forces along the probe/drogue rotational axis, it was not a problem considering the restrained experiment, but it would be for a satellite. Finally, the internal parts of the mechanism, like the solenoids and linear motor are quite bulky and rearrangements would have to take place for a cubesat implementation.

These problems can be addressed. The spring loaded disk can be removed, avoiding the unwanted forces. Matching indentations and chamfers to the probe/drogue can be added, avoiding undesired rotational movements. The solenoids can be reoriented with the help of a simple bell crank mechanism.

2.0.2.15 IBOSS

The idea behind the Intelligent Building Blocks for On-Orbit Satellite Servicing ((KORTMAN *et al.*, 2015)) is to develop a modular system. There will be a big central core (Fig.29); with the propellant tank; and many additional building blocks around providing essential functions, such as solar panels, ADCS, etc. The modules will be moved and connected via a robotic manipulator. For this to work, it is necessary a highly capable connector, able to deal with electrical power, data, and heat transfer, as well as being mechanically sturdy. It was then developed the Intelligent Space System Interface (ISSI) for such purposes.

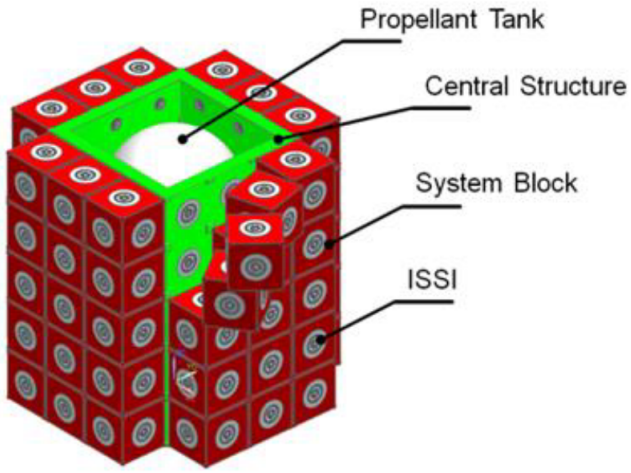

Figure 28 – IBOSS artistic representation of the proposed architecture with the core component and the many additional modules.

The connector is androgynous and retractable, so it won't stick out the surface and avoid difficulties on transport and delivery. Data is transmitted optically between modules

(with a trans-receiver at the center of the connector) and electrical power is transmitted via two concentric spring supported copper rings. The current prototype is 160mm in diameter and would have to be reduced by approximately 60% to fit into a 3U cubesat, which should be possible considering the symmetrical scalable design.

The latching sliding cam mechanism is very complex comparable to other solutions. After the mating surfaces are in touch, alignment pins are extended and penetrate into the chamfered alignment holes. After that, retractable teeth are extended and rotated to latch the surfaces and promote pressure between then. It is mentioned that the connector should be designed to tolerate large misalignments(KORTMAN *et al.*, 2015), but no tests or simulations are available to demonstrate that ability. There is also no mention of any electro-magnetic alignment assistance. A video of the mechanism in action can be found on the official website[16]. It is one of the only connectors available for sale on this report at this moment, but there is no information available about on-orbit testing. The precise mechanism is described at the European Patent "PCT/EP2015/056923".

[16] https://www.iboss.space/

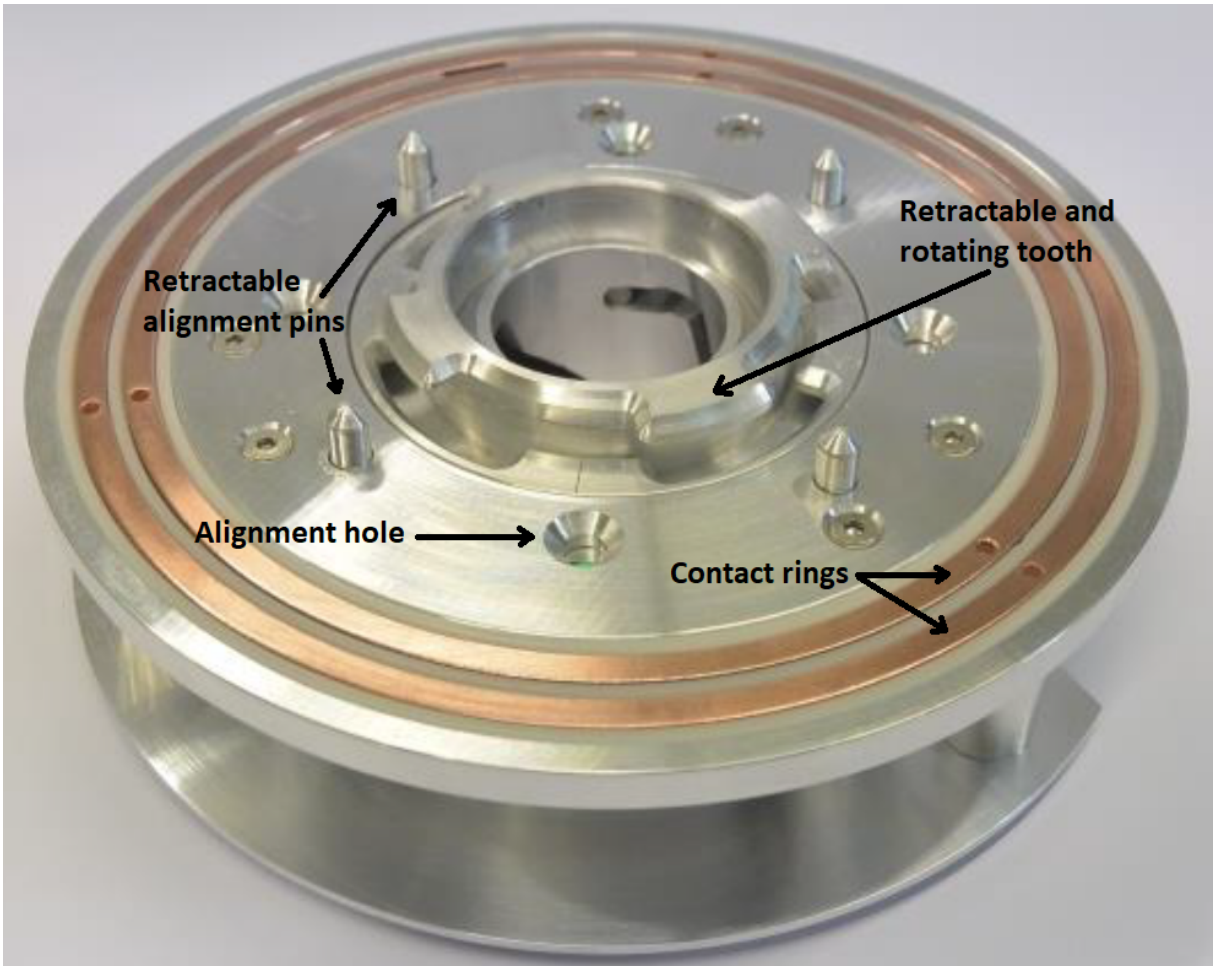

Figure 29 – IBOSS connector. Retractable rotating latching mechanism at the center, four retractable alignment pins and their hole on the side. Slip rings at the edge for electrical power transfer.

2.0.2.16 AUTOPORT

AUTOPORT is yet another student project from the Padova university. It was specially developed for UAVs planetary exploration, allowing for the transfer of data and electrical power. As stated by the group, it is a very simple and easily scalable probe/drogue system with radial latching (OLIVIERI *et al.*,) (Fig.30).

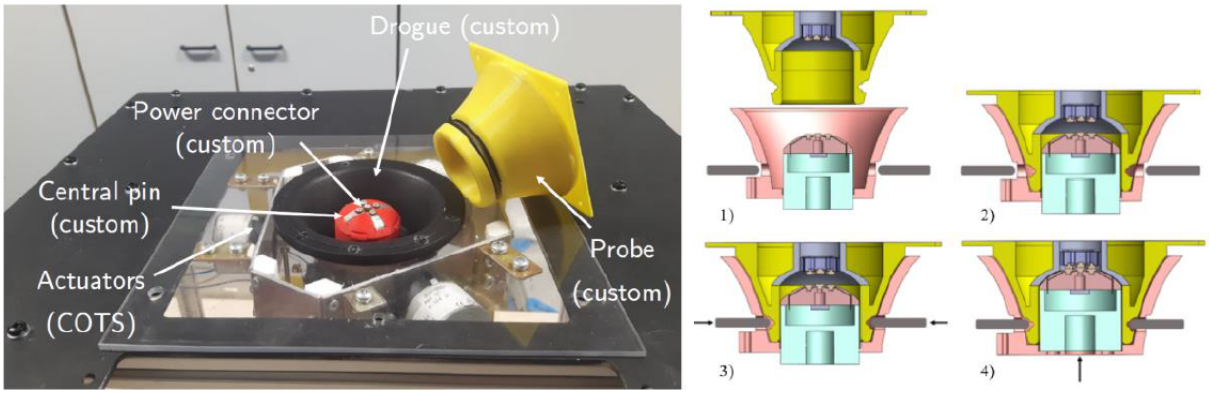

Figure 30 – AUTOPORT test rig on the left. Latching mechanism on the right.

An interesting element of this design is the hollow probe that aligns with the central pin (red part at Fig.30) and supposedly provides better linear and angular alignment. The connector does not present radial alignment constraints, so the 5 connections for transferring electrical power, on the top of the central pin, were made radially symmetric. Furthermore, a wireless power system was embedded balancing the individual batteries. The connections are made by contact rivets that requires an axial compression force of 43N. Data communication is done by wifi. The probe itself is completely passive. The system was prototyped with PLA in additive manufacturing, but is intended to be made in carbon fiber. FEM analysis was performed using the software ANSYS[17] to ensure it would withstand the necessary forces and practical experiments were devised to analyse the docking angles and displacements (Fig.31).

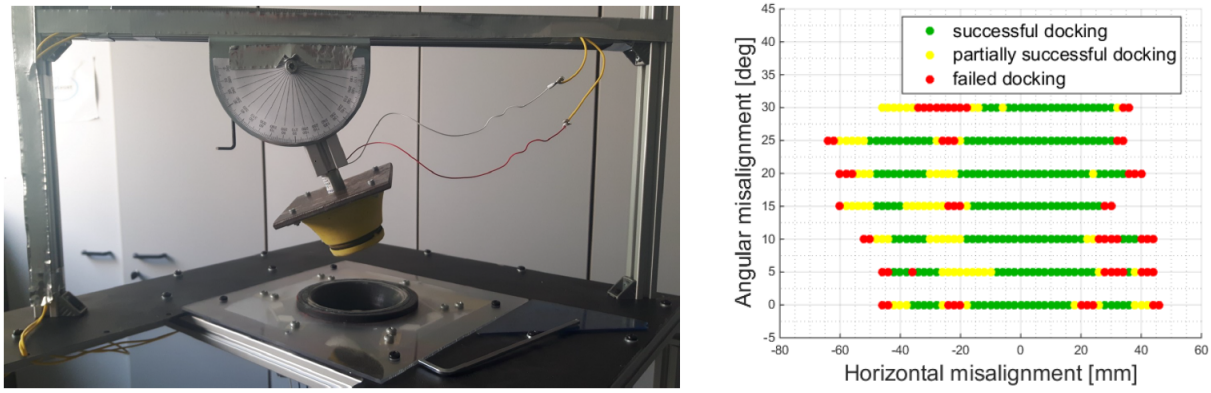

Figure 31 – AUTOPORT alignment test rig on the left. Test results on the right comparing linear and angular misalignment for successful docking.

The relative navigation sensing was based on visible LEDs and a small 2D RGB camera using (SANSONE *et al.*, 2015) as reference. They argued it is easier computationally

[17] https://www.ansys.com/

and less susceptible to noise.

2.0.2.17 TransTerrA

The electro-mechanical interface presented here(WENZEL; CORDES; KIRCHNER, 2015) is a connector made to transfer electric power, data, and high mechanical loads between different heterogeneous modules that shall be used for planetary surface exploration. The project as a hole is called TransTerrA[18] and the gendered connector is an improvement on the last developed connector, the RIMRES project[19] (DETTMANN *et al.*, 2011).

The connector contains 36 "pogo-pins" that are able to supply at least 10A of current and allow for Ethernet connection. It is made to be dust resistant, allowing for up to a 2mm layer, so it could be used for diverse planetary conditions. There is a central chamfered pin that, once inserted into the other connector, is pulled up by an active mechanism. The alignment and rotation constraint is made by four conical shaped pins(Fig.32). There are also ArUco markers at the edges of the passive connector and a mini camera at the active one. The two connectors are aligned using the markers and the final docking approximation is done "blindly" by the manipulator in charge of the movement.

The alignment tolerance of the connector is not bad, at ±5mm and 7°. The size is not optimized for cubesats, being 15x15cm, but could easily be miniaturized. The strong aspect of this connector is the extreme simplicity and apparent robustness. The latching mechanism is show in the detail at Fig.33

[18] https://robotik.dfki-bremen.de/en/research/projects/transterra.html
[19] https://robotik.dfki-bremen.de/en/research/projects/rimres.html

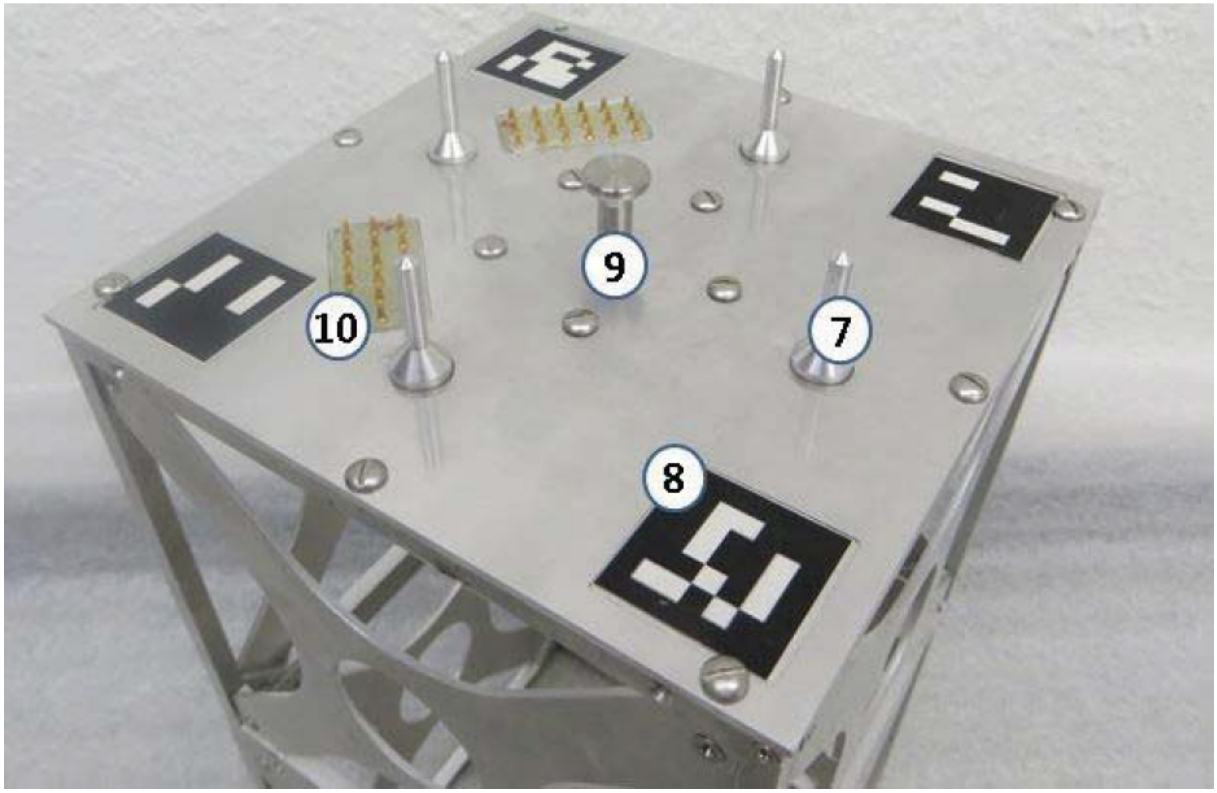

Figure 32 – TransTerrA connector. (9) chenfared pin, (10) electrical connections, (7) alignment pins, (8) ArUco markers.

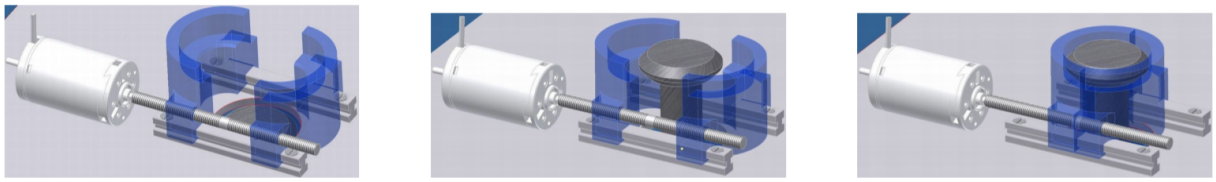

Figure 33 – TransTerrA connector latching mechanism sequence.

2.0.2.18 NASA Magnetic Capture Docking System

Not a lot of information is available on this connector. It was developed for the Mini AERCam program from NASA (FREDRICKSON *et al.*, 2003), a small free floating robot to be used for remote inspection. The connector is a type of probe/drogue mechanism with a lot of alignment tolerance (up to 6cm and 30°). The drogue is made to be attached to a much larger spacecraft and it has alignment teeth to lock the radial movement of the spacecrafts, it has a ball latching mechanism to ensure a rigid connection and the system relies on magnetic forces for the final approaching stage. Fig.34 shows the probe and the drogue. The system as a whole was tested on-orbit (NASA. . . ,) but no specific information about the connector is available.

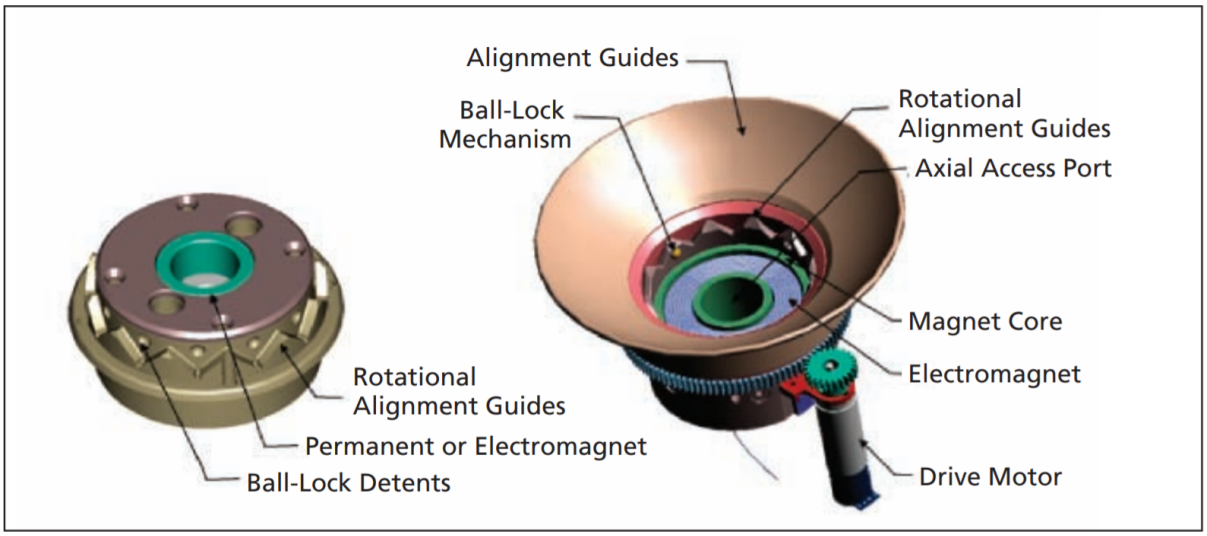

Figure 34 – NASA electromagnetic connector for miniature satellites artistic representation.

2.0.2.19 Semiandrogynous

The work performed by this University of Padova's team resulted in a shape shifting semiandrogynous connector, meaning it is able to actuate itself in order to become the drogue or the cone as in Fig.35. The current prototype is fitted to be used on a 6U or bigger cubesat, but can easily be scaled downwards (OLIVIERI; FRANCESCONI, 2016). The idea of using cam mechanism was also used on the IBOSS project, but here is a translational one instead of a rotating one. Although a clever mechanism, it is very complex and quite bulky. The misalignment tolerances are high (5° angular and 15mm laterally) but the resisting tensile force is very low (3N).

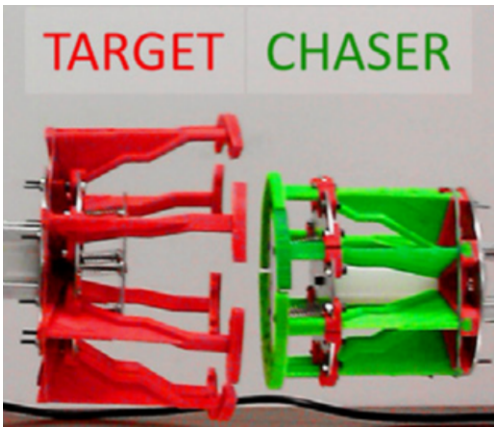

Figure 35 – Semiandrogynous connector in docking process. The chaser one on the left opening up for "grabbing" the target one on the right.

2.0.3 Rovers and Robot Connectors

Modular robotics is an area where multiple small semi autonomous (identical or not) parts are able to connect to each other, cooperate and perform multiple tasks that the individual would not be able to perform. It is clear to see that the connector here plays a vital role, and considering the small nature of most of those systems, integrating some of these concepts can be valuable to a space application(YAN *et al.*, 2018).

	Androgynous	Rigid connection	Mechanical	Latch type	Power	Data	Thermal	Redundancy	Marker	Angular orientation	No. of orientations
MTRAN				Magnetic	X	X				X	4
SINGO	X	X	X	Clamp				X		X	4
CAST		X	X	Hook						X	2
CEBOT			X	Hook					X		1
ATRON		X	X	Hook		X					1
Telecube	X			Magnetic	X	X		X		X	2
PolyBot	X	X	X	Rotational	X			X		X	4
AMAS		X	X	Hook				X		X	4
SMORES	X			Magnetic						X	2
GENFA	X	X	X	Rotational	X			X		X	4
ACOR			X	Hook	X			X			1
SWARM	X	X	X	Rotational	X			X			1
Phoenix Tool		X	X	Hook	X			X		X	1
Phoenix Satlet		X	X	Clamp	X	X		X		X	1
SSRMS LEE		X	X	Snare	X	X		X			1
DEXTRE (OTCM)		X	X	Clamp	X	X					1
iSSI	X		X	Rotational	X	X	X	X	X	X	4
EMI		X	X	Clamp	X	X		X	X	X	4
Berthing and Docking		X	X	Hook				X		X	∞
EM-Cube	X			Magnetic				X	X	X	2

Figure 36 – Compilation of connectors from modular robots

2.0.4 Connector's Actuation System

As previously discussed, there are many advantages to having your connector actuated. For instance, having no extra protuberances on the surface of the spacecraft so not to have to rely on the "extra space" on the cubesat dispenser and may even help in a misalignment situation. A multi-degree actuation system could be used to help orient the connector before docking. Even a single degree of freedom could result in a higher tolerance for misalignments. There are many ways of applying this actuation without the use of a full serial manipulator. For now, some possibilities are going to be presented. These possibilities can be combined, so to have, for example a retractable mechanism with a gimbal on top. The axis of rotation perpendicular to the mounting surface is the least significant one. When using traditional orthogonal reaction wheels for the ADCS, it is easy to act upon this axis with only one wheel. Furthermore, if the connector is positioned on the top surface of the cubesat, that represents the axis with less moment of inertia, thus more easily controlled by the ADCS. It is also important to notice that the mass of

the connector is not negligible compared to the cubesat, thus any acceleration on it will most likely have to be counteracted by the ADCS system.

2.0.4.1 Retractability

Fig.37 shows two connector types; they are represented as a probe/drogue connector but can be assumed of being of any kind. The left one (extended connector) has a connector that sticks out of the surface and the right one has a retractable connector. We are considering the situation where the lateral and angular alignment of the satellites is so big that the probe completely misses the drogue. The two spacecrafts are approaching as represented by the velocity vector and the contact point is marked in red. Fe and Fr are the forces acting on the system on the Center Of Mass (C.O.M.) of the satellites. These forces arise from the sudden deceleration of the bodies caused by the impact, and they create torque forces at the point of contact. De and Dr are the moment arms of these torques. It is clear to see that, while the retracted connector experiences a positive torque, the extended one experiences a negative torque. This means that the first will naturally be pushed into alignment while the letter will be pushed further away from alignment. We can see that as long as the force is projected on the x axes on a point left of the contact point, the torque will be positive, and the opposite is true. It is also easy to see that the retracted connector will always be favorable on these scenarios. The conclusion is that a retractable connector is more tolerant to big misalignments, and if a considerable magnetic force is present between the connectors, the system may even recover naturally from a failed docking situation.

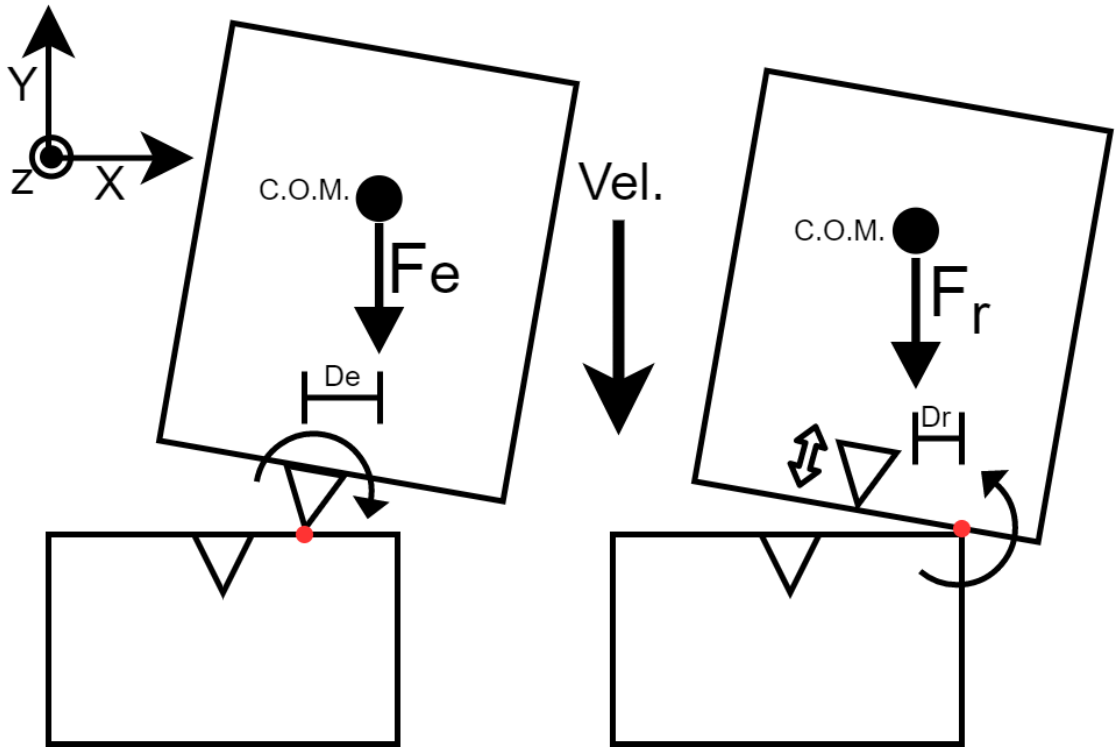

Figure 37 – Forces acting on docking of misaligned spacecrafts with and without retractable connectors

A simple and space efficient way of achieving this feature would be, for example, to use an external worm gear system to move the connector up and down. The motor could then be positioned outwards and in a compact manner.

2.0.4.2 Cartesian

A cartesian option would move the connector in purely translational matter, with the axis of movement orthogonal to each other. A 1 DOF system parallel to the surface (Fig. 38.a) would mostly make sense on a non-symmetrical connector. A 2 DOF system with the actuation plane parallel to the spacecraft surface (Fig. 38.b) could be useful on all types of connectors. Considering for instance Fig.8 (Padova Probe/drogue connector), clearly indicating the coupling between angular and lateral alignment. This is also relevant for systems where the final approximation is dependent on magnetic attraction (OAAN and AAReST projects). Which means that the requirements for translational and attitude control of the spacecraft can be reduced.

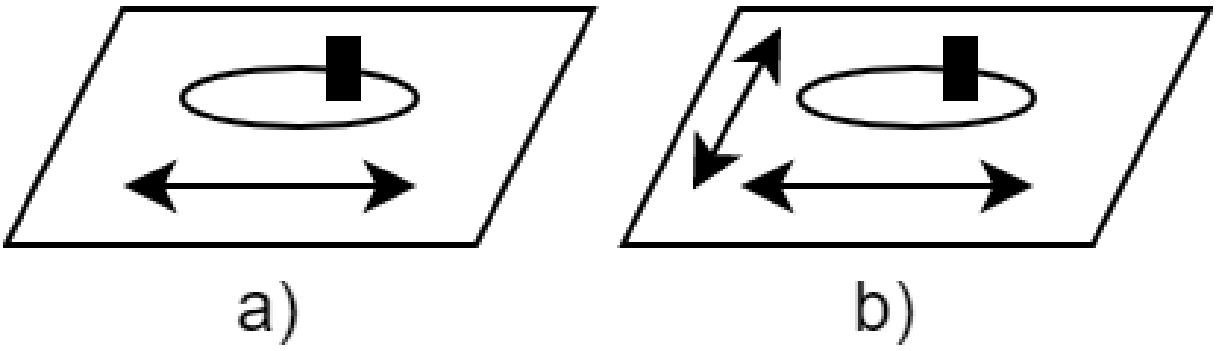

Figure 38 – Cartesian movement of a possible active docking connector.

2.0.4.3 Delta Robot

A delta robot is a category of parallel robots, which is defined as a closed kinematic chain. In particular, the delta robot allows for purely translational movements, just like a Cartesian would. A possible advantage of using this type of actuation is a simple mechanical convenience. On figure39 there is a drawing of a classical delta robot on the left and a simple illustration for a connector actuating mechanism on the right, where the parallelogram represents the top face of the cubesat. This configuration would allow for a retractable connector with extra two DOF parallel to the surface. An added advantage of parallel robots is the increased rigidity. Springs could be easily added on the linear rails to allow for shock absorption.

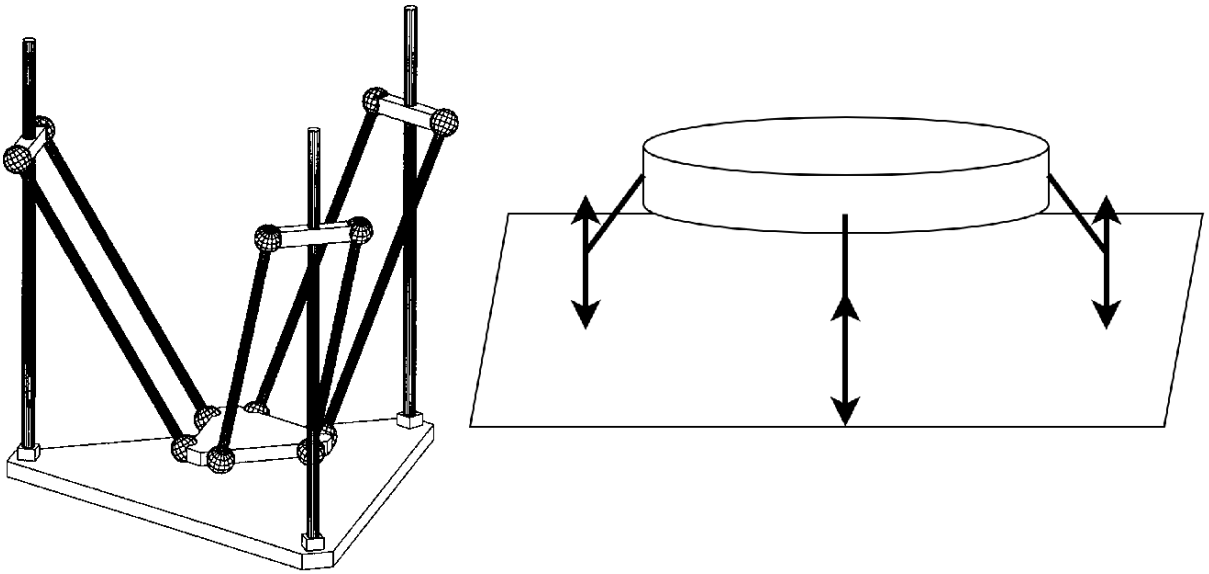

Figure 39 – Classical delta mechanism at the left and possible implementation for a cubesat connector at the right.

2.0.4.4 Zero Torsion Mechanism

A zero torsion mechanism is also considered a parallel, or closed chain mechanism. Like the delta, it is also popular in industry. The advantage of the zero torsion is that it provides 2 degrees of rotation and one degree of translation. For this application, it would result in the possibility of having a retractable connector that is also able to aid on angular alignment. Fig.40 highlight a few arrangement possibilities.

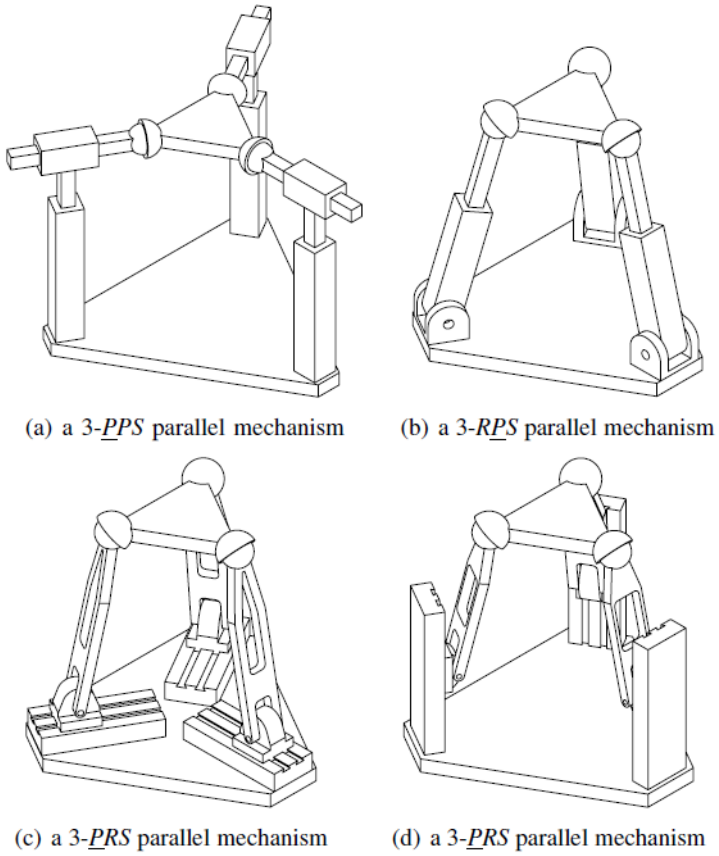

(a) a 3-*PPS* parallel mechanism (b) a 3-*RPS* parallel mechanism

(c) a 3-*PRS* parallel mechanism (d) a 3-*PRS* parallel mechanism

Figure 40 – Example of zero torsion mechanisms.

2.0.4.5 Gimbal Mechanism

A gimbal mechanism is a simple system that purely rotates a center piece, usually with 3DOF. It is possible to implement one to facilitate the alignment of the connectors. There is a common problem called gimbal lock, but it could easily be avoided by the simple fact that the amplitude of movement would probably be very limited.

3 CUBESAT MANIPULATION

A reliable manipulation system is recognized as a key technology for the future of space exploration. There is a lot of work that has been done for full sized satellites, including the famous CANADARM [1], currently working at the ISS.

For nano spacecrafts however, there are very little examples of on-orbit manipulation. Here, manipulation referees mainly to the addition of serial robotic manipulators, with relevant end-effector, capable of acting upon objects outside the body of the spacecraft it has been added to. Relevant end-effectors include: specialised or generic grippers, docking connectors, cameras, sensors, etc.

3.0.1 AMODS

The Autonomous Mobile On-orbit Diagnostic System (AMODS) project [2] is been developed by the United States Naval Academy. It is a complete system, including up to three assessment and repair (3U) cubesats called "RSats", and one (also 3U) "tug satellite" called BRICsat, responsible for transporting and maneuvering the RSats. The goal is for the complete system to be available for less than $300.000,00. This report will focus on the RSats, considering it is the one that has two manipulators integrated.

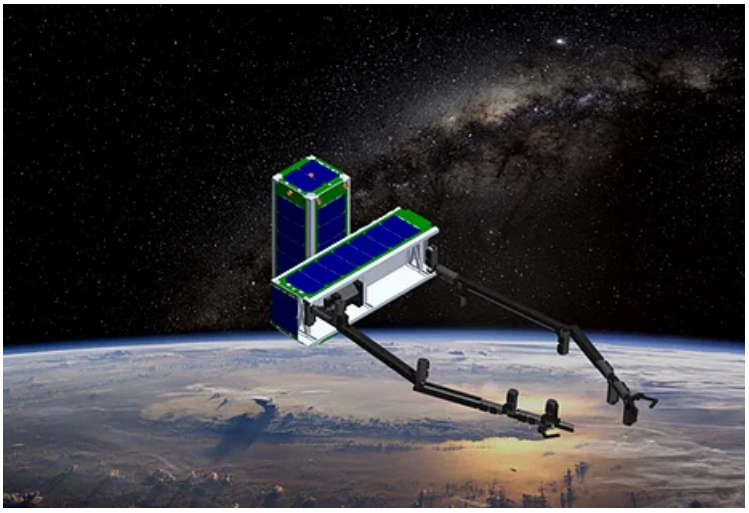

Figure 41 – Artistic representation of the AMODS mission. The cubesat in the vertical position represents the BRICsat, tugging to different orbits and maneuvering the RSat, which is equipped with two robotic arms. One BRICsat should be capable of tugging up to three RSats.

[1] https://www.asc-csa.gc.ca/eng/iss/canadarm2/canadarm-canadarm2-canadarm3-comparative-table.asp

[2] https://www.amods.org/

The developers envision two main possibilities: to preemptively embed one or more RSats into a big satellite and deploy it if necessary or to launch it and rendezvous it with a BRICsat in case of an anomaly (HANLON *et al.*, 2016)(HANLON, 2016).

Each arm is equipped with a commercial off-the-shelf (COTS) radio, camera, electrical power system (EPS), one micro controller for each joint and a couple of Arduino micro-controllers. This introduces cost savings and redundancy. The latter is given by the fact that these double subsystems are able to cross-talk and fill in the roll of a damaged part. Even the EPS is able to handle the two arms if necessary. Regarding mechanical construction, the joint actuators were chosen so that the end-effector has a 10mm accuracy and the links are connected directly to the motor shaft. Considering that each arm has seven degrees of freedom (DOF), this results in a tolerance of $\pm 0.25°$. The prototype was developed using additive manufacturing(HANLON *et al.*, 2017). The resulting design is two very compact 0.6m meters arms. They are held in place during launch with a fishing line (that is later burned) to avoid vibration stresses.(WENBERG *et al.*, 2016) (see Fig. 43)

During tugging, the arms move in a mirrored fashion, so their angular momentum cancels each other. It should also be noted that the arms of the RSat, whenever possible, are positioned on such a way to try to move the center of mass of the BRICSat/RSat system close to the geometric center of BRICSat (Fig.42), to optimise the propulsion system (that is only present at BRICSat).

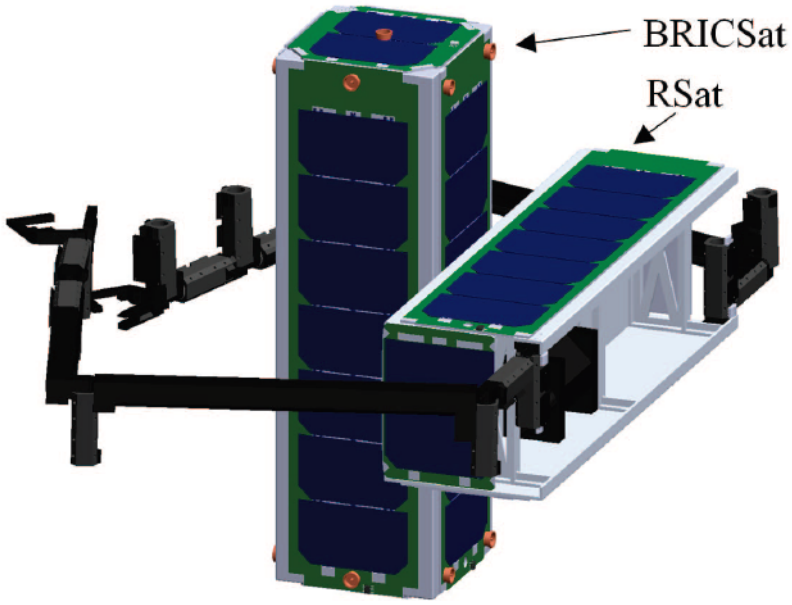

Figure 42 – BRICSat/RSat system with the two manipulators positioned in a way to bring the system's center of mass close to BRICSat's geometrical.

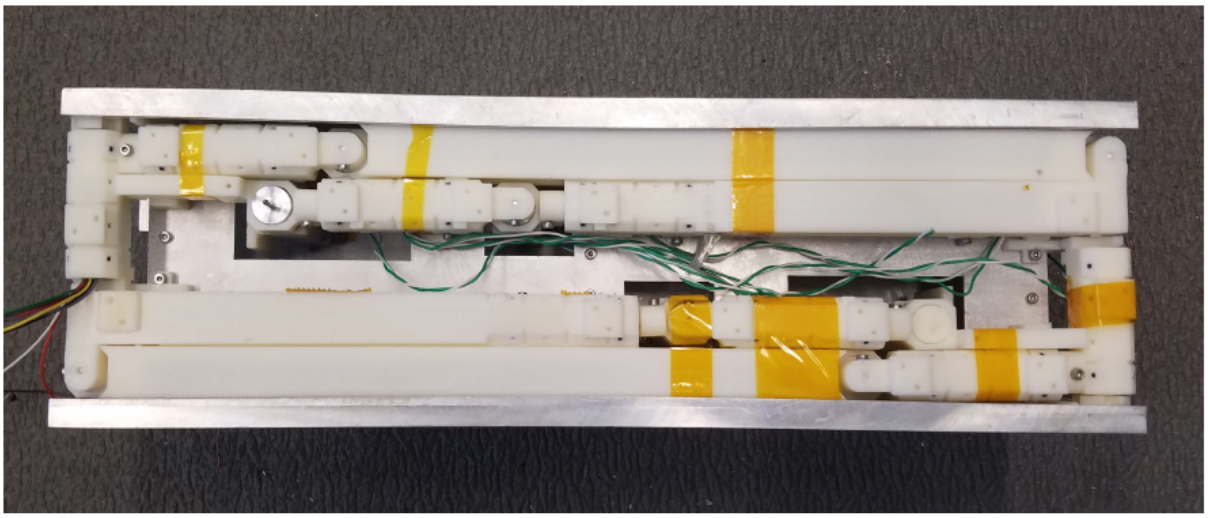

Figure 43 – RSat picture with its arms (white plastic) folded into the structure.

Furthermore, the RSat is completely dedicated to its manipulation capabilities, lacking any extra on-board instrumentation or ADCS capability. As we can see on Fig.44, most of the satellite's body volume is used for storing the arm and the rest is used for the electronics components. This is possible because the robot relies on the inertia of the heavy satellites it is intended to interact with.

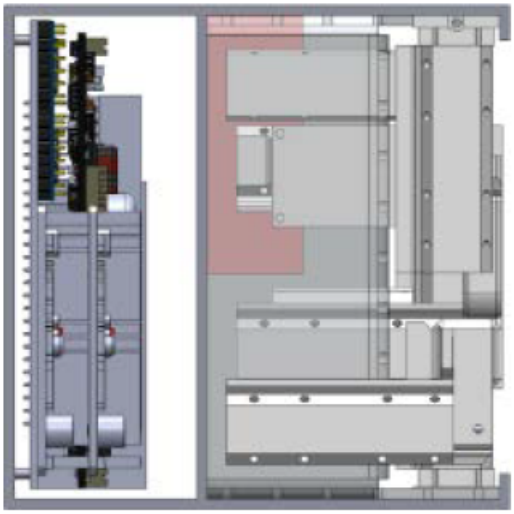

Figure 44 – At the left, we see the space reserved for the on-board electronics. At the right, the space filled with the folded robotic arm from an Rsat.

BRICSat is equipped with GPS and Star Tracking technology for long term navigation and with cameras and LIDAR (Light Detection And Ranging) for precisely positioning the RSats. The latter is equipped with one central camera at the satellite's body and one at the end of each arm. Furthermore, there is one laser diode on each end of the grippers for detecting the presence of an object between the fingers.

The development program was divided in three phases (HANLON *et al.*, 2016):

1. Phase one: Launch of a first BRICsat prototype (BRICsat-P) in may of 2015 and launch of a second improved prototype (BRICsat-D) in September 2016. The goal was to validate the propulsion system.

   The first part can be considered a success. BRICSat-P operated as expected (HANLON, 2016), but there is no official information available about the outcome of BRICSat-D (WENBERG *et al.*, 2017).

2. Phase two: Launch of the first RSat prototype (RSat-p) to validate the manipulator in 2017.

   Unfortunately, according to unofficial sources [3] the spacecraft lost contact with the control center after its deployment.

3. Phase three: 2018 launch of a fully operational BRICsat and three RSats to validate the whole system.

   The mission website[4] is not been kept up to date, and the author was not able to assess the current state of this phase by any other means.

The US Naval Academy letter re-branded the mission as Intelligent Space Assembly Robot (ISAR)(WENBERG *et al.*, 2018a). The project improved some of RSat's hardware adding 3D cameras, improving the processing power and modifying the arm construction(WENBERG *et al.*, 2018b) and also realizing some ground testing (WENBERG *et al.*, 2017). According to an unrelated source(JACKSON *et al.*, 2020), the mission was successful and the cubesat was capable of latching into a target spacecraft. The author of this report was not able to find official information sources confirming or denying the claim.

It could be possible to develop an even more compact system, by implementing small changes. There is at least a five year gap between the start of AMODS's development and many technologies have become more available and more developed. This means that it may be possible to develop a system that incorporates the BRICSat's features of navigation and attitude control and an RSat's like arm for inspection and manipulation. This would reduce the complexity, the cost and deployment time of the system. Here are some of the author's suggestions to improve on the design:

1. Implement higher grade material for the linkages, carbon fiber rods for example.

2. Save space on the electronics side by developing custom circuit boards, instead of soldering existing ones to each other.

[3] https://twitter.com/planet4589/status/1102595829808930817?s=20
[4] https://www.amods.org/

3. Avoid the usage of through-hole components, as they add bulk in relation with surface mounted devices (SMD).

4. Look for higher efficiency motors like Brushless DC (BLDC) instead of stepper ones.

5. Implement strain wave or cycloidal compact gearboxes if needed.

3.0.2 REMORA

REMORA is a system designed to avoid collisions of on orbit satellites and debris(MCCORMICK *et al.*, 2018). The goal is to develop a small (6 or 12U, Fig.45) cubesat equipped with a robotic arm, propulsion elements, ADCS and a variety of sensors. The spacecraft will use its manipulator to attach itself to a large satellites, serving as a GPS beacon for sub-meter accuracy tracking and use its own propulsion system to alter the craft's orbit if necessary. REMORA will attach into features like engine nozzles and other accessible points, the maneuver itself will be aided my ground control and be commanded to the spacecraft after a complete assessment of the target object. The project started its development in 2017 at NASA's Jet Propulsion Laboratory (JPL). The precision tracking, combined with the orbit maneuvering capabilities for decommissioned satellites and big debris should be a powers tool on avoiding dangerous on-orbit collision.

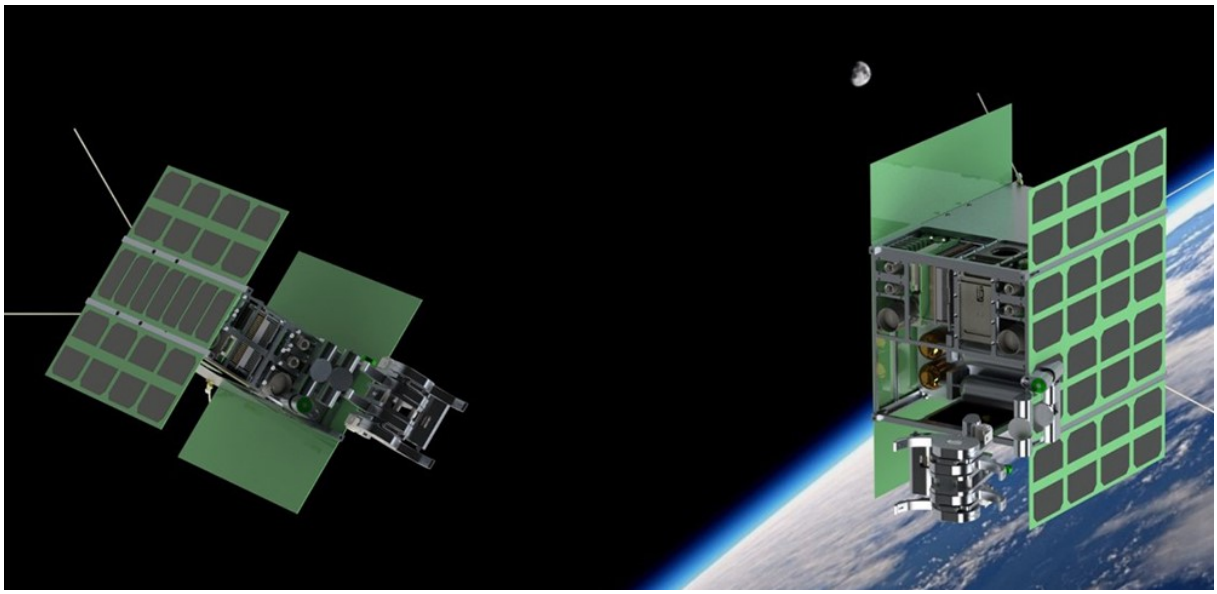

Figure 45 – Two possibilities of the REMORA spacecraft, 6U on the left and 12U, on the right.

The arm has five degrees of freedom, it reaches up to 0.4m considering the proposed end-effector and can be stowed into the volume of a 1U satellite (Fig.46). Faulhaber 1226012 12-mm BLDC motors were coupled with 1024:1 planetary gear reductions and a subsequent 5:3 gear train to increase the torque output of each joint. An analytical

analysis showed that a 1N force on the end-effector would result, in the worst case scenario, on a maximum torque of only 44% of a joint's stall torque. The structure is a hollow monocoque (presumably out of aluminium) design to save mass.

The total mass of the arm/end-effector subsystem is around 1.14kg and the expected accuracy is ±5mm. The configuration of the arm is Yaw-Roll-Yaw-Yaw-Yaw. Multiple end-effectors were proposed for different missions and a traditional 1DOF claw type prevailed.

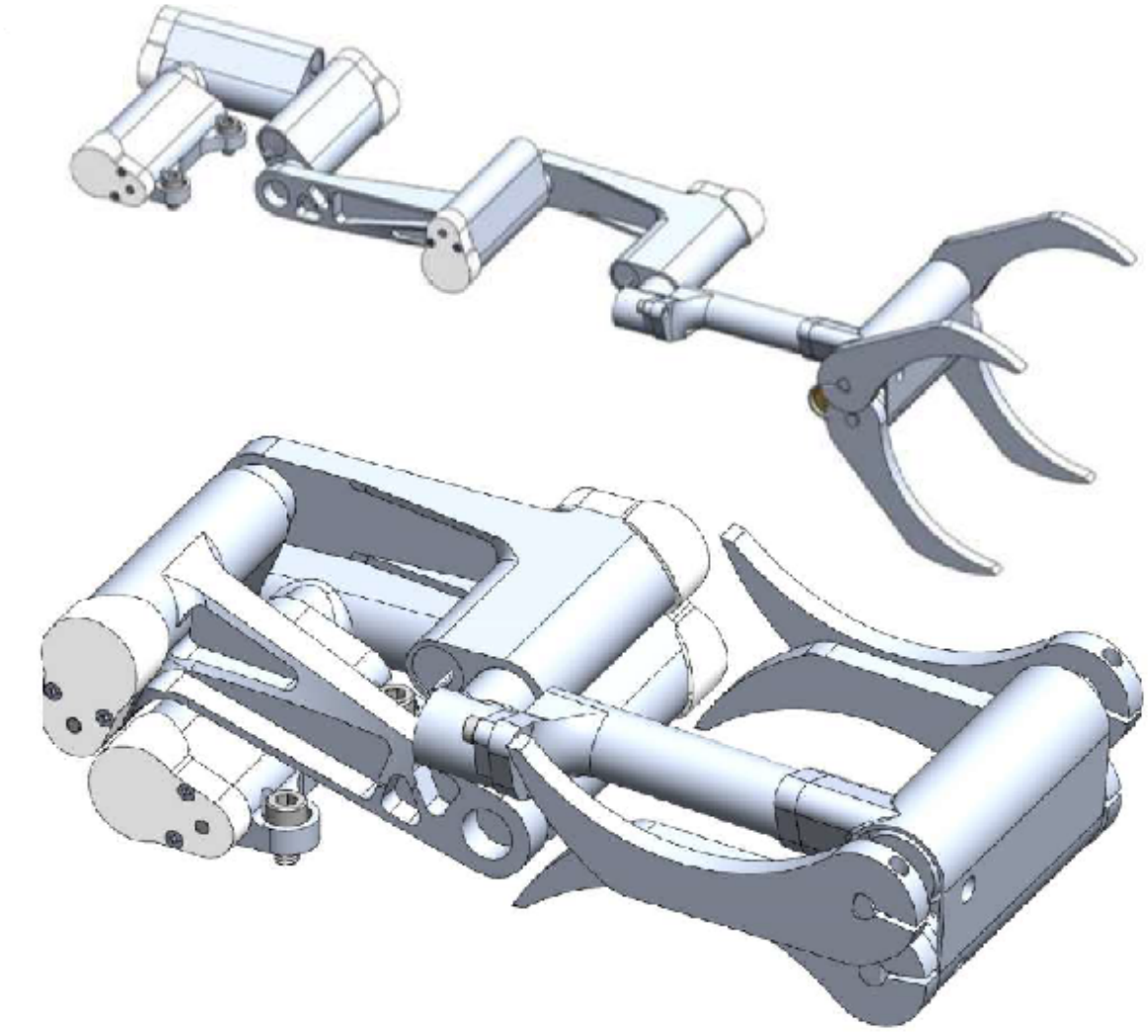

Figure 46 – REMORA manipulator on its extended configuration (top) and on its stowed configuration (bottom). The arm/end-effector stowed configuration results in a volume of 20x10x5cm.

Combining an ADCS and a propulsion system together with a robotic arm is a very

effective solution. The only disadvantage of the system proposed is the limited manipulator with 5 DOF, susceptible to singularities and limiting its dexterity. This would limit the scope of missions possible.

Figure 47 – REMORA manipulator prototype extended.)

3.0.2.1 C-FORM

JPL is developing this manipulator for 6U cubesats. The goal is to have two arms per cubesat and have docking connectors as end-effectors. Many of them can link up and form a satellite cluster via Cluster Forming On-board Robotic Manipulators (C-FORM). The many advantages of this is the extra DOFs the formation will have for pointing and attitude control and it allows the satellites to be more spaced than if docking without the manipulator arm (Fig.51).

The team investigated some use cases (Fig.48) and divided them into four categories that take advantage of using a manipulator in the formation: construction, positioning, reconfigurability and arm manipulation.

Construction	Positioning	Reconfigurability	Arm Manipulation
Synthetic aperture radar	Real-time data transmission	Large distributed array (adaptability to different missions)	Satellite inspection with camera
ISARA reflectarray	Large solar panel pointing	Sample transfer to and from ISS	Satellite repair
Optical mirror	Data relay for deep space communications	Replaceable parts to extend mission life	Satellite sabotage
Large Solar Sail	Data relay for far side of moon in L2 halo orbit	New payload modules to expand capabilities of larger satellites	Capture space debris
Altimeter	Interferometry	Steerable radar to cover large swaths	In-orbit assembly

Figure 48 – Different applications for C-FORM cubesat clusters based on the four main advantages of the manipulator usage: (MCCORMICK *et al.*, 2017)

The arm has 5 DOFs and a Yaw-Roll-Yaw-Yaw-Yaw configuration. It is able to be stowed into almost a 0.5U volume (10X10x5.4cm) and has a 43cm reach when unfolded. The reason it is able to be compact stowed is that it uses deployable telescopic links. They are kept under tension from an internal linear spring and a holding wire, when the arm unfolds itself from the spacecraft's body it burns the wire and releases the mechanism. The paper goes deeper into the details of mechanism itself (MCCORMICK *et al.*, 2017).

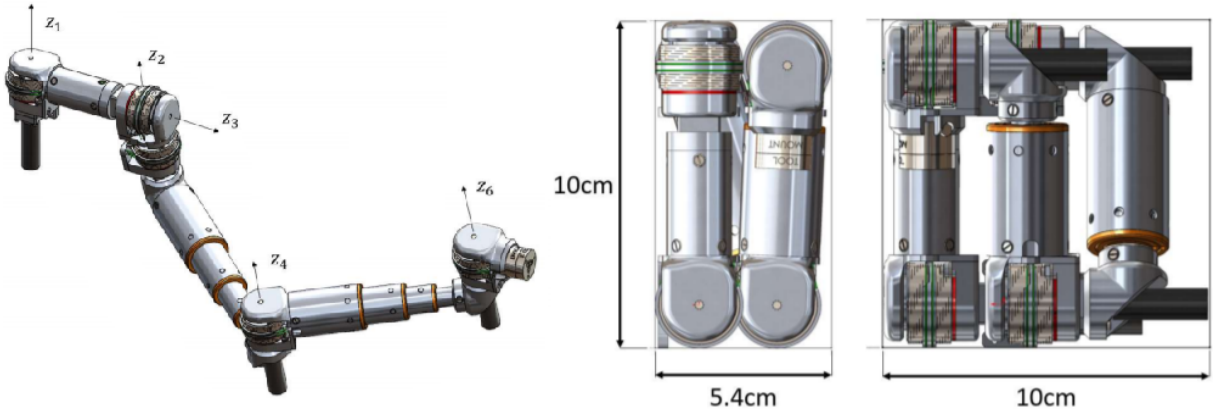

Figure 49 – Miniature arm with deployable telescopic links.

Once the team's goal was to use the linked arms for precise pointing, the accuracy of the end-effector was set by design at 1mm. This led to the use of strain wave (commercially known as harmonic gears) reducers, with virtually no backlash. Another measure to ensure the accuracy is on the feedback system. Due to their great robustness, it utilises resolvers for measuring the absolute angle of each joint. Magnetic encoders; without sensitive optics; are readily available nowadays and could be a valid and cheaper substitute. Another

requirement was the use of motors with NASA flight heritage, so they were constrained to use *Aeroflex 10-mm* stepper motors.

The team decided to add breaks on the joints, so to maximise the holding torque without powering the motor and to protect the gearbox from excessive loads. They decided to make their custom break out of nitinol "muscle wire", that is a shape-memory alloy (Fig.50 at the right). When current is passed through the wire it heats up and contracts, causing the joint to break. A possible alternative to the braking system would be to use more resilient non-backdrivable reductions, such as a worm or a cycloidal gear reduction.

The paper then describes the docking system. It is made to be attached at the end-effector of the arm, so it has to be exceptionally small. For the capturing, a fast mechanism was needed but the motor used on the joints is not powerful enough. To solve this issue, they implemented a small linear motor, actuated by the expanding force of heated paraffin. This strong, though slow, motor activates a spring mechanism that is released by the contact of the docking connector to its target(Fig.50 at the left).

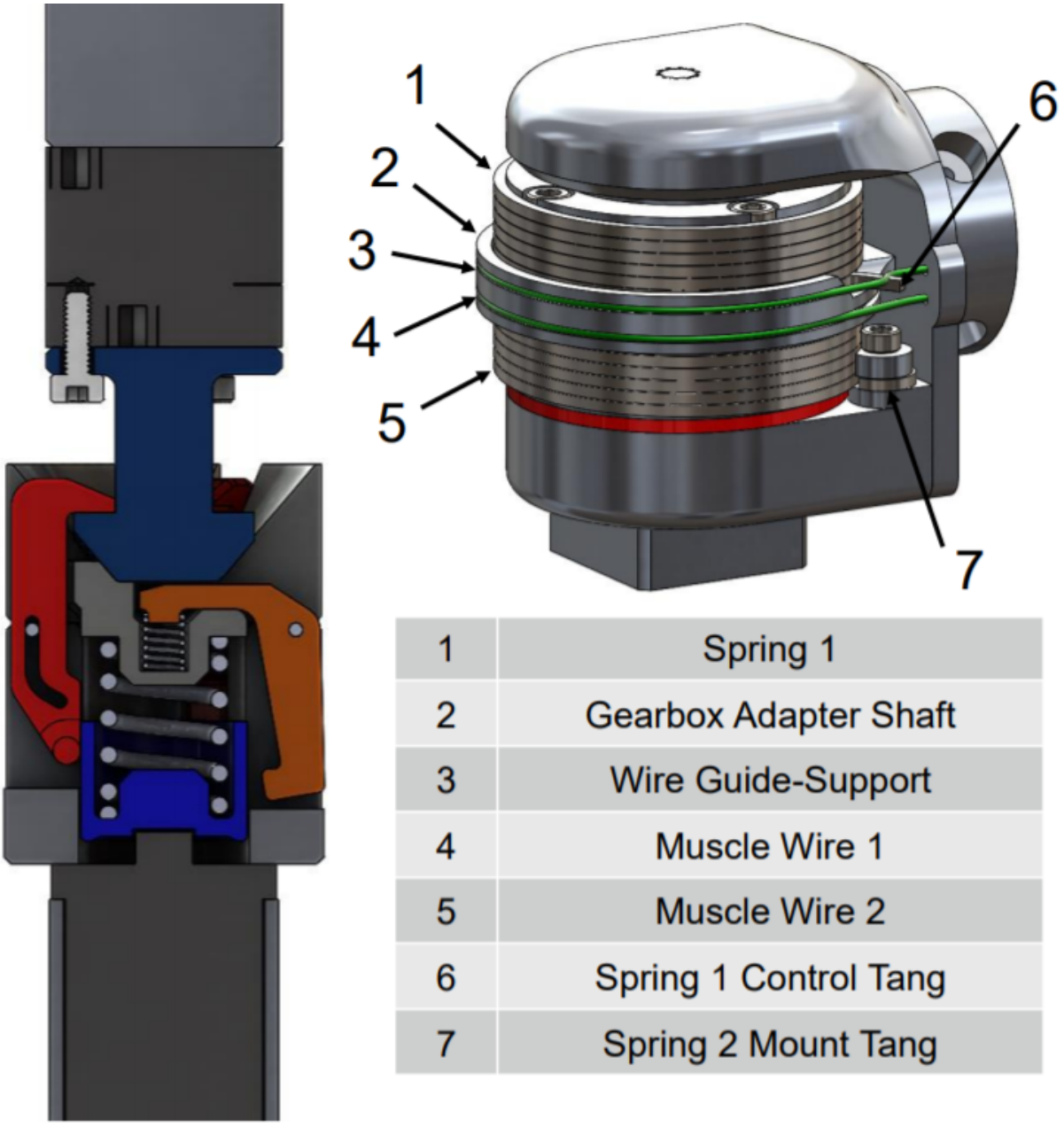

1	Spring 1
2	Gearbox Adapter Shaft
3	Wire Guide-Support
4	Muscle Wire 1
5	Muscle Wire 2
6	Spring 1 Control Tang
7	Spring 2 Mount Tang

Figure 50 – Docking mechanism on the left and breaking mechanism on the Right.

(MCCORMICK *et al.*, 2017) then creates an approximate model of the system to estimate the necessary orbiting maneuvers and the performance of the sensors. (DEVELOPMENT...,) explores in depth positioning and rendezvous control aspects of the mission.

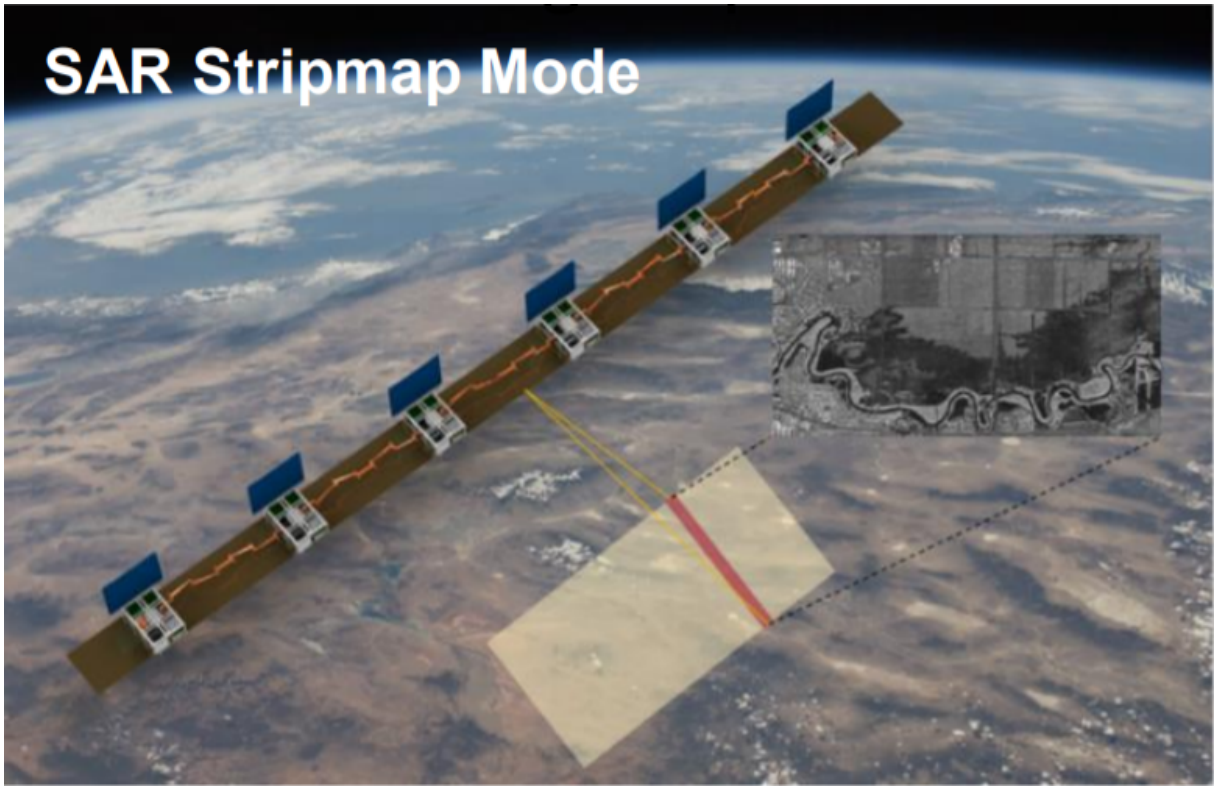

Figure 51 – Cubesats in formation flight (C-FORM) using manipulators for docking and alignment.

3.0.3 Micro satellites

Microsatellites are larger that cubesats, their mass goes from 10 to 100Kg. At this range, it is possible to identify more examples of rendezvous and manipulation. Even though the focus of this report is on nanosatellites, these bigger systems may be able to provide useful development insights.

3.0.3.1 KRAKEN

KRAKEN[5] is a project from *Thethers Unlimited* to develop a generic micro manipulator for LEO environment. The standard KRAKEN configuration is a 1 m, 7 degree-of-freedom arm that can stow in a 19x27x36cm volume (Fig.52). Not compact enough for a cubesat, but useful for microsats and internal use at the ISS.

[5] https://www.tethers.com/robotic-arm/

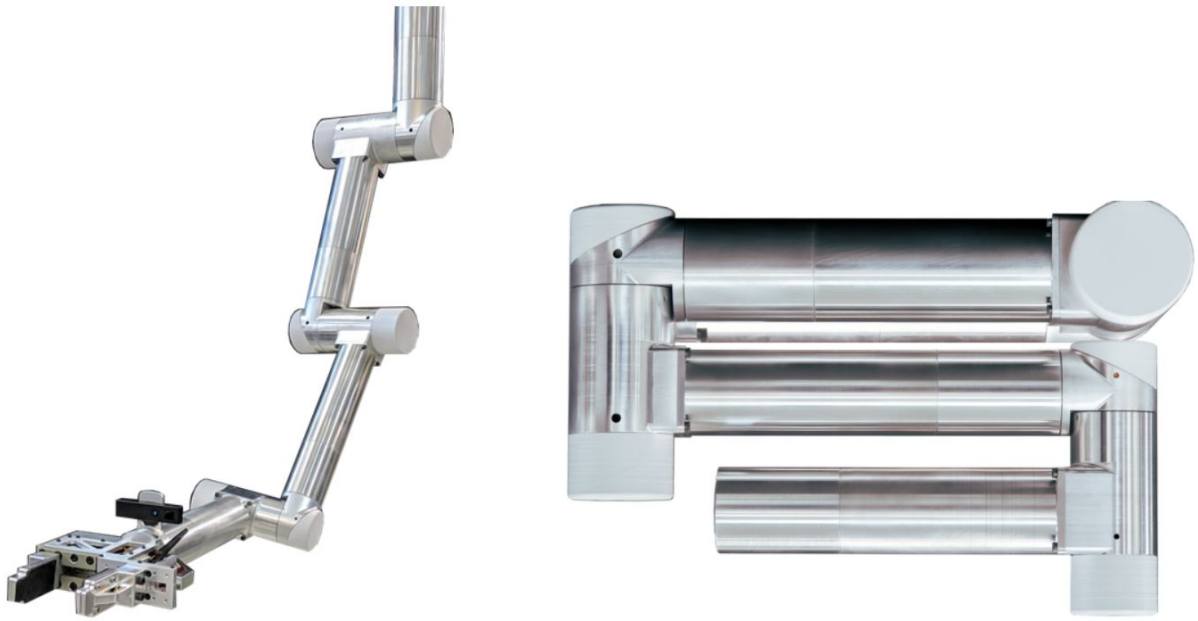

Figure 52 – KRAKEN robotic arm for microsatellites in the stowed position at right and extended position at left.

3.0.3.2 DEOS

The Deutsche Orbitale Servicing Mission (DEOS [6]) was commissioned by the German Aerospace Center (DLR) in 2011(RANK *et al.*, 2011). It was supposed to be a spacecraft equipped with a robotic arm and fully maneuverable. The goal of the mission was to force LEO reentry onto uncooperative satellites and to dock and service cooperative ones. A COTS 3m long arm, with space proven joints from mission ROKVISS (HIRZINGER *et al.*, 2005), would be used for the operation. A simple docking connector was developed for the cooperative targets and a simple gripper for the non-cooperative ones(Fig.53).

[6] https://www.spacetech-i.com/products/missions-satellites/deos

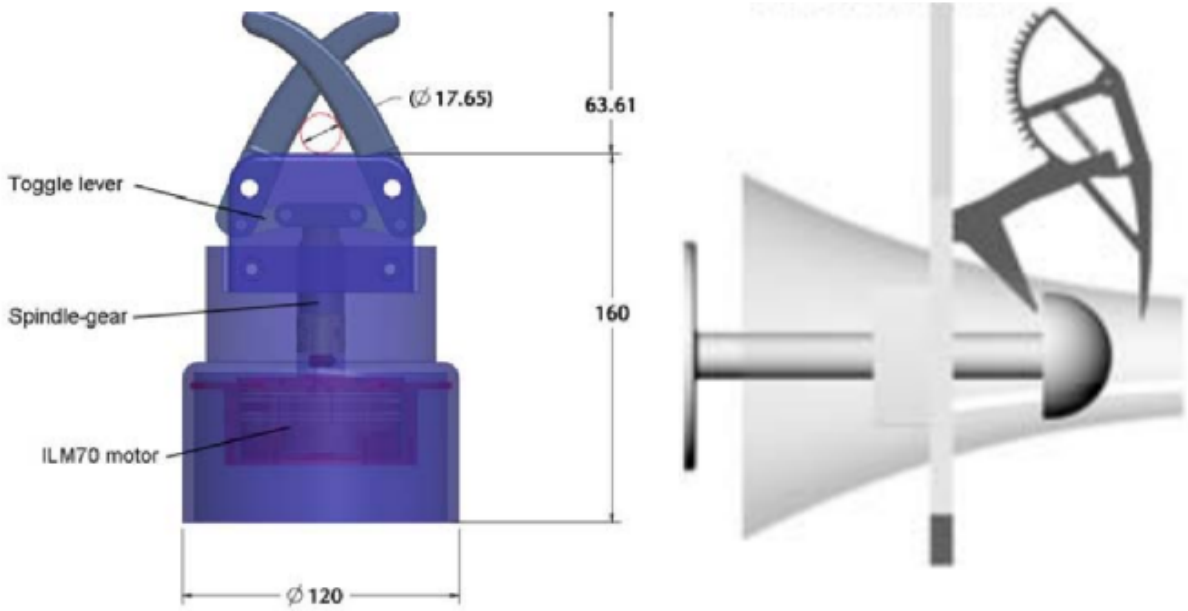

Figure 53 – DEOS gripper to the left and docking connector to the right.

4 POSITION ACTUATION AND SENSING OVERVIEW

Position actuation refers to the capability of performing angular and lateral movements on-orbit. Position sensing refers to the ability of measuring the satellite's angular and lateral position in relation to the earth, distant stars or other satellites. Each system has pros and cons and they can be combined to perform the necessary task. The goal here is to highlight the possibilities and major differences between them. (DAFFALLA; TAGELSIR; KAJO, 2015) offers a quick review of traditional sensors and actuators and (WESTON *et al.*, 2018) the state of the art of those components on the market.

4.0.1 Attitude sensing

This subsection explores possible sensors for attitude determination on the flight phase where there is yet no docking or manipulation taking place. The requirements for attitude accuracy here usually comes from the payload on the satellite, they can be very loose or very tight. If there is no payload on-board requiring high pointing accuracy, it is still useful to have a minimum capability of attitude determination for stabilizing the spacecraft prior to the docking or manipulation engagement. Table54 is taken from (CHAN *et al.*, 2019), that surveys a few sensors with their average expected accuracy. The company is very ambitious and projects such as on-orbit disassembly and recycling of space debris have been proposed to be realized with the manipulator.

Sensors	Accuracy (degree)	Mass(g)	Power(mw)
Coarse sun sensor	0.1-5	0.01-2	0-3
Fine sun sensors	0.005-0.1	0.01-2	0-3
Magnetometer	0.5-5	0.03-1.2	< 1
Star tracker	0.003-0.01	2-5	5-20
Fixed horizon sensor	0.1-1	0.5-3.5	0.3-5
Scanning horizon sensor	0.03-1	1-5	5-10
Gyroscope	Drift 0.001-0.01/hour	0.1-15	$< 1 - 200$

Figure 54 – Comparison between common attitude sensor.

4.0.1.1 Star Tracking

Star trackers are considered the most accurate attitude estimation systems today, and are very common[1]. They can also be very compact, are present in most missions

[1] shorturl.at/loCLN

and in some cases they are already incorporated within the ADCS system. In some cases there are more than one positioned orthogonally to each other. Their pointing accuracy is usually lower on the roll axis. The smallest models are expected to have a volume close of approximately 50x50x50mm. Care must be taken to avoid orienting the sensor towards the sun, a baffle is usually present for avoiding this problem(BAFFLING...,).

4.0.1.2 Sun Tracking

Sun tracking is also very common, it is divided in coarse and fine sensors. Although fine sun trackers can be very precise, they must be utilized with other sensors, once it gives only two axis determination. Coarse sensors can be very imprecise, up to 15° of accuracy in some cases. Their accuracy also varies a lot depending on its orientation in relation to the sun. More information is available at the *SatSearch* website[2]

4.0.1.3 Fixed horizon Sensing

This is a type of earth sensor. They can be precise, when there is a camera with a fixed focal length that is aimed at the earth's horizon and is able to recognize its outline. They can also be a course sensor based on infrared readings of the surface to estimate the satellite's position. It is a less common sensor, but can be useful due to the fact that earth is usually easy to identify, which grants a robustness for the sensor.

4.0.1.4 Magnetic Field Orientation

Magnetometers are ubiquitous. It would be hard to find a mission, more so in LEO, that does not implement them. They are usually implemented as MEMS and detect the orientation of the earth's magnetic field. In the case of this report, care must be taken if a strong electromagnet is present at the spacecraft. It could saturate the sensors, given that it is calibrated to sense the low earth's field.

4.0.1.5 Gyroscopes

Mechanical gyroscopes are rare at cubesats due to their bulkiness and unavoidable measurement drift. MEMS, fiber optic (FOGs) and piezo ones are available though. They measure directly the rotation speed and would be thus recommended for applications where precise speed measurements are necessary. Attitude estimation can also be extracted by integration, which usually introduces errors.

4.0.1.6 GNSS

GNSS receivers are also one of the most utilised sensors. They can be very small and reliable, but it's accuracy is in the order of meters. It is important to use a system

[2] shorturl.at/kHR14

that is able to receive signals from all possible constellations for ensuring robustness. A more precise variation of the sensor, suitable to relative navigation is presented at 4.0.2.1.

4.0.2 Relative Navigation sensing

The goal here is to underline possible sensors for relative navigation. That is, the ability to estimate the position of the spacecraft in relation to another, instead of earth or outer space. With the exception of the Phase Difference GPS, this is done by measuring a satellite position directly in relation to another, instead of comparing the measurement of both against and external reference. It is common to make use of more than one of these sensors simultaneously to achieve the best results. The accuracy requirements here doesn't come from the payload, but from the connector or the manipulator alignment requirements.

Regarding the range, it should be chosen a system with the lowest bound possible, so a docking or manipulation procedure can be monitored until the last moment. It is possible to determine two minimum upper bound requirements. A smaller one, that needs to be accurate enough to position the satellite in its angular and lateral alignment requirements. And a bigger one that doesn't need to be as precise, but only to allow for an initial positioning upon arriving at the target. Using the missions presented as a reference, two meters for the smaller bound and ten meters for the big one should fulfill all docking and manipulation requirements with ease. If the sensors allow for higher upper bound ranges, it is a welcome advantage, but not required. These bounds are represented at Fig.55. The ranging problem is usually related to the focal distance and aperture angle of the sensors.

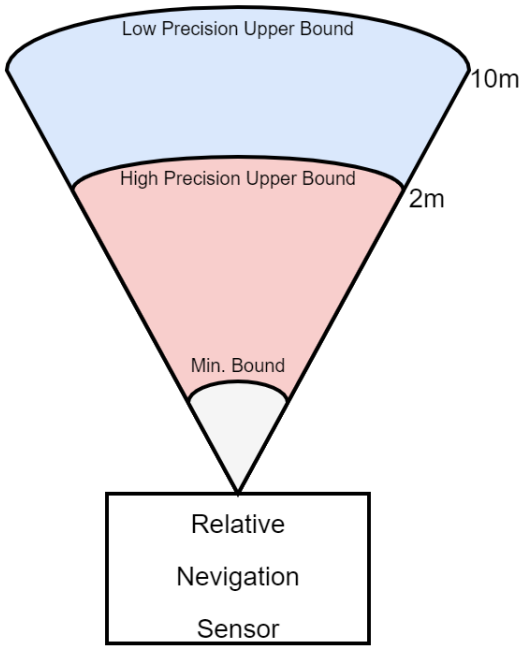

Figure 55 – Relative navigation sensor bounds. Not in proportion.

Resolution is an important factor, it must be compatible with the necessary requirements. According to table 10 a 10mm and 1.5° accuracy would suffice most docking case scenario encountered. For manipulation, an accuracy of 10mm, 5mm and 1mm are expected from the AMODS, REMORA and C-Form project, respectively. Although AMODS includes a dedicated camera at the End-effector to allow for higher accuracy when grabbing the target's rails. A 2° and 5mm accuracy would probably fulfill most Relative Navigation sensing requirements. If extra accuracy is required for the manipulator, a camera at the end-effector should be added. (PIRAT *et al.*, 2018) Agrees with a fine alignment precision of at least 1cm and a coarse range of 10m.

4.0.2.1 CDGPS

Carrier-Phase Differential Global Position System (CDGPS) is a type of GPS that can be installed on two rendezvousing spacecrafts. Instead of measuring both spacecrafts position in relation to the GPS satellite constellation and using this to determine the relative position of the two bodies, CDPGS uses the signal to measure directly the distance and orientation between them. Real time wireless communication between the docking spacecrafts is necessary.

Millimeter accuracy have been reported using hardware in the loop simulations of CDGPS(LEUNG; MONTENBRUCK, 2005). It is also worth noticing that the technology is mature with multiple flight heritage(MONTENBRUCK *et al.*, 2011). The only mission on this report to use this technology was the OAAN, reporting an accuracy of sub centimeter

Name/Company	Accuracy [mm]	Size [mm]	Update Freq. [Hz]
PIKSI/Swift navigation	≤15	48x71	≤10
PX1122R/NavSpark	≤10	12x16	≤10
VN-310/Vectornav	≤10	31x31	n.a.
RTKITE GNSS/ North Survey	±15	47x54	≤10
ZED-F9P/ Ublox	≤10	17x22	≤8
AP104/absolute precision	≤8	46x71	≤10

Table 2 – Comparing table between small RTK GNSS receivers.

(65). The COTS products are know as Real-time kinematic (RTK) GNSS. A few of then are show on the table 2.

4.0.2.2 Hall sensor

A hall-sensor measures the strength of a magnetic field. They are commonly used as cheap sensors for measuring the relative position of an object, fitted with a magnet, and another, fitted with the sensor. The HotDock system utilizes three of them to determine the relative position between two connectors at very close distance. The arrangement can be seen in Fig.66, where they are interspersed among permanent magnets. Hall sensors can be unipolar or bipolar, which means that they react with one specific pole or both poles of a magnet, respectively. They can work on a wide range of temperatures, in some cases from -40 to +150°C. A reasonable amount of calibration may be required, but they can be used for angular(LINEAR. . . , a) and linear measurements(LINEAR. . . , b). Other relative navigation sensors may present a dead band at very close distances, the use of hall sensors can be a cheap option to integrate and fill this gap.

4.0.2.3 IR Trans-receiver

The ARCADE mission had a simplified IR sensing system consisting of two IR LED's and one receptor. By modulating the light emission and using simple geometry (Fig.56), the team was able to achieve the necessary accuracy requirement of 5mm and 1.5°. It is worth noticing that those are average values and considerable filtering was necessary to be implemented. Also, the experiment conditions were very limited, with only two DOF available. This simplistic sensor should then be avoided for on-orbit operations.

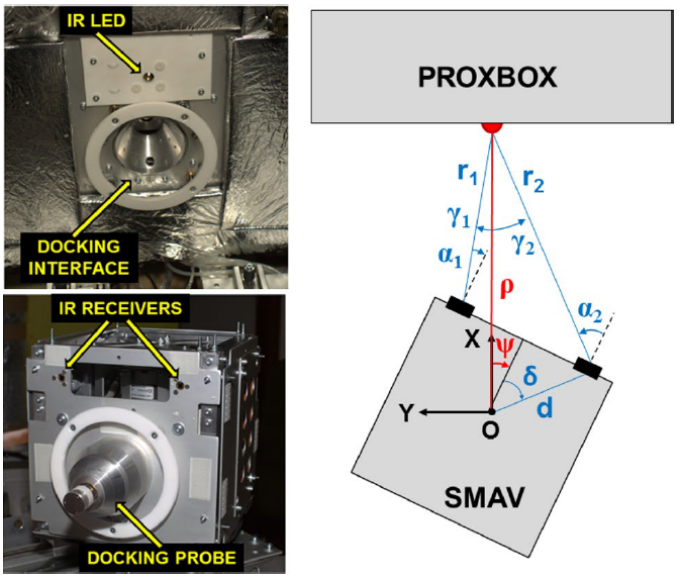

Figure 56 – IR transreceiver system developed by the ARCADE project.

4.0.2.4 Depth Cameras

A normal colored camera attributes one intensity value from each of the three color components (RGB) to each pixel. A depth camera attributes a fourth value, that is the distance from it to that point in real life, depth (RGB-D). There are multiple ways of measuring this fourth value, and it usually requires the fusion of different types of sensors and projectors.

Structured Light uses visible (or some times infrared) light. It projects a pattern at the surface of the object and determines the depth value by the distortion of this shape, which is captured with a simple camera. It is very information dense, but very low range and susceptible ambient noise and light conditions.

Stereo cameras are actually two cameras. They are placed at a certain distance apart and by tracking specific features present in both images captured, it is possible to determine the distance from these points. They are resistant to environmental noise and often are equipped with IR projectors, in that case they would be classified as active rather than passive. By using IR receivers they can then work in dark or poorly lighted situations. They generally require more processing power to keep track of the necessary points, but that is often done by the on-board processing of the COTS device itself and made available via API. It is recommended to use global shutter cameras for moving applications. Since it needs to track determined points, the accuracy is dependent on the texture of the target, but it is realistic to expect centimeter accuracy(HOW...,).

Time of Flight (TOF) cameras and scanners forms the LIDAR category. Here the properties of the light emitted and received are used, like the time (Pulsed Light) or phase difference between them (Continuous-wave). Pulsed Light is better suited for

Name	Range cm	Accuracy mm	Type	Operating Temp. $[^{\circ}C]$	RGB Camera
ifm O3D311	30-1000	± 7	TOF camera	-10 to 50	No
ifm O3X100	5-300	± 5	TOF camera	-10 to 40	No
e-Con Systems Tara	50-300	-	Stereo Cam.	-30 to 70	Yes
Intel D415	16-1000	-	Active IR Stereo Cam.	0 to 85	Yes
Intel D435	10.5-1000	-	Active IR Stereo Cam. Global Shutter	0 to 85	Yes
Sense Photonics SenseOne	50 - 1000	± 5	TOF camera	-	No
DUO MC	23 - 250	-	Stereo Cam	0 to 45	Yes

Table 3 – Table comparing COTS depth cameras small enough to fit on the smaller face of a 3U cubesat.

outdoor environments and long range application. Continuous-wave is recommended for indoor environments and shorter ranges. LIDAR scanners are suited for very long ranges if necessary. Traditionally, LIDAR scanners implements rotating mirrors to direct one or multiple IR beans, but recently solid state ones are available. On the other hand, TOF cameras use 2D sensors, like a traditional camera would. A LIDAR scanner would most likely not be a good choice for relative navigation, but a LIDAR camera would.

Considering the low volume available for a cubesat application, it is desirable to invest in integrated solutions that may combine more than one sensor, which is inexactly what depth sensors usually do. More than that, it is common for the embedded processor to be in charge of fusing the information and delivering a precise result, although it is usually required to perform calibration procedures outside the factory. There are many different manufacturers[3]. Unfortunately, since the need for these types of sensors is not usual for satellites, there is no one COTS space hardened available. The closest to it would be the Ones produced by FRAMOS[4] that are industry rated.

The table3 gathers depth cameras that would fit to be positioned on the smallest face of a 3U cubesat, not considering cable management. Other critical information is added for comparison. Notice the range and resolution varies with size, reflectivity and distance of the target.

[3] https://rosindustrial.org/3d-camera-survey
[4] https://www.framos.com/en/industrial-depth-cameras

4.0.2.5 2D Cameras

A Perspective-n-Point (PnP) pose problem, is the problem of estimating the 3D pose and orientation of a known object, given only the 2D projection of such[5]. For this to be possible, it is necessary to know the mathematical model of the camera and the real dimensions of the object. The bigger the amount of points known in the object; that are possible to be traced into the 2D projection; the better will be the pose and orientation estimation. Efficient Perspective-n-Point (EPnP) deals with at least 6 points. That is why multiple missions presented use 2D cameras and fiducial LED's, that serve as reference points. (PIRAT *et al.*, 2018) reports a performance of 1mm and $\leq 2^{\circ}$ with a single monocular camera and addresses many issues related with the use of this technology for cubesat applications. This is considered a traditional method, once the reference points are determined and arranged by design. There are other approaches to the problem (CHEN *et al.*, 2020).

For instance, the use of deep networks allow for the training process to determine the reference points and to fine tune the necessary parameters. This machine learning approach is deemed significantly more robust and precise and even allow for the fusion of RGB and depth information as in (WANG *et al.*, 2019)[6]; which was considered the state of the art in 2019. But a significant drawback of this technique is the vast amount of training data necessary. For mundane objects, this may not be a big problem, but for a spacecraft on a LEO background, it can be difficult to do a proper training. Some implementations resort to simulate data instead of captured, but the robustness of the final result is affected.

The 6D pose estimation of objects can also be obtained from a fusion of traditional methods and machine learning. Currently, this approach has obtained very good results. Accuracy of up to 1.67cm and 2.5degree were obtained by (LIU; HE, 2019). Another advantage here is the reduced computational resources than one based solely on machine learning.

(SANSONE *et al.*, 2015) Suggests visible and IR LED fiducials to reduce even further the computations costs. The idea is to use underexposed images and filtering to take a photo of the environment, the result is a dark image with only the visible LEDs highlighted. It also uses one IR LED and a filtered receiver. The brightness of the received light is used to estimate the distance from the source, which is particularly useful for low rotation angles, where the fiducial technique is worse. The accuracy reported is of 10 mm and $\leq 2^{\circ}$ up to one meter away.

[5] https://rb.gy/tgpkp1
[6] https://github.com/j96w/DenseFusion

4.0.2.6 IR Cameras

Not considering TOF cameras, IR cameras can be used like a simple 2D camera for approximation of the position and orientation of an object. On the CPOD project, the 3D thermal reflectivity profiles of the two spacecrafts were stored on-board the chaser cubesat. IR cameras were then used to approximate the relative position and orientation. It is the same process described on the 2D camera section, but in a different wavelength.

4.0.2.7 External references

The problem of relative navigation sensing was tackled by missions like SPHERES by using close by references. This is a valid approach for spacecrafts that are used inside a space station, so to use it as a reference. Ultrasound and IR beacons or even cameras can be positioned at the walls of the station and easily determine the position of both spacecrafts. Other than the presence of a gas medium, the lighting conditions at the station would also be stable, making any RGB image based system easily implementable.

4.0.3 Attitude Control

This section outlines some of the available commercial technologies for altering the angular position; the attitude; of the spacecraft in orbit. This is an essential ability for multiple payloads and for docking and manipulation itself.

Component	Performance	TRL Status
Reaction Wheels	0.001 – 0.3 Nm peak torque, 0.015 – 8 Nms storage	9
Magnetorquers	0.1 Nm peak torque, 1.5 Nms storage	9
Star Trackers	25 arcsec pointing knowledge	9
Sun Sensors	0.1° accuracy	9
Earth Sensors	0.25° accuracy	9
Gyroscopes	$1°h^{-1}$ bias stability, $0.1°h^{-1/2}$ random walk	9
GPS Receivers	1.5 m position accuracy	9
Integrated Units	0.002° pointing capability	9

Figure 57 – Figure from (WESTON *et al.*, 2018) comparing ADCS types and their general characteristics. The table may be slightly outdated due to the release date of the study, nevertheless it is useful.

4.0.3.1 Reaction Wheels

Reaction wheels are very traditional for attitude actuation and many options are available[7], they are able offer fine control and high torques. They are movable components, which exposes them to mechanical failure. For that reason, from big satellites to micro ones, it is not unusual to have redundant wells. In cubesats, it is commonly implemented only 3 orthogonal ones. Some of their key aspects are Momentum Storage, Maximum Torque and Maximum RPM.

4.0.3.2 Magnetorquers

Magnetorquers, sometimes called torque rods, are simple electromagnets that interacts with earth's magnetic field. Their torque is generally low, but can be used for long stretches of time for consuming low power. They are mainly used for detumbling the satellite and for desaturation of the reaction well when it hits the maximum RPM. The higher the Magnetic Moment [A.m^2] produced, the higher the torque generated at the same point at the earth's magnetic field. Residual Magnetic Moment is the result of hysteresis on the material and should be as small as possible.

4.0.3.3 Thrusters

Thrusters can be utilized for attitude determination, preferably when they are positioned with a significant torque moment arm. Nevertheless, a tendency observed on the missions reported is to decouple translational en angular displacement. For this, the thrusters were usually positioned close to the center of mass of the spacecraft or in a way that ensured the resultant torque would be zero. Assembly and manufacturing misalignments are inevitable so a complete decoupling is impossible. More details about thrusters are presented at Sec.4.0.4.

4.0.4 Translational Control

Translational control is very important in cubesat docking and manipulation contexts. The level of accuracy required (sub centimeter) is not common, so they are usually not optimized for that. That is why the Minimum Impulse Bit [mN.s], that is equivalent to the system's "resolution", becomes an important factor to be considered. Some missions opted for developing their own propulsion systems for improved control.

[7] shorturl.at/mqtCZ

Product	Thrust	Specific Impulse (s)	TRL Status
Hydrazine	0.5 – 30.7 N	200-235	7
Cold Gas	10 mN – 10 N	40 – 70	GN2/Butane/R236fa 9
Alternative (Green) Propulsion	0.1 – 27 N	190 – 250	HAN 6, ADN 9
Pulsed Plasma and Vacuum Arc Thrusters	1 – 1300 μN	500 – 3000	Teflon 7, Titanium 7
Electrospray Propulsion	10 – 120 μN	500 – 5000	7
Hall Effect Thrusters	10 – 50 mN	1000 – 2000	Xenon 7, Iodine 3
Ion Engines	1 – 10 mN	1000 – 3500	Xenon7, Iodine 4
Solar Sails	0.25 – 0.6 mN	N/A	6 (85 m^2), 7 (35 m^2)

Figure 58 – Figure from (WESTON *et al.*, 2018) comparing thrusters types and their general characteristics. The table may be slightly outdated due to the release date of the study, nevertheless it is useful.

4.0.4.1 Cold Thrusters

Cold gas thrusters are simply pressurised tanks with actuated valves and an exhaust nozzle. Their simplicity makes them a very common choice for cubesats and sometimes they come in units with many exhaust nozzles integrated. The speed and precision of the actuator defines the Minimum Impulse Bit. They offer a good balance of high thrust and good control accuracy, but are usually low on specific impulse.

4.0.4.2 Non-pressurized Cold Gas Propulsion

This is a novel option, the exhausted gasses comes from the sublimation process of a substance (the fuel) and is controlled by the heating of it. Only one example of such a system for cubesats was found, the *I2T5* from *ThrustMe*[8].

4.0.4.3 Electric propulsion

Electric propulsion is an umbrella term for multiple types of thrusters such as Pulsed Plasma and Vacuum Arc Thrusters, Electrospray Propulsion and Ion Engines. In general, they offer low thrust values, but high specific impulse for their low fuel consumption. Regardless of Fig.57, nowadays there are electric propulsion systems with TRL 9.

[8] https://www.thrustme.fr/products/i2t5

4.0.4.4 Hydrazine

Hydrazine are chemical thrusters. Like cold gas, they have a high thrust and good accuracy. They are a mature technology for big spacecrafts, but relatively new for cubesats. Their high toxicity must be taken into account when considering this system. Other chemical propulsion methods are available with similar performance.

4.0.4.5 Green Propulsion

Green propulsion thrusters are also chemical engines, but with non-toxic reagents. There are more Green options available at the market than toxic ones, such as hydrazine. The simplified procedures for dealing with then may also facilitate logistics and delivery times.

4.1 Position Actuation and Sensing

This section condenses the information about translational and attitude control and determination for all the previously mentioned missions with information available. Here, relative navigation refers to the satellite's ability to close rendezvous another one on the docking or manipulation process. Attitude estimation refers to the satellite's ability to determine its orientation prior to the relative navigation stage. For microsat mission proposals (bigger than cubesats) only the relative navigation sensing was considered, for the difference in weight and size would render actuation comparisons useless.

4.1.0.1 Padova Probe/drogue

(SANSONE; BRANZ; FRANCESCONI, 2018) a good review of relative navigation estimation available in literature and proposes one for the Padova Probe/drogue connector project. The system makes use of 8 LED's divided in two patterns, ensuring that the small one will stay inside the camera's field of view for longer (below 0.38 m), while the bigger provides better accuracy. Some LED's protrude from the surface plane to enhance the system's sensibility to rotation. They make use of underexposed pictures to filter out ambient noise and capture mostly the LED's light.

Experimental testing on a 2 DOF motorized table showed an alignment accuracy better than 5mm and 1.5° , even though the system struggled with z distance estimation, something that has been observed on other cases of systems like this. Different dynamic tests were carried out and similar good results were observed.

Figure 59 – Padova probe/drogue connector proposed LED fiducial pattern.

The hardware used was adequate for indoor tests, not on-orbit environment.

4.1.0.2 AAReST

The AAReST mission depends on magnetic attraction for the final docking phase. Nevertheless, it is equipped with a TOF LIDAR camera (Softkinetic DS325) for relative position estimation. The module also contains a traditional RGB camera and IMU capability. It is made for indoor environments, has a nominal range of 1m and a resolution better than 14mm. Its biggest dimension is 105mm, which would make it impossible to be mounted on certain orientations on a 3U cubesat. Softkinetic was acquired by Sony in 2017.

It also has specific requirements for attitude control. The MirosSat (3U) have much looser requirements, once it needs mostly to navigate to the broad capturing area. On the other hand, the CoreSat (15U) have very restrictive requirements, once it is responsible to maneuver the craft after docking and, being a telescope, have to be accurate and stable. It accomplishes this by having 4 reaction wheels arranged in a pyramid shape, also providing redundancy. The analysis on the next tables are divided between these two systems.

The ADCS was developed by the South African company CubeSpace[9]. Unfortunately, the reaction wheels used don't seem to be available commercially. The on-board computer was also developed from the same company and the sensors necessary for attitude estimation were embedded into the CubeSense Module (CUBESENSE...,). The MirrorSat ADCS system is identical to the QB-50 satellites launched in 2014 and also similar to the STRaND-1 satellite [10]. At the time of the article (UNDERWOOD *et al.*, 2015), the QG-50 program[11] had launched only two spacecrafts but currently that number is up to 36.

Information for the MirrorSat ADCS is available at pg.129 at (AAREST...,). It has one coarse sun sensor, one CMOS Camera Digital Sun Sensor, one CMOS Camera Digital Earth Sensor, 3-Axis Magnetoresistive Magnetometer, 3-Axis Magnetorquer(2Rods & Coil), Pitch-Axis Small Momentum Wheel (45g) and GPS receivers. Estimation capability is better than 0.2° (CUBESENSE...,). Table 4 summarized these variables. Regarding the thrusters, nine of them were fitted solely on the MirrorSat, for more details at the propulsion system, pg.33 form (AAREST...,) is recommended.

[9] https://www.cubespace.co.za/
[10] https://earth.esa.int/web/eoportal/satellite-missions/s/strand-1
[11] https://www.qb50.eu/

MirrorSat (∼ 6.1kg)	**Reaction wheels**	-	**Magnet Torquer**	-	**Thrusters**
Momentum Storage $[mN.m.s]$	1.7	**Nominal Mag. Mom.[A.m^2]**	n.a.	**Number of Thrusters**	9
Maximum Torque $[mN.m]$	n.a	**Saturation Mag. Mom. [A.m^2]**	0.2	**Total Impulse [N.s]**	n.a.
Maximum RPM	n.a	**Residual Mag. Mom. [A.m^2]**	n.a.	**Nominal Thrust [mN] (each thruster)**	$5 < 10$
Number of wheels	1	**Number of Magnetorques**	3	**Delta-V [m/s]**	10
-		-		**Minimum Impulse Bit [mN.s]**	0.01 - 0.02
Final Pointing accuracy			$\pm 2°$		

Table 4 – Attitude and translational control of the MirorSat.

For the CoreSat, more powerful reaction wheels were implemented, and more precise sensors used (pg.132 at (AAREST...,)). On top of the other sensors cited, it was added two star trackers CubeStars[12] and two IMUs based on the STIM210 multi-axis MEMS gyro[13]. And the pointing requirements are summarized on table 5.

CoreSat (∼32kg)	**Reaction wheels**	-	**Magnet Torquer**	-	**Thrusters**
Momentum Storage $[mN.m.s]$	30	**Nominal Mag. Mom.[A.m^2]**	0.4	**Number of Thrusters**	0
Maximum Torque $[mN.m]$	2	**Saturation Mag. Mom. [A.m^2]**	0.8	**Total Impulse [N.s]**	-
Maximum RPM	5600	**Residual Mag. Mom. [A.m^2]**	n.a.	**Nominal Thrust [mN] (each thruster)**	-
Number of wheels	4	**Number of Magnetorques**	3	**Delta-V [m/s]**	-
-		-		**Minimum Impulse Bit [mN.s]**	-
Final Pointing accuracy			$\pm 0.1°$(3-sigma).		

Table 5 – Attitude and translational control of the CoreSat.

4.1.0.3 OAAN

The OAAN project is the only one that aims to use an external positioning source for the relative navigation. Instead of trying to directly measure the other satellite's position and maneuver in relation to it, it will use GPS. More specifically, a Carrier-Phase Differential Global Position System (CDGPS). It measures the phase difference of the GPS carrier wave at two locations (the two docking satellites), which provides relative

[12] https://www.cubespace.co.za/products/adcs-components/cubestar/
[13] https://www.sensonor.com/products/gyro-modules/stim210/

position measurement accurate within 2 cm. They used the "Piksi Multi GNSS Module"[14] from *Swift Navigation*. One requirement of the system is that the antenna should face away from earth. The final docking stage is done by magnetic attraction, so this system is precise enough to position the satellite within the capture volume. The team carefully tested the equipment and came to the conclusion that the products are consistent with manufacturer specifications (PEI, 2017), although heavy filtering was necessary. Fig.65 summarizes their results.

Error Type	North	East	Down
White Noise (cm)	0.43	0.325	0.87
Bias Stability (cm/time step)	0.48	0.36	0.96

Figure 60 – Table resuming experimental tests with the "Piksi Multi GNSS Module" after filtering(PEI, 2017).

A four cold gas thruster setup was arranged in a tetrahedron shape in the middle of the satellite to provide solely translational movement. A series of thrust characterisations were performed, mostly to obtain an adequate measurement of the Minimum Thrust Impulse Bit (MIB).

As one can read on the paper (PEI, 2017). "The Attitude Determination and Control System (ADCS) is provided by Blue Canyon Technologies (BCT)[15]. The "XACT" unit is a fully assembled COTS product with flight heritage. The XACT provides precise three-axis attitude control using reaction wheels, magnetic torque rods, and integrated control algorithms. For attitude sensors, it contains a star tracker, sun sensor, and magnetometer. The star tracker is used during fine pointing mode operations." The precise model used can be tracked by visual reference to be the XACT-15, whose available characteristics (MASON *et al.*, 2017) are present on the table 6.

[14] https://www.swiftnav.com/piksi-multi
[15] https://www.bluecanyontech.com/

OAAN mission (~ 5 **kg**)	**Reaction wheels**	-	**Magnet Torquer**	-	**Thrusters**
Momentum Storage $[mN.m.s]$	15	**Nominal Mag. Mom.[A.m^2]**	n.a.	**Number of Thrusters**	4
Maximum Torque $[mN.m]$	n.a.	**Saturation Mag. Mom. [A.m^2]**	n.a.	**Total Impulse [N.s]**	n.a.
Maximum RPM	8000	**Residual Mag. Mom. [A.m^2]**	n.a.	**Nominal Thrust [mN] (each thruster)**	300
Number of wheels	3	**Number of Magnetorques**	n.a.	**Delta-V [m/s]**	n.a.
-		-		**Minimum Impulse Bit [mN.s]**	22
Final Pointing accuracy		$\pm 0.003°$ (1-sigma) for 2 axes; $\pm 0.007°$ for 3rd axis			

Table 6 – Attitude and translational control of the OAAN cubesat.

4.1.0.4 PACMAN

The relative maneuver sensing was done by integrating a 2D camera and the on-Board IMU. The Raspberry Pi NoIR Camera v2. It is located at the centre of the CUBE top plate, with its optical axis oriented towards the direction of motion of the module (Fig. 61). The system also makes use of fiducial LED's and was extensively tested at (DUZZI *et al.*, 2017). They performed static and moving tests and results were very promising, even with limited processing resources, with the maximum error limited to a range of about 3:5mm, ±1mm and ±5mm along the x, y and z-axis respectively. Angle accuracies archived on the tests are seen on Fig.62.

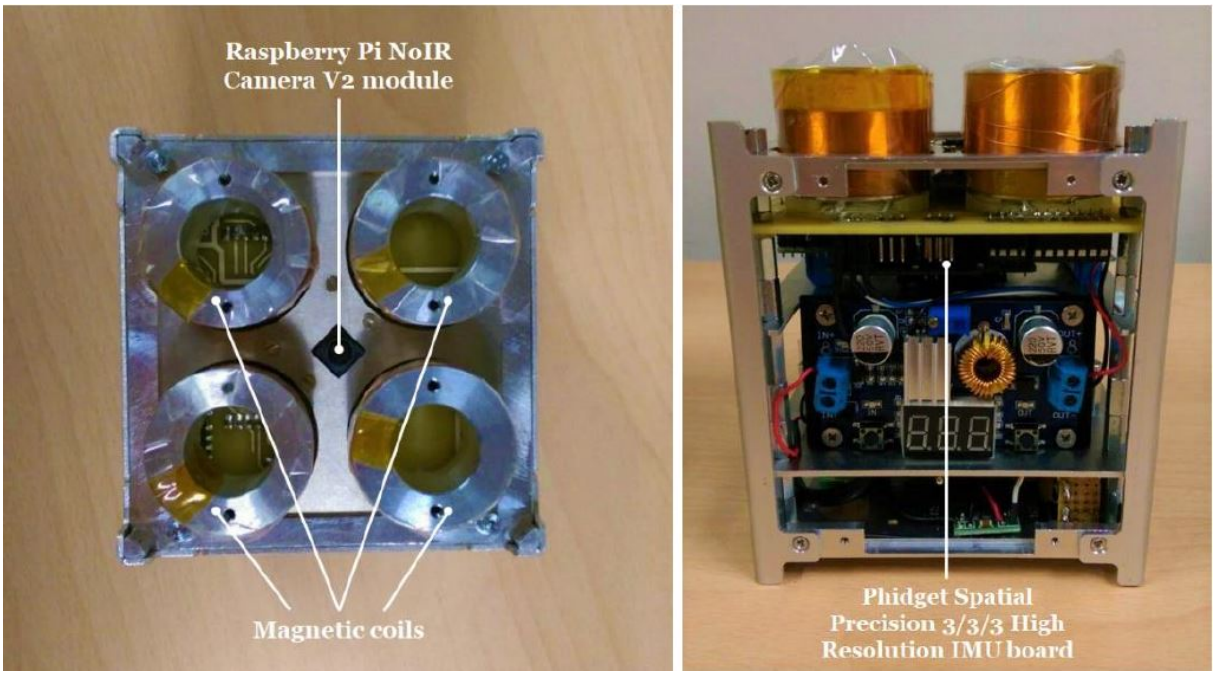

Figure 61 – PACMAN cubesat.

	μ [deg]	σ [deg]
roll (ϕ)	2.79	4.61
pitch (θ)	0.04	2.69
yaw (ψ)	-1.26	0.29

Figure 62 – PACMAN angular alignment error test results.

Even though the lab test results were very positive, on orbit application may face backlash. The camera and processor used are not made for space environments and light variations may be very detrimental to the system's performance.

4.1.0.5 CPOD

The CPOD mission includes an Integrated ADCS unit developed by Tyvak[16] roughly 1/2U size. It contains 3 reaction wheels, 3 magnetorquers and the attitude estimation hardware (CPOD. . . , 2015) (Fig.64). Next is a table summarizing the attitude and translational capabilities of the mission.

[16] https://www.tyvak.eu/

CPOD mission (∼6kg)	**Reaction wheels**	-	**Magnet Torquer**	-	**Thrusters**
Momentum Storage $[mN.m.s]$	10	**Nominal Mag. Mom.[A.m^2]**	0.1	**Number of Thrusters**	8
Maximum Torque $[mN.m]$	3	**Saturation Mag. Mom. [A.m^2]**	n.a.	**Total Impulse [N.s]**	186
Maximum RPM	10000	**Residual Mag. Mom. [A.m^2]**	n.a.	**Nominal Thrust [mN] (each thruster)**	25
Number of wheels	3	**Number of Magnetorques**	3	**Delta-V [m/s]**	31
-		-		**Minimum Impulse Bit [mN.s]**	0.2
Final Pointing accuracy			0.25°(3-sigma).		

Table 7 – Attitude and translational control of the CPOD cubesat.

For orbit maneuvering, the spacecraft is equipped with 8 cold gas thrusters concentrated on a module developed by VACCO[17]. This module is positioned on the center of the cubesat, close to the center of mass, as in Fig.63. The system size is approximately 1U(CPOD...,).

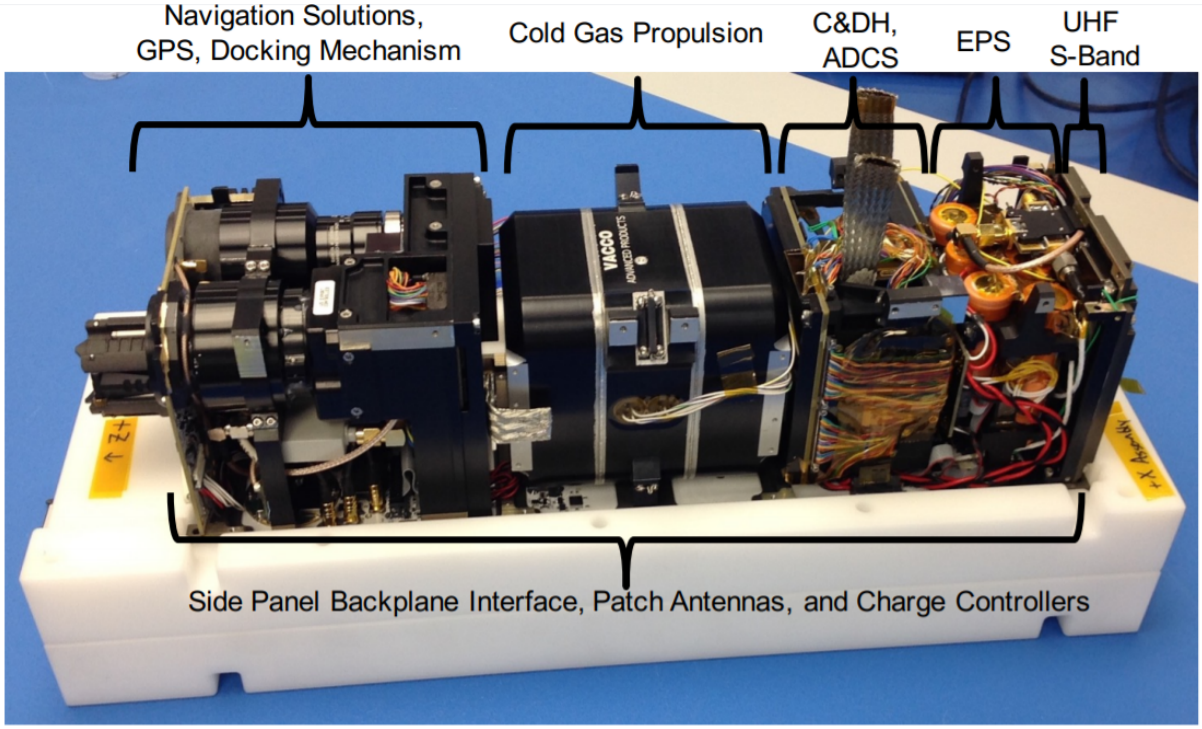

Figure 63 – Image taken from the presentation on the CPOD project(CPOD..., 2015).

The attitude estimation was also concentrated on the Tyvak Inertial Reference

[17] https://www.vacco.com/space/overview

Module (CPOD. . . , 2015). It contains two star trackers, inertial measurement unit (IMU), three reaction wheels, GPS receiver, Sun sensors, magnetometers, and three torque coils. Its estimation capability is 0.15° three sigma, according to (BOWEN *et al.*, 2015).

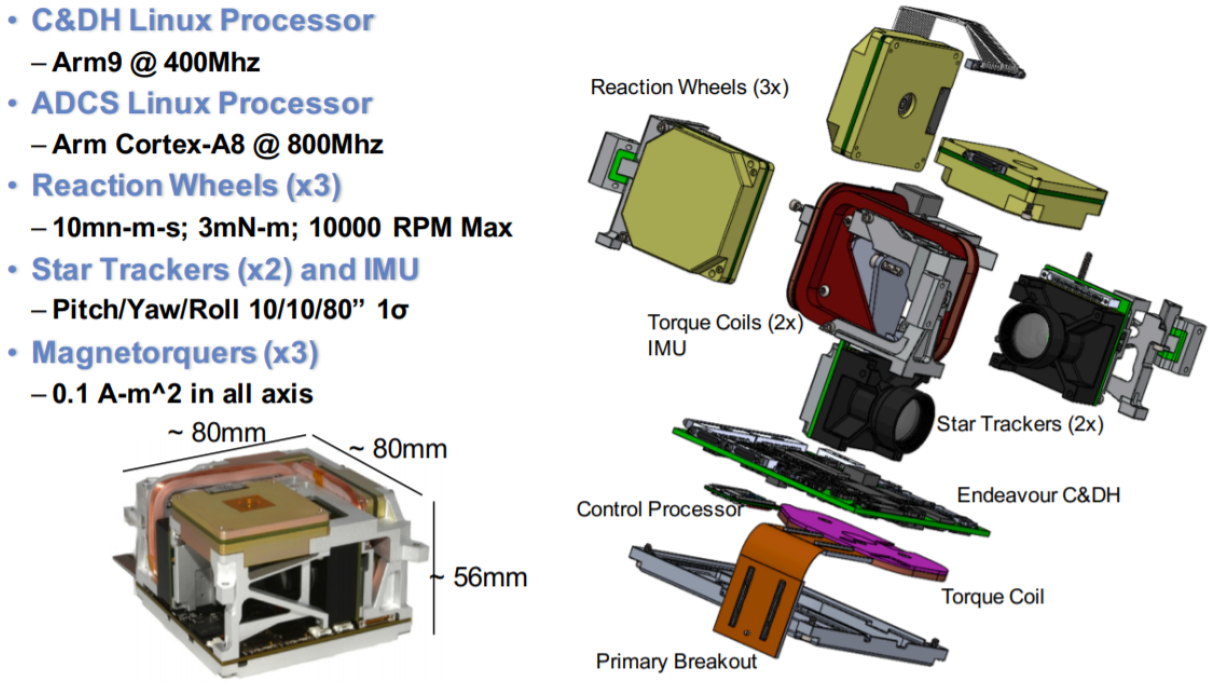

Figure 64 – Image taken from the presentation on the CPOD project(CPOD. . . , 2015).

For relative navigation, the satellite contains 4 cameras: narrow field of view visible, wide field of view docking visible, wide field of view IR, and narrow field of view IR. There is a 3D model of the cubesats on board, that are used for calculating each other's pose, using images on the visible range and thermal reflectivity. Using the OpenCV platform the system is able to compensate for a number of aberrations on the imaging system like Sun glint, Earth albedo effects, etc. As the spacecrafts get closer, LED's on the mating surfaces are used as fiducials. The accuracy of this system was not specified.

It is important to mention that even though the docking capability of this system has yet not been proven, the attitude control capabilities have. It was tested on the NANOACE mission [18]

4.1.0.6 Electromagnetic docking

The proposed attitude determination system for this system(Sec. **??**) is the *MAI-400 3axis RCS*[19]. It is an integrated module with three reaction wheels, a 3-axis magnetometer,

[18] https://www.tyvak.eu/missions/
[19] https://www.adcolemai.com/wp-content/uploads/2019/02/AMA-MAI-400-Datasheet.pdf

two IR Earth Horizon Sensor (IREHS), three electromagnets (magnetorquers) and an ADACS computer.

CPOD mission (∼ 3.2kg)	**Reaction wheels**	-	**Magnet Torquer**	-	**Thrusters**
Momentum Storage $[mN.m.s]$	11	**Nominal Mag. Mom.[A.m^2]**	0.108	**Number of Thrusters**	-
Maximum Torque $[mN.m]$	0.64	**Saturation Mag. Mom. [A.m^2]**	n.a.	**Total Impulse [N.s]**	-
Maximum RPM	10000	**Residual Mag. Mom. [A.m^2]**	n.a.	**Nominal Thrust [mN] (each thruster)**	-
Number of wheels	3	**Number of Magnetorques**	3	**Delta-V [m/s]**	-
-		-		**Minimum Impulse Bit [mN.s]**	-
Final Pointing accuracy				n.a.	

Table 8 – Attitude and translational control of the the proposed cubesat.

For the relative navigation, the group proposes the implementation of the reference (NALLAPU *et al.*, 2018). This work is relatively incomplete more details should be offered for consideration.

4.1.0.7 SIROM

The only thing that can be added is regarding SIROM's relative navigation sensing performance. 24 ArUco markers were utilized for visual reference, once they were used to extract a 6D pose estimation on the connector in relation to the camera, that was attached to the end-effector of the manipulator arm. LEDs were added to the base of the connector to ensure stable lighting in dark condition. The system utilized remarkably simple hardware; Raspberry Pi Zero (used as a control computer) and Raspberry Pi Camera Module v2 (as a visual servoing sensor); and software (OpenCV with Python 2.7). These are obviously not space qualified hardware, and after further testing with a rover, significant latency (10 to 15s) was observed. They were able to obtain the necessary accuracy out of the system; $\pm 5.5m$ and $\pm 1.65°$; but to use ArUco markers on the final design would probably not be optimal, given the large area necessary for attaching it.

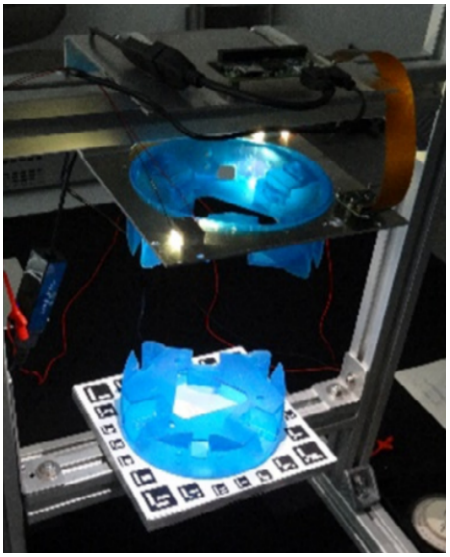

Figure 65 – SIROM alignment test rig with ArUco markers and LED lighting.

4.1.0.8 HotDock

There is no official sensing or actuation recommendation for to be used with the connector. The only disclaimer in that sense is the use of hall-effect sensors for measuring the final alignment between two connectors. Fig.66 show the arrangement of permanent magnets and sensors that allows for the measurement while also assisting on the alignment itself.

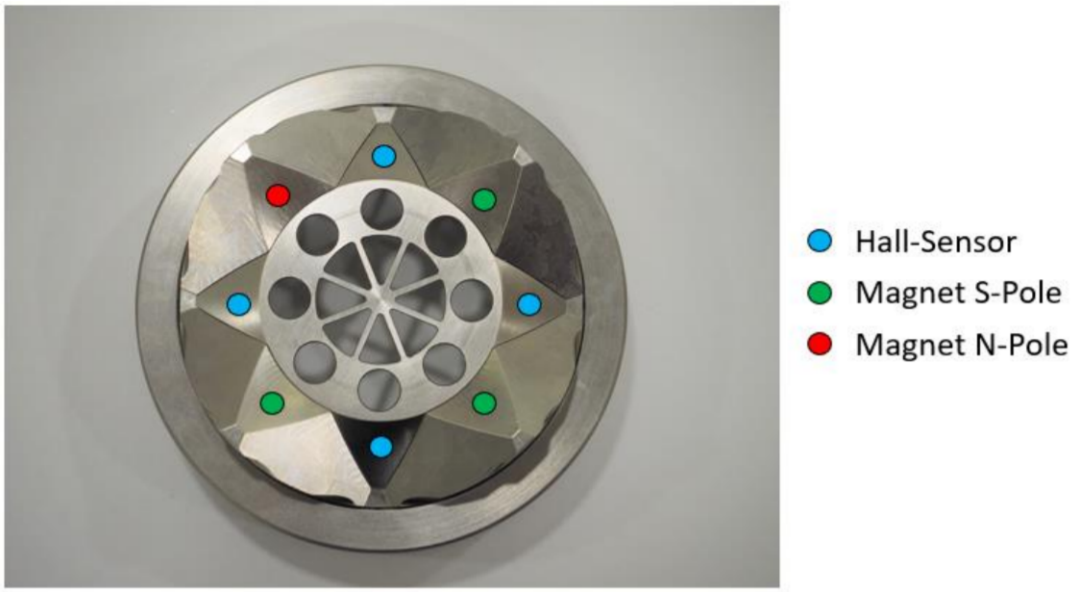

Figure 66 – HotDock's permanent magnets and hall sensors alignment.

4.1.0.9 ASSIST

For relative navigation sensing, a hybrid system was proposed. For the approach phase, the utilization of scanning LIDARS coupled with retro-reflectors was chosen. The

system was considered superior thanks to "robust to lighting conditions, very high accuracy in range, LOS and attitude and extended operating range" (up to 5km). For the closer phase, a visual-servoing approach was selected based on 9 markers at the drogue connector (Fig.67).

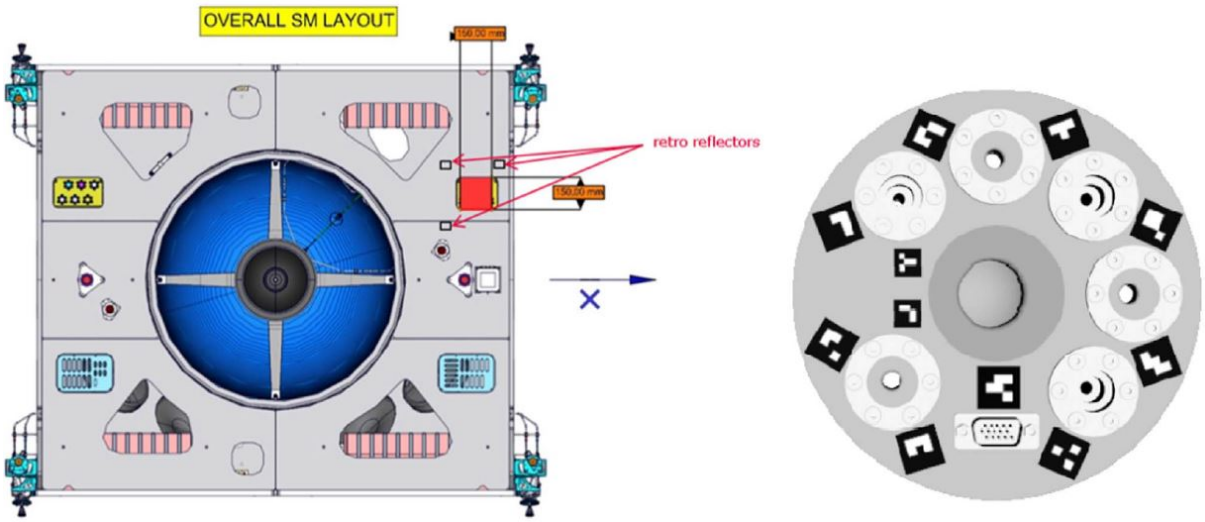

Figure 67 – ASSIST connector outlining the retro-reflectors and the 2D markers.

4.1.0.10 ARCADE

Arcade was a simplified mission with dimensions not completely compatible with a cubesat and put through conditions not analogous to an on-orbit environment. There was one rotational DOF tested, and it was controlled by a costume made brushless reaction wheel. There is not extra information available.

4.1.0.11 AUTOPORT

AUTOPORT was thought to be a Mars UAVs connector, thus the attitude actuation system is not relevant to this report. However, the relative navigation sensing system is slightly unusual. It uses two sets of visible LED fiducials. The bigger set (blue ones in Fig. 69) are used for bigger distances and precise measurements. The smaller set (red ones in Fig. 69) is used for close distances when the bigger falls out of sight, enabling measurements up to 10cm close. All the processing is embedded, running C++ on a Raspberry Pi 3 using OpenCV 3.1. The authors remind that the amount of LED used is important and so is their position. They chose 5 LED's on the given non symmetrical configuration.

Static tests on a table showed that the lateral accuracy may not be very good for some conditions, sometimes going up to 8mm. But the angular accuracy never exceeds

0.9°. Dynamic tests with the table moving up to 5mm/s showed similar results, although concerns were raised about the poor sampling performance of the camera.

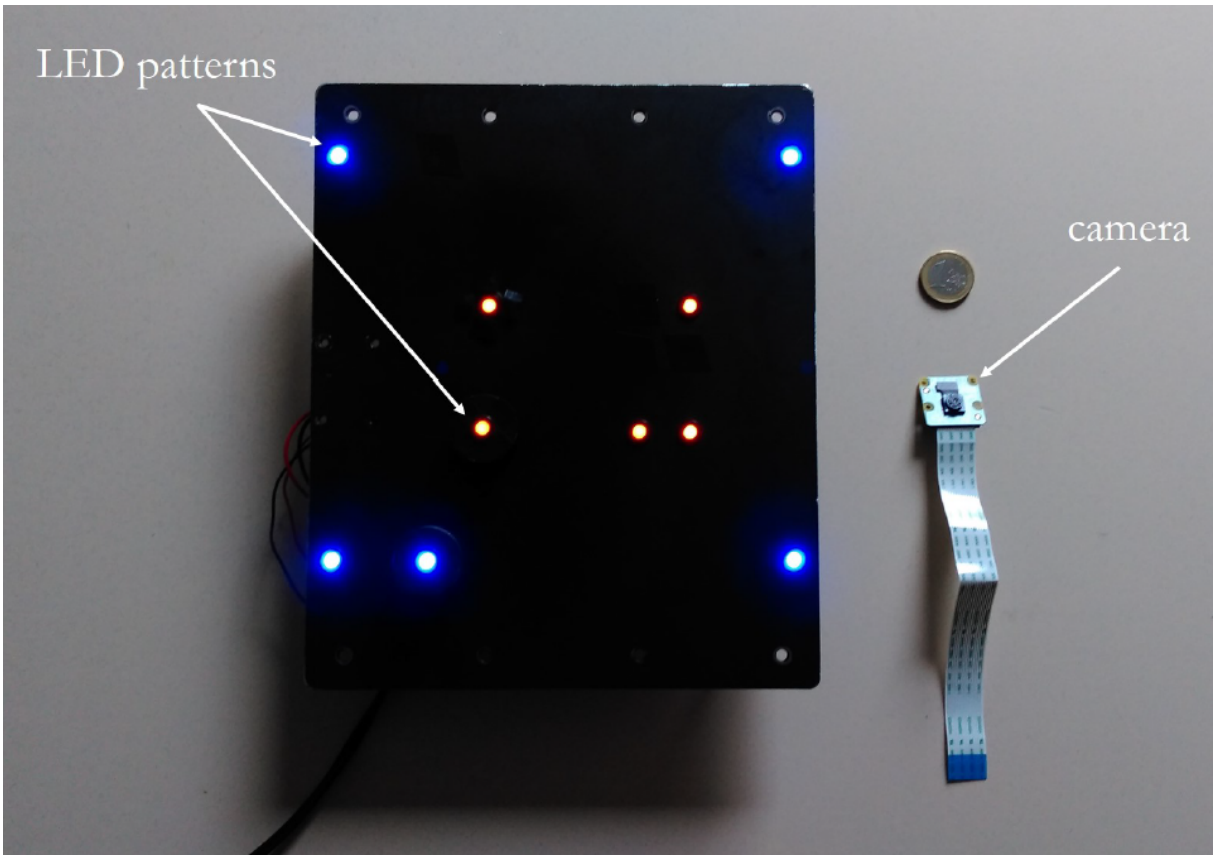

Figure 68 – AUTOPORT fiducial markers pattern.

4.1.0.12 AMODS

The AMODS program was divided between the RSat and the BRICSat. RSat lacks any attitude actuation or propulsion capabilities, but does have a depth camera for relative navigation sensing. According to (WENBERG *et al.*, 2018a), the chosen one is the Duo-M 3D stereoscopic vision camera[20]. It sits in the middle of the satellite pointed at the manipulators. It creates a 3D mash or the environment in order to allow for the trajectory planning or the arms. In the order hand, the B-Sat has well defined attitude requirements, such as 0.5° of pointing accuracy and to be able to reduce tumbling to a maximum of 1°/s. Some information was given, but not the exact models used. In (HANLON *et al.*, 2017) reads "[B-Sat]... employ a COTS ADCS system that provides a torque of 0.635 mNm, which is approximately 25% of the motors expected torque...". It is important to outline that the presence of moving arms with a non-negligible mass is taken into consideration on the ADCS design.

[20] https://duo3d.com/product/duo-mini-lv1

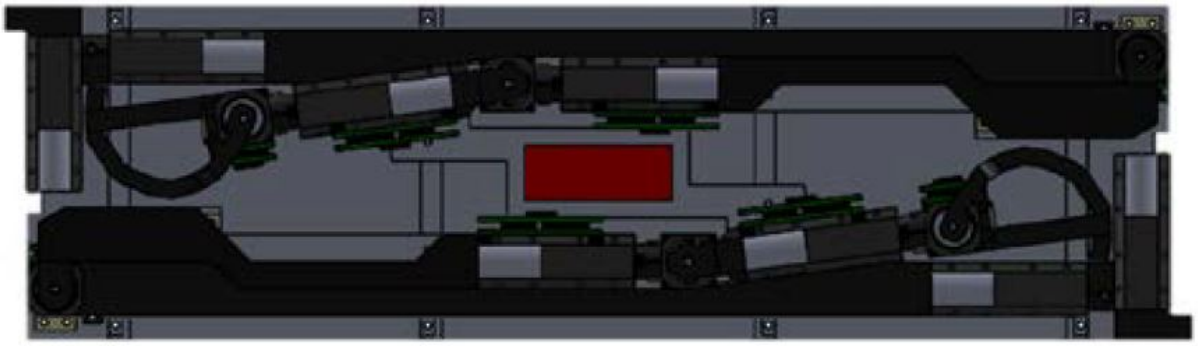

Figure 69 – ISAR satellite (previously called AMODS) with its stowed arms and the depth camera, outlined in red at the middle.

For the propulsion system at BRICSat, the requirements were ±20mm at lateral positioning accuracy. For this, the group used a costume Micro-Cathode Arc Thrusters (μcat) developed by the George Washington University(KEIDAR *et al.*, 2013) with 3000s of Specific impulse and 1mN of thrust. 14 of these thrusters were attached to all the six faces of the satellite. Even so, they are used for fine maneuvering. For big delta-V maneuvers, a cold gas system is employed (more than 80 m/s based on a 4 kg satellite).

4.1.0.13 REMORA

REROMA will be a complete satellite, with propulsion, ADCS and manipulation abilities. It is fitted with a star tracker, sun sensors, and GPS transceiver. According to the paper (), attitude control and propulsion is accomplished by the use of thrusters.

For relative navigation sensing, there is significantly more information available. On the paper, reads:

"REMORA has two separate imaging systems, two German Orbital System PicoSatellite CAM1 (apparently not commercially available anymore) imagers for long range navigation, and four GumStix CASPA VL[21]imagers for proximity operations during the rendezvous and attachment phase. Figure 71 shows a representation of the camera's field of view.

PicoSatellite CAM1 cameras are expected to be implemented into future missions. They will provide REMORA with the ability to track the debris object from at least 15 km separation distance, and also provide 10 cm per pixel images from 1 km ... to characterize the debris object's behavior before planning a final approach. Having two operational cameras is preferred to provide better object characterization through stereoscopic imaging, but the mission can be completed with one camera, providing redundancy in the design.

[21] https://www.gumstix.com/caspa-vl.html

The Gumstix CASPA VL imagers have flight heritage from the European Romit2 CubeSat and are also expected to be implemented into the upcoming MarCO mission. The cameras are placed in a fashion to allow for stereoscopic imaging to enable distance measurements during REMORA's final approach and attachment phases. Four cameras are included, with only two being needed for mission success, providing redundancy in the design."

Figure 70 Show some of the discussed components.

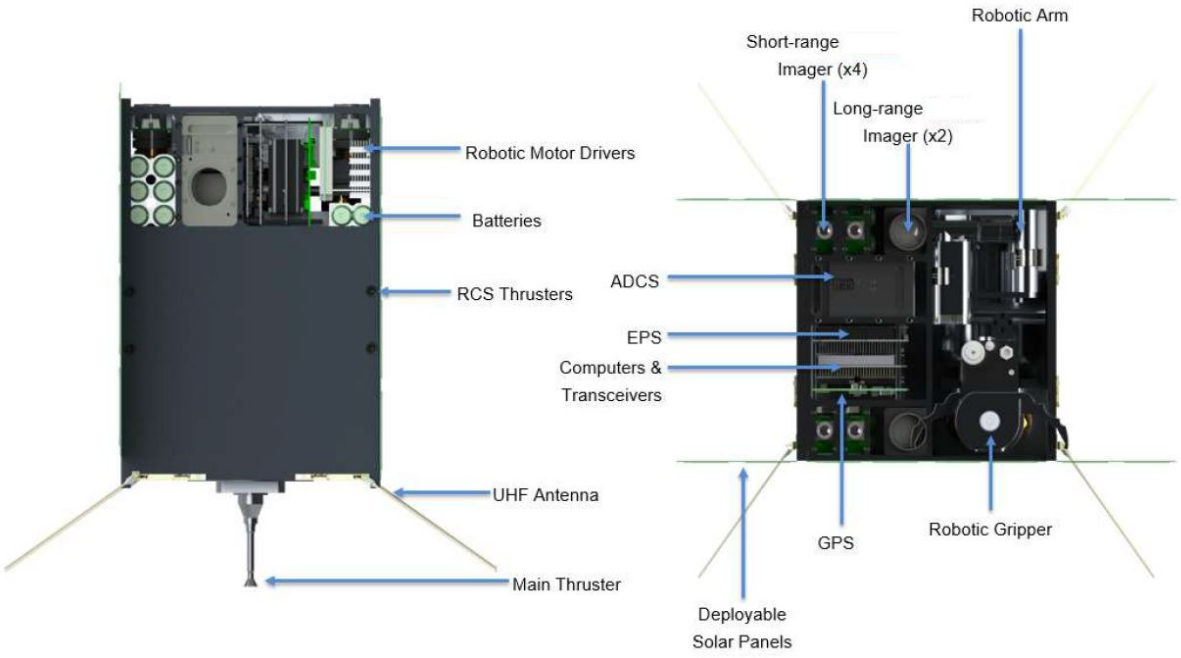

Figure 70 – REMORA satellite labeling important components.

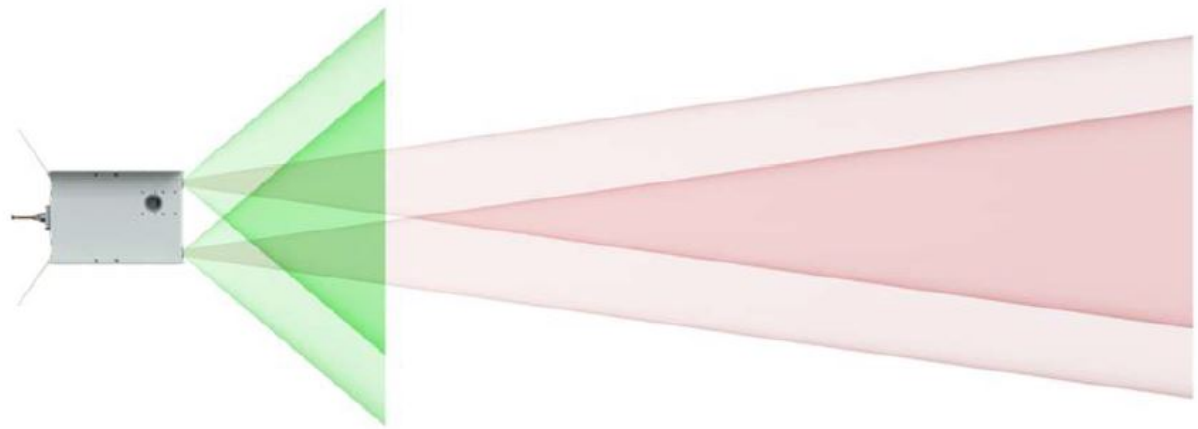

Figure 71 – REMORA satellite field of view with it four cameras for close and distant relative navigation.

4.1.0.14 C-Form

The miniature robotic manipulator developed by JPL for formation flight is a capable system. The proposed mission is a 9.5kg 6U unit that integrates two manipulators, one ADCS system, two propulsion systems and four close range cameras. They also left extra space and power available for the payload. They based a great deal of these systems on the CPOD mission. For instance, the same cold thruster module was used for close proximity maneuvering, the *Vacco Reaction Control Propulsion Module*(CPOD...,). Also, the same camera system, with two RGB cameras and two IR cameras; for relative navigation sensing; and the same Tyvak Inertial Reference Module from Tyvak(CPOD..., 2015). The main difference was the addition of a second thrust module for performing orbital maneuvering, the *Vacco ADN Micro Propulsion system*(ADN...,).

The pointing accuracy was not calculated, but the group performed a simulation maneuvering the satellite from a 1km distance to a precise location 50cm away from the target and was able to stay within ±1cm around the position goal.

5 CONCLUSION

The final goal of this report is to assess the state of the art about cubesat docking connectors and manipulators. One can easily see that these technologies are not commercially available yet. Docking connectors and robotic manipulators for big spacecrafts are nothing new, and some of these technologies are just becoming commercially available for microsatellites, such as the IBOOS (Sec.2.0.2.15) and the HotDock (Sec.2.0.2.12) connectors and the KRAKEN (Sec.3.0.3.1) manipulator. For nanosatellites, docking connectors are just now making the transition from lab research into the commercial environment and manipulators are still more on the embryonic research state. The most developed docking connector; TRL 8; is on the SPHERES project (Sec. 2.0.2.1), and even so it has only flown inside the ISS for a limited amount of time. When it comes to commercial developments, there are the C-POD (Sec. 2.0.2.6) and the RACE (Sec. 2.0.2.9) missions. The first one has flight proven their hardware, but not performed an on-orbit docking yet, even though the launch was scheduled for 2021. The latter one started its developments in 2019 and reasonable delays arose with the covid-19 pandemic. When it comes to manipulation, the most advanced project is AMODS (Sec. 3.0.1), with some of its main technologies being already flight proven. The REMORA project (Sec. 3.0.2) is still at the prototyping stage, and the JPL's manipulator (Sec. 3.0.2.1), although the most technologically advanced, haven't publicly presented a prototype.

Another relevant matter is about the separation between the docking and the manipulation problem. Some connectors (Sections 2.0.2.15, 2.0.2.16 and 2.0.2.17) are made to be used in conjunction with manipulators. That was viable thanks to their mission profiles, the bigger size of their attached systems and the fact they were made to be used also for connecting modules (instead of spacecrafts). Similarly, JPL's manipulator (Sec. 3.0.2.1) was devised to have a docking connector as an end-effector. That was one of the proposed and initial ideas, but by no means the only one or the most generic, as it was outlined by the team themselves, the AMODS (Sec. 3.0.1) and REMORA (Sec. 3.0.2) projects. The clear conclusion then is that docking and manipulation are essentially separate. The combination of these technologies may allow for specialized missions, but docking cubesats does not requires a manipulator and manipulators don't need to have a docking connector as an end-effector in order to be usefull.

5.0.1 Docking Connectors Conclusion

Appendix A presents Table.10, a compilation of the main characteristics of the connectors presented so far. It is organized in the same order presented. Items 1 to 7 are connectors already optimised for the cubesat format and 8 to 18 are bigger connectors liable

for miniaturization. From a simple inspection, we can see that electrical connections are not common in the first group, given their small area. Thus wireless communication prevails. Also, the use of electromagnetic alignment assistance is ample, probably due to the fact that performing precise attitude control on light spacecrafts is hard and the resources are limited. Inspecting the whole table and comparing it to the mission descriptions, we see that a latching mechanism is essential for relevant restraining forces and considerably reduces the mission's power budget than relying solely on magnetic forces. Soft docking is also a rare feature and causes significant complexity in the design. Gendered and androgynous connectors are equally distributed around the table. Regarding angular tolerances, is is well within the state of the art at cubesat pointing capabilities, currently at the arcsecond range. Lateral alignment, on the other hand, is a much harder task, for it depends on the precise activation of thrusters and accurate relative navigation sensing. It is important to highlight that the presence of an electromagnet at the connector may cause saturation of the magnetometer sensors on-board the spacecraft. The magnetic fields generated will also interact with earth's magnetic field and possibly affect the satellite's attitude. Activation of the electromagnet, if present, must be kept to a minimum. A reasonable goal would be to develop a COTS connector unit that could be bolted into a satellite's structure with power and data connections.

Regarding attitude sensing and actuation, it must be divided in two parts: payload sensing and actuation requirements and docking sensing and actuation requirements. The attitude actuation must be set according to the most rigorous of the two parts, that would usually be the payload for missions aimed at remote sensing or IOT. The attitude estimation for the payload shall make use of traditional sensors, like star trackers and accelerometers. Not unusually, these are already integrated into the ADCS unit. On the other hand, the attitude estimation for rendezvous and docking is not traditional and should make use of one or more of the technologies highlighted at section 5.2. For orbit maneuvering, a precise set of thrusters must always be present for the rendezvous. In case the mission requires big orbital manoeuvrings, a second set of less precise thrusters, but with greater Delta-V, can be added. These could also be valuable for detumbeling purposes.

Here are the author's suggestions about the development of a demonstrator mission for on-orbit cubesat docking.

- Like the C-POD mission (Sec. 2.0.2.6), deploy two 3U units as one 6U unit. After release, they break apart and maneuver into docking.

- Use one set of precise thrusters, such as the cold-gas one proposed by JPL (Sec. 4.1.0.14) and C-POD (Sec.4.1.0.5). Electric thrusters ones such as the one proposed by the AMODS team (Sec. 4.1.0.12) can be used for orbit maintenance.

- Add one ADCS unit with actuation and sensing integrated like the ones present in sections 4.1.0.5, 4.1.0.3, 4.1.0.14 and 4.1.0.2.
- For relative navigation, in case a sturdy TOF camera is found viable; preferably the *Intel D435* at Sec.4.0.2.4; would be ideal. The point could be compared to a 3D model of the satellite and the RGB camera present could also be used with the fiducials. A stereo camera could also be used, like in the AMODS project (Sec. 4.1.0.12). In case neither seems viable, a small 2D camera combined with fiducials LED's could be enough (Sec. 4.0.2.5).
- Make use of CDGPS (Sec. 4.0.2.1). The technology is relatively new for space exploration but has extensive use on the ground. NASA's mission OAAN (Sec. 4.1.0.3) showed very good experimental results. It could be used as a conventional GNSS receiver and for improving position estimation for the relative navigation.
- An androgynous connector with 90° symmetry resembling the HotDock connector (Sec.2.0.2.12).
- A hook latching mechanism like the one present at the SIROM connector (Sec. 2.0.2.11).
- Make use of a non-backdrivable gearing system to save power once docked.
- A retractable connector such as in Sec.2.0.4.1.
- Add at least 6 IR and/or visible LED's at the satellites surface to be used as fiducials, such as in Sec.2.0.2.6. This was present in many proposals, it saves space and is more reliable than ArUco markers.
- Use electromagnets for alignment aid. One strong central one like in Sec. **??** and possibly smaller ones on the side to aid on angular alignment, see Sec. 2.0.2.5 and 4.1.0.8. This would allow looser alignment requirements, once the satellites could be positioned at a capturing cone and be brought together by the magnetic force.
- Make use of hall sensors, such as in the HotDock project (Sec. 4.1.0.8), for it is very cheap and can possibly cover ranges blind to other sensors.
- Make use of the so called "Pogo-pins" for data transferring as in Sec. 2.0.2.17 and 2.0.2.12. Tabs can also be used, but preferably for power transferring, such as in Sec. 2.0.2.1.
- The communication between two connectors could be made with specialized protocols such as *SpaceWire* (Sec. 2.0.1). Integrated electronics into the connector could be responsible for the external communication, and the required serial protocols and

GPIOs, outlined in section 2.0.1, could be converted and offered internally to the satellite (see figure 72).

- Some connectors like 2.0.2.15 and 2.0.2.12 offer thermal transferring capabilities. That would be too bulky and most likely be unnecessary for cubesats.

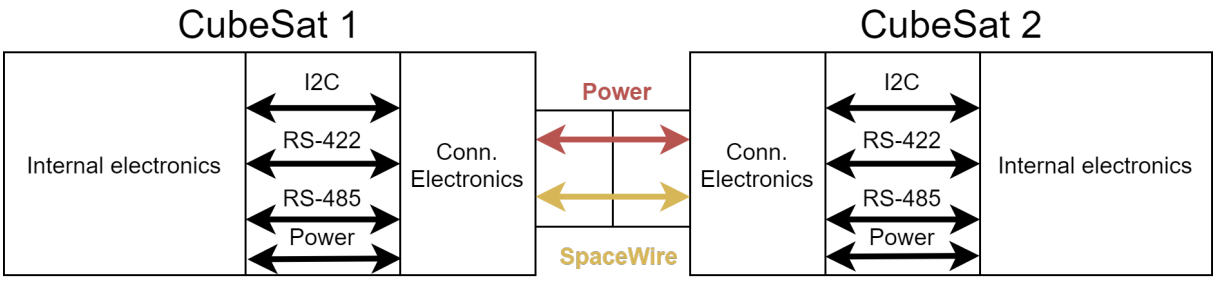

Figure 72 – Proposed communication protocols inside and between two spacecrafts.

A mock-up mechanical CAD of the proposed connector is shown in Fig.73.

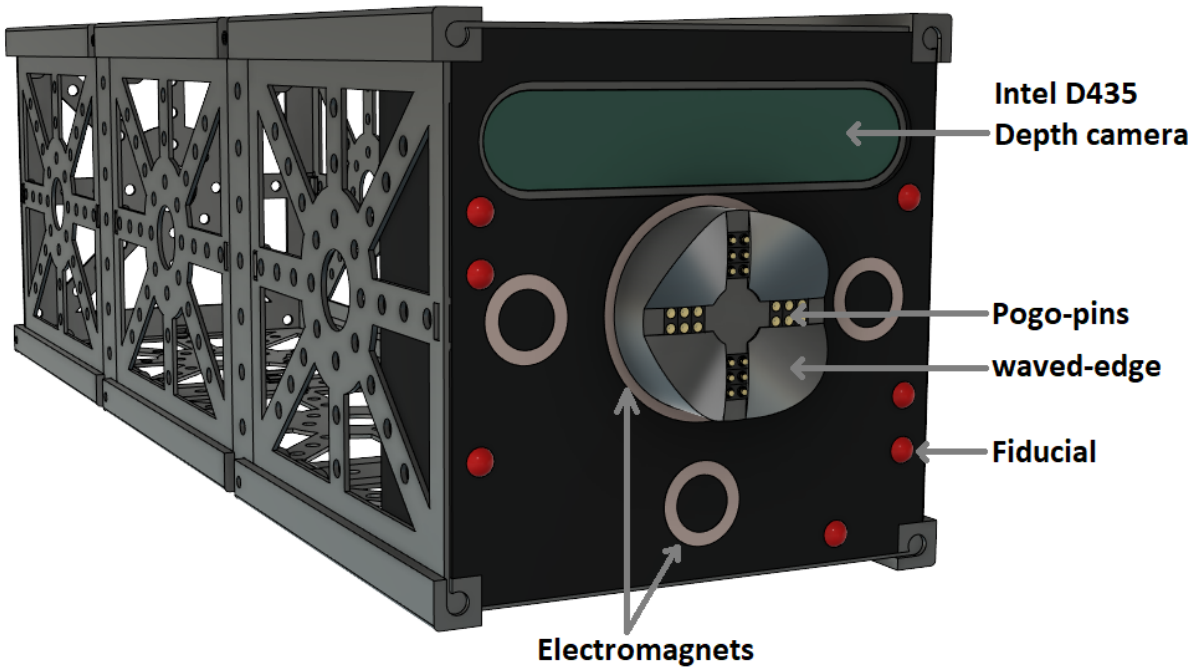

Figure 73 – Mock-up of the proposed connector with a wave edge retractable connector, 7 LED fiducials, 12 "pogo-pins" and 1 *Intel D435* depth camera. This particular TOF camera could be replaced for other ones a stereo camera or a miniature 2D camera. The latching connector was not added in the rendering due the fact that an adequate mechanism is not yet determined.

It is also valid to talk about the development process. A common procedure amongst the connectors proposed is:

1. Develop the mechanical CAD of the connectors.
2. Monte Carlo Kinematic simulations to determine maximum docking misalignments.
3. Multi body simulations for refining the docking alignment envelop.
4. Build a first prototype of the connectors with additive manufacturing for saving costs.
5. Test the prototype on a controlled table to validate the kinematic simulations
6. Test the prototype on an air bearing table to validate the multi body simulation.
7. Build a full metal connector and repeat the testing for validation.

At any point of this listing it is possible, and even recommended, to go back and alter the CAD or the prototype in case new insights for improvements occur. A common multi-body simulation software used is Adams [1], and the Padova probe/drogue connector (Sec. 2.0.2.2) also uses it for the kinematic analysis. The ASSIST (Sec. 2.0.2.13) mission also used the GNCDE (Guidance Navigation and Control Development Environment) simulator[2] for both the kinematics and dynamics simulations.

It is also important to highlight the contributions of the Padova University, having developed many of the connectors presented (Sections 2.0.2.2, 2.0.2.5, 2.0.2.10, 2.0.2.16, 2.0.2.19).

(WENZEL *et al.*, 2017) and (YAN *et al.*, 2018) offer good reviews of the basic components necessary for the development of a docking connector. Also Fig.36 should be further explored for the development of a compact latching mechanism. (VINALS *et al.*, 2018) gives some insight into the SIROM (Sec. 2.0.2.11) mechanism.

5.0.2 Cubesat Manipulation Conclusions

Table 9 compares some key aspects of the manipulators presented for cubesats. The first thing noticeable is the variety of applications. Unlike for nanoconnectors, the development of a nanomanipulator would probably have to be tailored for different types of mission. The REMORA project (sec. 3.0.2), for example, has half of its stowed space dedicated to the end-effector and the JPL manipulator team (Sec.3.0.2.1) had to develop a specialised mechanism. Figure 48 presents a few options of missions to take advantage of a nanomanipulator. Stowed size, nominal power consumption and the number of DOFs is also very dependent on the mission profile. (JACKSON *et al.*, 2020) Is a recent work that goes into deep details into the forces involved with the use of a manipulator with non-negligible mass on a free floating spacecraft.

[1] https://www.mscsoftware.com/product/adams
[2] https://www.gmv.com/en/Products/gncde/

Here are the author's suggestions about the development of a demonstrator mission for on-orbit cubesat manipulation.

- A 6U mission, with two sets of thrusters, one precise and one with high delta-v. They could be both cold gas based, such as the mission proposed by JPL at section 4.1.0.14 or electric and cold gas as on AMODS (Sec. 4.1.0.12).

- An ADCS unit with actuation and sensing integrated like the ones present in sections 4.1.0.5, 4.1.0.3 and 4.1.0.14.

- For relative navigation, in case a sturdy TOF camera is found viable; preferably the *Intel D435* at Sec.4.0.2.4; it would be ideal. The point cloud could be compared to a 3D model of the satellite and the RGB camera present could also be used with the fiducials. A stereo camera could also be used, like in the AMODS project (Sec. 4.1.0.12). In case neither seems viable, a small 2D camera combined with fiducials LED's could be enough (Sec. 4.0.2.5).

- Make use of CDGPS (Sec. 4.0.2.1). The technology is relatively new for space exploration but has extensive use on the ground. NASA's mission OAAN (Sec. 4.1.0.3) showed very good experimental results. It could be used as a conventional GNSS receiver and for improving position estimation for the relative navigation.

- Have two manipulators symmetrically positioned at the cubesat for canceling each other's moment of inertia with mirrored movements, as it was proposed with the AMODS project (Sec. 3.0.1).

- Use deployable prismatic links as in Sec. 3.0.2.1. It is a simple mechanism that saves a lot of space.

- Start with a 5 DOF arm. The zero gravity environment facilitates the use of standard joint actuators throughout the arm, thus facilitating a future addition of DOFs.

- Make use of a non-backdrivable gearing system. This would avoid the use of complex braking systems (as in Sec. 3.0.2.1) and save power. In case a worm gear mechanism is selected, it could be used to rotate the the axis of the actuator and save space.

- Add micro IR or RGB cameras at the end-effectors so to facilitate positioning and manipulation, as it was proposed with the AMODS project (Sec. 3.0.1).

- Stow the two arms like in the AMODS project (Sec. 3.0.1) can be advantageous to make a better use of empty space caused by the actuator sticking out of the arm.

	Stowed Size cm	Power W	Stretched Size m	DOFs	Mass kg	Configuration	Accuracy mm	Main Usage
AMODS	30x10x6.2 (2 arms)	n.a.	0.6	7	n.a.	Y-R-Y-Y-R-Y-R	10	Assessment
REMORA	20x10x5	15	0.40	5	1.14	Y-R-Y-Y-Y	±5	Cleaning
C-FORM	10x10x5.4	16.5	0.43	5	0.46	Y-R-Y-Y-Y	1	Docking

Table 9 – Comparison between nanosat manipulators. At the 7th column, "Y" means yaw and "R" means roll.

As stated at different points, the use of docking connectors and manipulators are closely related to on-orbit services including assembly, manufacturing, inspecting, cleaning, maintenance, recycling and refueling. These capabilities are the key for mission that will enable a more sustainable and human friendly space exploration on LEO and beyond.

REFERENCES

AAREST presentation. Disponível em: http://www.its.caltech.edu/~sslab/AAReST_Docs/AAReST_Surrey_DDR_2014.pdf.

ADN Micro Propulsion System. Disponível em: https://www.vacco.com/images/uploads/pdfs/MicroPropulsionSystems.pdf.

BAFFLING Buffs. Disponível em: https://www.colorado.edu/aerospace/sites/default/files/attached-files/bafflingbuffs_pdd.pdf.

BARBETTA, M. *et al.* Arcade-r2 experiment on board bexus 17 stratospheric balloon. **CEAS Space Journal**, Springer, v. 7, n. 3, p. 347–358, 2015.

BOESSO, A.; FRANCESCONI, A. Arcade small-scale docking mechanism for micro-satellites. **Acta Astronautica**, Elsevier, v. 86, p. 77–87, 2013.

BOWEN, J. *et al.* Cubesat proximity operations demonstration (cpod) mission update. *In*: IEEE. **2015 IEEE Aerospace Conference**. [*S.l.: s.n.*], 2015. p. 1–8.

BOWEN, J.; VILLA, M.; WILLIAMS, A. Cubesat based rendezvous, proximity operations, and docking in the cpod mission. 2015.

BRANZ, F. *et al.* Miniature docking mechanism for cubesats. **Acta Astronautica**, Elsevier, v. 176, p. 510–519, 2020.

BRIDGES, C. *et al.* Strand-2: Visual inspection, proximity operations & nanosatellite docking. *In*: IEEE. **2013 IEEE Aerospace Conference**. [*S.l.: s.n.*], 2013. p. 1–8.

BRINKMANNA, W. Modular active payload modules for robotic handlings in future orbital missions wiebke brinkmanna*, marko jankovicb, christoph stoefflerc, gonzalo guerra d, eduardo urgoitie, javier vinalsf, sebastian bartschg.

CHAN, M. *et al.* Productization of cubesat rendezvous and docking solutions. 2019.

CHEN, J. *et al.* Survey on 6d pose estimation of rigid object. *In*: IEEE. **2020 39th Chinese Control Conference (CCC)**. [*S.l.: s.n.*], 2020. p. 7440–7445.

CPOD presentation. 2015. Disponível em: https://digitalcommons.usu.edu/cgi/viewcontent.cgi?article=3291&context=smallsat.

CPOD Thruster Unit. Disponível em: https://cubesat-propulsion.com/reaction-control-propulsion-module/.

CUBESENSE Module. Disponível em: https://www.cubesatshop.com/wp-content/uploads/2016/06/CubeSpace_CubeSense_Brochure_2016_01.pdf.

DAFFALLA, M. M.; TAGELSIR, A.; KAJO, A. S. Hardware selection for attitude determination and control subsystem of 1u cube satellite. *In*: IEEE. **2015 International Conference on Computing, Control, Networking, Electronics and Embedded Systems Engineering (ICCNEEE)**. [*S.l.: s.n.*], 2015. p. 118–122.

DETTMANN, A. *et al.* Heterogeneous modules with a homogeneous electromechanical interface in multi-module systems for space exploration. *In*: IEEE. **2011 IEEE International Conference on Robotics and Automation**. [*S.l.: s.n.*], 2011. p. 1964–1969.

DEVELOPMENT OF MINIATURE ROBOTIC ARM MANIPULATORS TO ENABLE SMALLSAT CLUSTERS. Disponível em: https://www.ideals.illinois.edu/bitstream/handle/2142/97516/WENGER-THESIS-2017.pdf?sequence=1.

DONG, S. *et al.* Self-assembling wireless autonomously reconfigurable module design concept. **Acta Astronautica**, Elsevier, v. 62, n. 2-3, p. 246–256, 2008.

DUZZI, M. *et al.* Electromagnetic position and attitude control for pacman experiment. *In*: **Proceedings of the 10th International ESA Conference on Guidance, Navigation & Control Systems, Salzburg, Austria**. [*S.l.: s.n.*], 2017. v. 29.

DUZZI, M. *et al.* Pacman experiment: A cubesat-size integrated system for proximity navigation and soft-docking. ResearchGate, 2018.

ECKERSLEY, S. *et al.* Future rendezvous and docking missions enabled by low-cost but safety compliant guidance navigation and control (gnc) architectures. *In*: BRITISH INTERPLANETARY SOCIETY. **Proceedings of The 15th Reinventing Space Conference**. [*S.l.: s.n.*], 2017.

FREDRICKSON, S. E. *et al.* Mini aercam: development of a free-flying nanosatellite inspection robot. *In*: INTERNATIONAL SOCIETY FOR OPTICS AND PHOTONICS. **Space Systems Technology and Operations**. [*S.l.: s.n.*], 2003. v. 5088, p. 97–111.

HANLON, E. *et al.* Leveraging the autonomous mobile on-orbit diagnostic system to initiate a doctrinal shift in spacecraft operations. *In*: **Space Operations: Contributions from the Global Community**. [*S.l.: s.n.*]: Springer, 2017. p. 53–86.

HANLON, E. A. Design features and flight results for the autonomous mobile on-orbit diagnostic system (amods). *In*: **AIAA SPACE 2016**. [*S.l.: s.n.*], 2016. p. 5618.

HANLON, E. A. *et al.* Amods: Autonomous mobile on-orbit diagnostic system. *In*: IEEE. **2016 IEEE Aerospace Conference**. [*S.l.: s.n.*], 2016. p. 1–10.

HAYS, A. B. *et al.* Dynamic simulation and validation of a satellite docking system. *In*: INTERNATIONAL SOCIETY FOR OPTICS AND PHOTONICS. **Space Systems Technology and Operations**. [*S.l.: s.n.*], 2003. v. 5088, p. 77–88.

HAYS, A. B. *et al.* Advancements in design of an autonomous satellite docking system. *In*: INTERNATIONAL SOCIETY FOR OPTICS AND PHOTONICS. **Spacecraft Platforms and Infrastructure**. [*S.l.: s.n.*], 2004. v. 5419, p. 107–118.

HAYS, A. B. *et al.* Advancements in kc-135 microgravity testing of an autonomous satellite docking system. *In*: INTERNATIONAL SOCIETY FOR OPTICS AND PHOTONICS. **Spacecraft Platforms and Infrastructure**. [*S.l.: s.n.*], 2004. v. 5419, p. 119–129.

HIRZINGER, G. *et al.* Rokviss-robotics component verification on iss. *In*: **Proc. 8th Int. Symp. Artif. Intell. Robot. Autom. Space (iSAIRAS)(Munich 2005) p. Session2B**. [*S.l.: s.n.*], 2005.

HOTDOCK: Design and Validation of a New Generation of Standard Robotic Interface for On-Orbit Servicing. Disponível em: https://www.researchgate.net/publication/344871962_HOTDOCK_Design_and_Validation_of_a_New_Generation_of_Standard_Robotic_Interface_for_On-Orbit_Servicing.

HOTDOCK User Manual. Disponível em: https://www.h2020-mosar.eu/wp-content/uploads/2020/06/MOSAR-WP2-D2.7-SA_1.0.0-HOTDOCK-User-Manual-.pdf.

HOW to Choose a 3D Vision Technology. Disponível em: https://roscon.ros.org/2017/presentations/ROSCon\%202017\%203D\%20Vision\%20Technology.pdf.

JACKSON, L. *et al.* Downsizing an orbital space robot: A dynamic system based evaluation. **Advances in Space Research**, Elsevier, 2020.

KEIDAR, M. *et al.* Micro-cathode arc thruster for nanosatellite propulsion. *In*: **33rd International Electric Propulsion Conference (IEPC-2013), George Washington University, Washington, DC**. [*S.l.: s.n.*], 2013.

KORTMAN, M. *et al.* Building block based iboss approach: fully modular systems with standard interface to enhance future satellites. *In*: **66th International Astronautical Congress (Jersualem, Israel**. [*S.l.: s.n.*], 2015.

LEUNG, S.; MONTENBRUCK, O. Real-time navigation of formation-flying spacecraft using global-positioning-system measurements. **Journal of Guidance, Control, and Dynamics**, v. 28, n. 2, p. 226–235, 2005.

LI, W.-J. *et al.* On-orbit service (oos) of spacecraft: A review of engineering developments. **Progress in Aerospace Sciences**, Elsevier, v. 108, p. 32–120, 2019.

LINEAR Hall Effect Sensor Angle Measurement Theory, Implementation, and Calibration. Disponível em: https://www.ti.com/lit/an/slya036a/slya036a.pdf?ts=1604659852284&ref_url=https\%253A\%252F\%252Fwww.google.com\%252F.

LINEAR Hall Effect Sensor Array Design. Disponível em: https://www.ti.com/lit/an/slya051/slya051.pdf?ts=1604658707818&ref_url=https\%253A\%252F\%252Fwww.google.com\%252F.

LIU, J.; HE, S. 6d object pose estimation without pnp. **arXiv preprint arXiv:1902.01728**, 2019.

MASON, J. P. *et al.* Minxss-1 cubesat on-orbit pointing and power performance: the first flight of the blue canyon technologies xact 3-axis attitude determination and control system. **arXiv preprint arXiv:1706.06967**, 2017.

MCCORMICK, R. *et al.* Development of miniature robotic manipulators to enable smallsat clusters. *In*: IEEE. **2017 IEEE Aerospace Conference**. [*S.l.: s.n.*], 2017. p. 1–15.

MCCORMICK, R. *et al.* Remora cubesat for large debris rendezvous, attachment, tracking, and collision avoidance. *In*: IEEE. **2018 IEEE Aerospace Conference**. [*S.l.: s.n.*], 2018. p. 1–13.

MCKENNA, E. **AAReST Spacecraft Electro-magnetic Docking System**. 2015. Tese (Doutorado) — MSc Thesis, University of Surrey, Guildford, UK, 2015.

MEDINA, A. *et al.* Towards a standardized grasping and refuelling on-orbit servicing for geo spacecraft. **Acta Astronautica**, Elsevier, v. 134, p. 1–10, 2017.

MILLER, D. L. **Development of resource-constrained sensors and actuators for in-space satellite docking and servicing**. 2015. Tese (Doutorado) — Massachusetts Institute of Technology, 2015.

MONTENBRUCK, O. *et al.* Carrier phase differential gps for leo formation flying–the prisma and tandem-x flight experience. **Paper AAS**, p. 11–489, 2011.

NALLAPU, R. T. *et al.* Smart camera system on-board a cubesat for space-based object reentry and tracking. *In*: IEEE. **2018 IEEE/ION Position, Location and Navigation Symposium (PLANS)**. [*S.l.: s.n.*], 2018. p. 1294–1301.

NASA Johnson Space Center's Miniature Autonomous Extravehicular Robotic Camera (Mini AERCam). Disponível em: https://er.jsc.nasa.gov/seh/AERCAM/aercam.pdf.

NOHMI, M. Mission design of a tethered robot satellite "stars" for orbital experiment. *In*: IEEE. **2009 IEEE Control Applications,(CCA) & Intelligent Control,(ISIC)**. [*S.l.: s.n.*], 2009. p. 1075–1080.

OLIVIERI, L. *et al.* Microgravity tests in preparation of a tethered electromagnetic docking space demonstration. *In*: **Proceedings of the 68th International Astronautical Congress, Adelaide**. [*S.l.: s.n.*], 2017.

OLIVIERI, L. *et al.* Docking mechanisms for nano and micro satellites.

OLIVIERI, L.; FRANCESCONI, A. Design and test of a semiandrogynous docking mechanism for small satellites. **Acta Astronautica**, Elsevier, v. 122, p. 219–230, 2016.

PEI, J. Ground demonstration on the autonomous docking of two 3u cubesats using a novel permanent magnet docking mechanism. *In*: **55th AIAA Aerospace Sciences Meeting**. [*S.l.: s.n.*], 2017. p. 0849.

PEI, J. *et al.* Autonomous rendezvous and docking of two 3u cubesats using a novel permanent-magnet docking mechanism. *In*: **54th AIAA Aerospace Sciences Meeting**. [*S.l.: s.n.*], 2016. p. 1465.

PIRAT, C. *et al.* Vision based navigation for autonomous cooperative docking of cubesats. **Acta Astronautica**, Elsevier, v. 146, p. 418–434, 2018.

RANK, P. *et al.* The deos automation and robotics payload. *In*: **Symp. on Advanced Space Technologies in Robotics and Automation, ASTRA, the Netherlands**. [*S.l.: s.n.*], 2011.

RAVINDRAN, A.; VANCE, L. D.; THANGAVELAUTHAM, J. Modeling, control and laboratory testing of an electromagnetic docking system for small satellites. *In*: **AAS Guidance and Control Conference, CO**. [*S.l.: s.n.*], 2020.

RIVERA, D. E.; MOTAGHEDI, P.; HAYS, A. Modeling and simulation of the michigan aerospace autonomous satellite docking system ii. *In*: INTERNATIONAL SOCIETY FOR OPTICS AND PHOTONICS. **Modeling, Simulation, and Verification of Space-based Systems II**. [*S.l.: s.n.*], 2005. v. 5799, p. 82–91.

RODGERS, L. Concepts and technology development for the autonomous assembly and reconfiguration of modular space systems. *In*: . [*S.l.: s.n.*], 2006.

RODGERS, L. *et al.* A universal interface for modular spacecraft. 2005.

ROGNANT, M. *et al.* Autonomous assembly of large structures in space: a technology review. 2019.

SANSONE, F.; BRANZ, F.; FRANCESCONI, A. A relative navigation sensor for cubesats based on led fiducial markers. **Acta Astronautica**, Elsevier, v. 146, p. 206–215, 2018.

SANSONE, F. *et al.* Low-cost relative navigation sensors for miniature spacecraft and drones. *In*: IEEE. **2015 IEEE Metrology for Aerospace (MetroAeroSpace)**. [*S.l.: s.n.*], 2015. p. 389–394.

STANDARD, E. **ECSS-E-ST-50-12C: SpaceWire-Links, nodes, routers and networks, Jul. 2008**.

STANDARD Interface for Robotic Manipulation of Payloads in Future Space Missions - Summary for publication. Disponível em: https://www.strath.ac.uk/media/departments/dmem/smestech/sirom/D7.2___OG5-D0_SIROM_Final_Report.pdf.

TIA-422, Revision B, January 2000 - Electrical Characteristics of Balanced Voltage Digital Interface Circuits. [*S.l.: s.n.*]: Telecommunications Industry Association (TIA), 2014.

TIA-485, Revision A, March 1998 - Electrical Characteristics of Generators and Receivers for Use in Balanced Digital Multipoint Systems. 2012.

UNDERWOOD, C. *et al.* Using cubesat/micro-satellite technology to demonstrate the autonomous assembly of a reconfigurable space telescope (aarest). **Acta Astronautica**, Elsevier, v. 114, p. 112–122, 2015.

VINALS, J. *et al.* Multi-functional interface for flexibility and reconfigurability of future european space robotic systems. **Advances in Astronautics Science and Technology**, Springer, v. 1, n. 1, p. 119–133, 2018.

WANG, C. *et al.* Densefusion: 6d object pose estimation by iterative dense fusion. 2019.

WENBERG, D. *et al.* Advancing on-orbit assembly with isar. 2018.

WENBERG, D. L. *et al.* Miniaturizing the robotic assembly of spacecraft: Isar development and on-orbit demonstration. *In*: **2018 SpaceOps Conference**. [*S.l.: s.n.*], 2018. p. 2704.

WENBERG, D. L. *et al.* Intelligent space assembly robot: Design and ground testing. *In*: **AIAA SPACE and Astronautics Forum and Exposition**. [*S.l.: s.n.*], 2017. p. 5180.

WENBERG, D. L. *et al.* Rsat flight qualification and test results for manipulable robotic appendages installed on 3u cubesat platform. 2016.

WENBERG, D. L. *et al.* Bricsat-d flight experiment: Demonstrating the feasibility of low cost diagnostic missions. *In*: **55th AIAA Aerospace Sciences Meeting**. [*S.l.: s.n.*], 2017. p. 0616.

WENZEL, W.; CORDES, F.; KIRCHNER, F. A robust electro-mechanical interface for cooperating heterogeneous multi-robot teams. *In*: IEEE. **2015 IEEE/RSJ International Conference on Intelligent Robots and Systems (IROS)**. [*S.l.: s.n.*], 2015. p. 1732–1737.

WENZEL, W. *et al.* Mechanical, thermal, data and power transfer types for robotic space interfaces for orbital and planetary missions-a technical review. European Space Agency, 2017.

WESTON, S. *et al.* State of the art: Small spacecraft technology. 2018.

WILDE, M.; CLARK, C.; ROMANO, M. Historical survey of kinematic and dynamic spacecraft simulators for laboratory experimentation of on-orbit proximity maneuvers. **Progress in Aerospace Sciences**, Elsevier, v. 110, p. 100552, 2019.

YAN, X.-T. *et al.* Integrated mechanical, thermal, data, and power transfer interfaces for future space robotics. **Frontiers in Robotics and AI**, Frontiers, v. 5, p. 64, 2018.

ANNEX

ANNEX A – CUBESAT CONNECTORS COMPARISON

Table 10 – Comparison between different connector types explored in section 3.2.

		Electric Contacts	Angular Tolerance	Lateral Tolerance [mm]	Type	Alignment Assistance	Mass [Kg]	Cantilevered Force [N.m]	Tensile Force [N]	Close Position Sensor	Comn. Protocol	Soft Docking	TLR
1	**UDP**	2	2°	20	Androgynous	Electro-magnetic Medium dependence	0.45	27.5	110	External ref. + Ultrasound + Camera	Bluetooth	No	8
2	**Padova Drogue/cone**	0	±5° @0mm lateral	±20 @10°	Gendered	-	150	n.a	> 25	Camera + LED Fiducial	-	No	4
3	**AAReST**	0	30° @30cm	600 @30cm	Gendered	Electro-magnetic High dependence	4	1	3	LIDAR + Camera	Wifi	No	4
4	**OAAN**	0	1.5	20	Androgynous	Perm. magnetic High depedence	n.a	n.a	n.a	CDGPS	n.a	No	4
5	**PACMAN**	0	8°	n.a.	Gendered	Electro-magnets High dependence	n.a.	n.a.	n.a.	Camera + LED Fiducial	-	Yes	6
6	**CPOD**	n.a.	n.a.	n.a.	Androgynous	Electro-magnetic Low depedence	n.a.	n.a.	n.a.	IR & Visible Cameras + LED Fiducial	n.a.	No	7
7	**ASDS**	0	6°	70	Gendered	Cable Medium dependence	n.a	n.a	n.a	n.a	n.a	Yes	6
8	**SIROM**	27	1.5°	10	Androgynous	-	1.5	50	1600	Camera + ArUco markers	Electrical	No	4
9	**HotDock**	48	10°	±15	Androgynous	Permanent magnets Low dependence	0.25 to 1.55	300	3000	-	Electrical	No	4
10	**ASSIST**	9	5	20	Gendered	Robotic arm High dependence	n.a.	3.56	131	LIDAR + Camera	Electrical	Yes	5
11	**ARCADE**	0	5°	n.a.	Gendered	Electro-magnetic Low dependence	1.25	n.a.	300	IR sens.	-	Yes	6
12	**IBOSS**	2	n.a	n.a	Androgynous	-	1.63	360	6000	-	Optical	No	4
13	**AUTOPORT**	5	±20°	40	Gendered	-	n.a.	~ 42	100	Camera + LED Fiducial	Wifi	No	4
14	**TransTerrA**	36	7°	±5	Gendered	-	n.a.	n.a.	800	Camera + ArUco markers	Electrical	No	
15	**NASA Miniature**	n.a.	30°	±60 @ 12.7 cm	Gendered	Electro-magnets High dependence	n.a.	n.a.	n.a.	Camera	Wifi	No	4
16	**Padova Semi-andro.**	0	5°	15	Semi Androgynous	-	n.a	n.a.	3	-	NFC	No	4